Body mass estimation from footprint size in hominins

Christopher B. Ruff[a,*], Roshna E. Wunderlich[b], Kevin G. Hatala[c], Russell H. Tuttle[d], Charles E. Hilton[e], Kristiaan D'Août[f], David M. Webb[g], Benedikt Hallgrímsson[h], Charles Musiba[i], Michael Baksh[j]

[a] *Center for Functional Anatomy and Evolution, Johns Hopkins University School of Medicine, 1800 E. Monument St., Baltimore, MD 21111, USA*

[b] *Department of Biology, James Madison University, MSC 7801, Harrisonburg, VA 22807, USA*

[c] *Department of Biology, Chatham University, Buhl Hall, Woodland Rd., Pittsburgh, PA 15232, USA*

[d] *Department of Anthropology, University of Chicago, 1126 East 59th Street, Chicago, IL 60637, USA*

[e] *Department of Anthropology, University of North Carolina, 301 Alumni Bldg., University of North Carolina, Chapel Hill, NC 27599-3115 USA*

[f] *Department of Musculoskeletal and Ageing Science, Institute of Life Course and Medical Sciences, University of Liverpool, 6 West Derby Street, Liverpool L7 8TX, UK*

[g] *Department of Anthropology and Sociology, Kutztown University, Kutztown, PA 19530, USA*

[h] *Department of Cell Biology & Anatomy, Alberta Children's Hospital Research Institute, McCaig Institute for Bone and Joint Health, Cumming School of Medicine, University of Calgary, 3330 Hospital Dr. NW, Calgary, Alberta T2N 4N1, Canada*

[i] *Department of Anthropology, University of Colorado Denver, NC Building, Suite 4002, 1200 Larimer Street, Denver, CO 80217, USA*

[j] *10878 Aviary Ct., San Diego, CA 92131, USA*

***Corresponding author:**

Email address: cbruff@jhmi.edu (C.B. Ruff)

Note: Contains corrections to the legend of Figure 7 and associated text on p. 23.

Abstract

While many studies relating stature to foot length have been carried out, the relationship between foot size and body mass remains poorly understood. Here we investigate this relationship in 193 adult and 50 juvenile habitually unshod/minimally shod individuals from five different populations—Machiguenga, Daasanach, Pumé, Hadzabe, and Samoans—varying greatly in body size and shape. Body mass is highly correlated with foot size, and can be predicted from foot area (maximum length × breadth) in the combined sample with an average error of about 10%. However, comparisons among populations indicate that body shape, as represented by the body mass index (BMI), has a significant effect on foot size proportions, with higher BMI samples exhibiting relatively smaller feet. Thus, we also derive equations for estimating body mass from both foot size and BMI, with BMI in footprint samples taken as an average value for a taxon or population, estimated independently from skeletal remains. Techniques are also developed for estimating body mass in juveniles, who have relatively larger feet than adults, and for converting between foot and footprint size. Sample applications are given for five Pliocene through Holocene hominin footprint samples from Laetoli (*Australopithecus afarensis*), Ileret (probable *Homo erectus*), Happisburgh (possible *H. antecessor*), Le Rozel (archaic *H. sapiens*), and Barcin Höyük (*H. sapiens*). Body mass estimates for *Homo* footprint samples appear reasonable when compared to skeletal estimates for related samples. However, estimates for the Laetoli footprint sample using the new formulae appear to be too high when compared to skeletal estimates for *A. afarensis*. Based on the proportions of A.L. 288-1, this is apparently a result of relatively large feet in this taxon. A different method employing a ratio between body mass and foot area in A.L. 288-1 provides estimates more concordant with skeletal estimates and should be used for *A. afarensis*.

Key Words: Foot; Body mass index; *Australopithecus*; *Homo*

1. Introduction

Hominin footprints have been discovered from a variety of temporal and geographic contexts stretching from the Pliocene to the Holocene, with a world-wide distribution (Lockley et al., 2008; Bennett and Morse, 2014; Duveau et al., 2019). They have provided important insights into past locomotor biomechanics (Leakey and Hay, 1979; Day and Wickens, 1980; White, 1980; Charteris et al., 1981; Robbins, 1987; Tuttle, 1987; White and Suwa, 1987; Schmid, 2004; Bennett et al., 2009; Raichlen et al., 2010; Crompton et al., 2012; Hatala et al., 2016a; Hatala et al., 2016b), sexual dimorphism (Tuttle, 1987; Hatala et al., 2016b; Masao et al., 2016; Duveau et al., 2019; Villmoare et al., 2019), and paleoecology and group composition (Hatala et al., 2016b; Roach et al., 2016; Altamura et al., 2018; Roach et al., 2018; Duveau et al., 2019; Hatala et al., 2020).

Feet represent the point of contact of the body with the ground during terrestrial travel, transmitting the forces produced by body weight and muscular contractions during gait. Footprints record motions of the foot against the substrate, but their outer dimensions often approximate foot size and therefore they can also be used to estimate body size. In the past the most common application in this regard has been the estimation of stature from footprint length (Beguen and Vallois, 1928; Pales, 1976; White, 1980; Behrensmeyer and Laporte, 1981; Tuttle, 1987; Anil, 1997; Atamtürk and Duyar, 2008; Fawzy and Kamal, 2010; Dingwall et al., 2013; Ashton et al., 2014; Bennett and Morse, 2014; Domjanic et al., 2015; Hatala et al., 2016b; Masao et al., 2016; Altamura et al., 2018; Atamtürk et al., 2018; Duveau et al., 2019). Foot length is well correlated with stature, with a foot length/stature ratio averaging about 15% across modern human populations (Martin, 1928; White, 1980; Robbins, 1986; Ashton et al., 2014; Bennett and

Morse, 2014; Duveau et al., 2019). Various regression-based equations have also been developed (see references above).

Methods for estimating body mass from footprint size have been much less investigated, despite the importance of body mass in many studies of past hominin biology and behavior (Ruff and Niskanen, 2018). Body mass rather than stature is the morphological variable most directly related to the mechanical requirements for maintenance of posture and movement, the metabolic requirements for sustaining life, and the neurological requirements for control of the body. It is thus the most appropriate characteristic for evaluating relative skeletal strength (robusticity), dietary sufficiency, and relative brain size (encephalization). It is also highly correlated with many other physiological, ecological, life-history, and behavioral variables (Calder, 1984; Schmidt-Nielson, 1984; Brown and West, 2000). Many methods for estimating body mass from hominin skeletal remains have been developed (Ruff and Niskanen, 2018). The ability to accurately estimate body mass from footprint size would greatly increase the potential number of individuals available for estimation, including in locations where only footprints have been found, and allow demographic analyses of groups of individuals that are rarely possible using skeletal remains (e.g., Hatala et al., 2017; Duveau et al., 2019).

A summary of eight past studies of body mass estimation from foot or footprint size are given in Table 1.[1] All of them have some limitations. Six of the eight studies were of habitually shod people (Robbins, 1986; Anil, 1997; Atamtürk and Duyar, 2008; Fawzy and Kamal, 2010; Bennett and Morse, 2014; Domjanic et al., 2015). Using footwear appears to have systematic effects on foot shape (Hoffmann, 1905; Ashizawa et al., 1997; D'Août et al., 2009; Hollander et al., 2017; also see below), although some past studies have been partially confounded by comparisons between different ethnic/geographic groups and other problems (Hollander et al.,

2017; Duveau et al., 2019). Regardless, direct applicability of equations derived from habitually shod modern populations to unshod past hominins is highly questionable (Dingwall et al., 2013; Hatala et al., 2016c). Only two studies that developed regression equations for predicting body mass from foot or footprint size examined habitually unshod people (Krishan, 2008; Dingwall et al., 2013). In one case (Krishan, 2008) this was not explicitly stated, but an earlier report on the same study sample noted that "all the subjects were villagers and most of them are in the habit of walking bare feet [sic]" (Krishan, 2007: 138).

The studies in Table 1 employed a variety of methods to assess foot or footprint size. In four studies measurements were taken of footprints as the subjects stood, recorded using pressure-sensitive paper (Robbins, 1986; Bennett and Morse, 2014) or ink on paper (Krishan, 2008; Fawzy and Kamal, 2010). In two other studies feet were measured directly on standing subjects (Anil, 1997; Atamtürk and Duyar, 2008) (Atamtürk and Duyar also measured footprints of their subjects but developed body mass estimation equations using only their foot measurements). In one study foot dimensions were extracted from 3-D laser scans of subjects standing on a glass plate (Domjanic et al., 2015). Only one study measured footprints made in a naturalistic environment (hydrated fine sediment taken from a fossil hominin footprint locality) (Dingwall et al., 2013). All of these differences in technique likely affected assessments of foot dimensions, and thus the applicability of resulting equations to other specimens. Except for Dingwall et al. (2013), all of the studies recorded foot or footprint dimensions while subjects stood on a hard, incompressible surface, which may distort foot dimensions relative to either footprints made in a softer surface or the anatomical dimensions of the feet themselves. For example, foot areas (maximum length × forefoot breadth) measured using pressure-sensitive paper on a hard surface are about 11% larger on average than those calculated from

anthropometric measurements of the relaxed foot of the same subjects (see Supplementary Online Material (SOM) Fig. S1, derived from data collected by Tuttle et al., 1990).

But perhaps the greatest limitation of previous studies of foot/footprint size and body mass is the nature of the study samples themselves (aside from whether they were habitually shod or unshod). All of the studies listed in Table 1 were either of single specific ethnic/geographic groups (Turkish, Egyptian, Croatian, Gujjar, Daasanach) or were of quite broad but unspecified mixed-ethnicity samples (US, British), the latter two including children as well as adults. As noted by a number of researchers (Atamtürk and Duyar, 2008; Fawzy and Kamal, 2010; Bennett and Morse, 2014; Ruff et al., 2018), the specific morphological characteristics of a group may have significant effects on foot to body size proportions, and thus estimation of body size in past specimens. It is particularly noteworthy that the only two previous studies of habitually unshod individuals were of narrowly defined lower latitude populations (Krishan, 2008; Dingwall et al., 2013). The most widely applied of these methods (Dingwall et al., 2013) was based on the Daasanach, who are characterized by a very linear body shape, as reflected in a low body mass index (averaging 18.4—see below). Body mass index (BMI) is calculated as [body mass (kg)/stature^2 (m)] $\times$ 100, and is commonly used as an index of body shape in modern populations (e.g., WHO, 1995; Leonard and Katzmarzyk, 2010; Ruff et al., 2018). No information on stature or BMI is available for the specific sample measured in the other study of an unshod population (Krishan, 2008), but it is likely that they were also characterized by at least a moderately low average BMI (Krishan, pers. comm.). Past studies have documented an effect of BMI on foot shape and plantar pressures during weight support (Ashizawa et al., 1997; Bennett and Morse, 2014; Domjanic et al., 2015). Given that many Plio-Pleistocene hominins were apparently relatively wide-bodied (Aiello, 1992; Trinkaus et al.,

1999; Weaver, 2003; Ruff, 2010; Arsuaga et al., 2015), implying a relatively high BMI, application of body mass estimation formulae derived only from linearly-built, low BMI modern populations to such specimens is potentially problematic (Dingwall et al., 2013; Ashton et al., 2014; Masao et al., 2016). As noted by Bennett and Morse (2014: 152), "Identifying the most appropriate modern analogue population for an extinct hominin species is challenging and those native to a site now may not be the most appropriate analogue".

Here we examine the relationship between body mass and foot size in 243 habitually unshod individuals representing five geographically dispersed populations of varying body size and shape. Methods for converting between foot and footprint dimensions are presented. Results are used to develop general body mass prediction equations from footprint size. We also investigate the effects of body shape on body mass prediction, using BMI as a shape index. While another body shape parameter such as bi-iliac (maximum pelvic) breadth/stature (Ruff, 1994) might have been preferable for this purpose, body breadth data were only available for one of our five modern reference samples, precluding such an analysis. Also, the number of earlier (pre-Late Pleistocene) hominin specimens with stature estimates and associated bi-iliac breadths is exceedingly small. In contrast, stature and body mass data were available for our entire modern sample and can be estimated from skeletal dimensions in a number of early hominin taxa. It should also be noted that BMI and bi-iliac breadth/stature are positively correlated among modern humans, as would be expected: $r = 0.60$, $p < 0.001$ [based on 58 sex-population means given in Ruff (1994) and Ruff et al. (2005)]. While using an index that itself contains body mass as a factor in estimating body mass may seem circular, in fact, as illustrated in the examples below, this shape index can be derived independently using skeletal estimates of body mass and stature in other related specimens, and then applied as an average taxon/population value within

estimation formulae. Further considerations in using this approach are included in the Discussion section.

We also investigate ontogenetic effects on foot scaling to body mass, using 50 juveniles drawn from the same modern samples, and develop a method for predicting body mass from footprint size in children and adolescents. In addition, we include a comparison between habitually unshod and shod individuals from the same population to assess the effects of shoe wearing on body mass prediction and develop a conversion factor for application of our formulae to habitually shod individuals. Finally, to demonstrate application of the new prediction equations, we apply them to five hominin footprint samples spanning from the Pliocene to early Holocene.

2. Materials and methods

2.1. Reference samples

The five habitually unshod samples used to develop body mass estimation equations are listed in Table 2, along with basic descriptive statistics on anthropometric dimensions. The samples encompass a wide range of body sizes and shapes, with adult individual values of body mass varying between 36 and 99 kg, stature 135–192 cm, and BMI 15.7–32.3. Four of the five samples also include juveniles.

Data for the Machiguenga sample were collected by Tuttle and colleagues in 1988 (Tuttle et al., 1990). The Machiguenga live in the Amazon jungle region of southeastern Peru and have a subsistence strategy combining hunting-gathering with horticulture. Footprint trails recorded using Shutrak pressure-sensitive paper, and anthropometric dimensions were obtained.

Hatala and colleagues collected data for the agro-pastoralist Daasanach tribe, near Ileret, Kenya in 2011-2012 (Hatala et al., 2016c). This was an expanded sample of the same tribe included in an earlier footprint study (Dingwall et al., 2013). Data obtained included anthropometric dimensions as well as footprint dimensions (in a re-hydrated substrate taken from a nearby Early Pleistocene site containing hominin footprints (Bennett et al., 2009)) and pressure-pad parameters taken while walking and running.

The Pumé (formerly Yaruro), hunter-gatherers who also practice some horticulture and inhabit savannah wetlands of southwestern Venezuela, were studied by Hilton and Greaves in 1993 as part of Greaves' 18-month ethnoarchaeological project (Hilton and Greaves, 2008). Both anthropometric measurements and footprint data (in a thin sandy layer over hard-packed dirt) were collected (Hilton, n.d.).

Data for the Hadzabe, hunters and gatherers from the Mang'ola game controlled area (Kisimangeda, Barazani, Gorfan and Chem Chem) within the Lake Eyasi Plateau in north-central Tanzania, were collected by Musiba, Hallgrimsson and Tuttle in 1997 (Musiba et al., 1997). They obtained both anthropometric and footprint measurements (using Shutrak). Among the 54 individuals included in the study, five reported that they had occasionally worn footgear (thongs).

Samoan data were collected by R. Wunderlich in 2015 at the Samoan Rugby Union in Apia, Samoa. Subjects were young (mean age 21.8 years) healthy athletes who grew up primarily barefoot or minimally shod and started wearing footwear daily only for sport participation. Data collected included anthropometric dimensions as well as plantar pressure distribution on a Novel EMED/E plantar pressure mat (Novel GmbH, St. Paul).

Ages of subjects included in the study samples ranged from 4 to 70 years. Investigation of ontogenetic trends, presented in Results, indicated that foot area shows a different scaling relationship to body mass in juveniles than in adults, with the normal adult proportion reached at about 16 years of age (also see Anderson et al., 1956). Therefore, the sample was divided into juveniles (under 16 years) and adults (16 years or over) for all analyses. No juveniles were available for the Samoan sample. No consistent age trends in foot area to body mass proportions were discernable among adults, so they are combined in analyses. Except for Samoans, mean ages of adults in all samples varied between 27 and 36 years, with only 10% (19 of 193 individuals) over 50 years of age. (Some Daasanach adults were only recorded as 'adult', so there may have been a few more individuals over 50 years of age in that sample.) As noted above, Samoans were younger, ranging in age between 17 and 33 years.

Although some sex effects on relative foot size and shape have been described (Ashizawa et al., 1997; Wunderlich and Cavanagh, 2001; Bennett and Morse, 2014), most of these studies were of habitually shod individuals, so may have been affected by cultural differences in footwear. Many of the effects also appear to be population-specific (Ashizawa et al., 1997; Bennett and Morse, 2014). Wunderlich and Cavanaugh (2001) found no sex difference in forefoot breadth relative to length, the most relevant foot shape variable for the present study, and Atamtürk and Duyar (2008) reported only a very minor effect of sex on prediction of body mass from footprint dimensions. In any event, it is often difficult or even impossible to determine sex from footprints, making application of sex-specific equations impractical. Therefore, sexes were combined in all analyses.

2.2. Dimensions

As is evident from the description of present study samples as well as the earlier review of previous studies, there are a number of ways of assessing foot or footprint size. Not all of the five unshod samples included here have associated footprint data, and in those that do, footprints were obtained and measured in different ways—under naturalistic conditions on a soft substrate, on a thin layer of sand over a hard surface, on pressure-sensitive paper on a hard surface, or using plantar pressure pads—which can affect dimensions (see above). Also, while the ultimate aim of this work is to apply our findings to hominin footprints that were all formed and preserved in soft substrates, those footprints themselves would have been made under different environmental conditions, which must be factored into interpretations (D'Août et al., 2010; Crompton et al., 2012; Bates et al., 2013; Morse et al., 2013; Bennett and Morse, 2014). Thus, we elected to focus initially on foot dimensions, measured anthropometrically, and their relationship to body mass, since these were consistently measured across all studies and should be universally applicable. Equations for converting footprint to foot dimensions were derived from the matched Daasanach data, where footprints were collected under naturalistic conditions (of a particular kind). These equations are presented to allow conversion of footprint data for use in our prediction equations, although the decision on how to convert data will rest with individual researchers, depending on the particular environmental circumstances of their footprint data set.

Foot dimensions were obtained by measuring the relaxed (i.e., not weight-bearing) (Machiguenga, Pumé, Hadzabe) or partially weighted foot during bipedal standing (Daasanach, Samoans), using standard anthropometric techniques (Cameron et al., 1981). The average difference between foot length and breadth measured under these two conditions is 3% or less (Tsung et al., 2003; Houston et al., 2006; Xiong et al., 2009). Two specific dimensions were used

here: foot length, measured as the maximum distance between the heel and front of the foot (whether that was the hallux or second toe), and forefoot breadth (hereafter 'foot breadth'), measured as the maximum distance across the metatarsal heads, or ball of the foot. Following Dingwall et al. (2013), we took the product of these two dimensions as 'foot area'. Foot area was always a better predictor of body mass (i.e., had a lower standard error of estimate and higher correlation) than either foot length or breadth alone, similar to findings of Dingwall et al. (2013) for Daasanach footprints. Thus, we focus here primarily on foot area. However, equations using just foot length or breadth are also given for applications where both dimensions may not be available. Foot 'index'—(foot breadth/foot length) × 100—was also calculated as an index of general foot shape. When both right and left feet had been measured, an average of the two sides was used in all analyses.

For development of footprint to foot size conversion factors, maximum footprint lengths (to either the hallux or second toe) and forefoot breadths obtained from an experimental study of the Daasanach sample moving over a natural substrate (Hatala et al., 2016c) were employed. Multiple footprints were averaged for 'normal walk' and for a combined 'jog and run' condition. Anthropometric dimensions had been taken on only the right side, so only right footprints were used in these comparisons. This limited the available sample to 34 individuals (26 adults, 8 juveniles) for 'normal walk' and 40 individuals (29 adults, 11 juveniles) for 'jog and run'. Adults and juveniles (under 16 years) did not differ in foot to footprint proportions (t tests, $p > 0.05$, all comparisons; also see SOM Figs. S2–S3), so were combined.

Ratios of foot to footprint dimensions are given in Table 3 for the 'normal walk' and 'jog and run' conditions. Scatterplots of area, length, and breadth for each condition are shown in

SOM Figs. S2a-f, and for foot index in SOM Fig. S3. Paired t tests were used to test for significant ($p < 0.05$) differences between foot and footprint dimensions, indicated in the table.

The average ratios given in Table 3 were used as conversion factors for fossil/archaeological footprints, but only when differences were significant in the Daasanach sample between footprint and foot dimensions. In other cases, the two dimensions were considered to be equivalent. Thus, for example, no conversion was used for foot/footprint area in the 'normal walk' condition, while a conversion would be used for this dimension in the 'jog and run' condition. The 'normal walk' condition was assumed for all prints or trackways considered here.

2.3. Habitually shod comparisons

For this analysis we used data derived from a study of footprint dimensions, measured using a pressure plate (RSscan Footscan), in three samples: habitually unshod Indians ($n = 69$), habitually shod Indians ($n = 138$), and habitually shod Europeans ($n = 48$) (all adults) (D'Août et al., 2009). Unshod Indians had never used footwear, except in extremely rare circumstances as an adult, e.g., when visiting a hospital. The degree of footwear use and constraint in the shod Indians was generally less than that of the European sample, with subjects walking mostly barefoot as children and as adults in the house, and many using flip-flops or open sandals. In addition to foot length and breadth, true foot contact area was measured from the pressure plate recordings. This allowed some comparisons between true contact area and our length × breadth 'area' dimension.

2.4. Applications of equations

To demonstrate use of the new body mass estimation equations, they are applied to data derived from five published studies of fossilized or archaeological hominin footprints, listed in Table 4. The samples represent a wide variety of time periods, taxa (or probable/possible taxa), and geographic areas. The following is a brief description of each sample; for more information the reader is directed to the references cited.

Laetoli The trackways discovered at Site G in Laetoli, Tanzania, dated to about 3.66 Ma, are the most famous footprints in the hominin fossil record and have been the subject of many analyses since they were reported in 1979 (Leakey and Hay, 1979; Day and Wickens, 1980; White, 1980; Charteris et al., 1981; Robbins, 1987; Tuttle, 1987; White and Suwa, 1987; Tuttle et al., 1990; Schmid, 2004; Raichlen et al., 2010; Crompton et al., 2012; Bennett et al., 2016; Hatala et al., 2016a). Three trails attributed to *Australopithecus afarensis*, G1, G2, and G3 (G2 and 3 overlapping), have been described. More recently, two trails from Site S at Laetoli—S1 and S2—were described and attributed to the same taxon, and possibly the same depositional layer (Masao et al., 2016). The one S2 footprint exhibits distortion in the width dimension, possibly due to slippage or taphonomic factors, so only its length is used here. Average footprint dimensions for both the G and S Site trails were obtained from Masao et al. (2016: Table 3). Body masses were derived in that study using equations based on an experimental study of the Daasanach (Dingwall et al., 2013), termed the '*H. sapiens*' method, as well as a range of fleshy foot length to body mass ratios based on reconstructions of A.L. 288-1 (Jungers, 1982; White and Suwa, 1987; Jungers, 1988a, b; McHenry, 1992), termed the '*Au. afarensis*' method. The trackways have traditionally been considered to have been made by adults, although the smaller G1 and G3 trackways may have been produced by juveniles (Masao et al., 2016). For the present purposes they are provisionally treated as adults (also see Discussion).

Ileret Hominin trackways near Ileret, Kenya, have been excavated and analyzed since 2005 (Bennett et al., 2009; Dingwall et al., 2013; Hatala et al., 2016b; Roach et al., 2016; Hatala et al., 2017; Roach et al., 2018; Villmoare et al., 2019). Dated to about 1.51–1.53 Ma, they have usually been provisionally attributed to *Homo erectus*. Body mass estimates for an increasing number of prints and trackways have been derived based on experimental studies of the Daasanach (Bennett et al., 2009; Dingwall et al., 2013; Hatala et al., 2016b) and A.L. 288-1's proportions (Dingwall et al., 2013). The most recent compilation of trackways and individual footprints for the FwJj14E and ET-2013-1A/ET-2014-1A sites given in Hatala et al. (2017: SOM Table S1) was used here, along with data for two additional A2 surface prints reported in Dingwall et al. (2013: Table 4). The main focus is on the nine established trackways, although data for the remaining 22 individual prints are also considered. Only prints with both length and breadth measurements were included. Mean dimensions for all prints within a trackway were used in analyses. All trackways are assumed to have been made by adults, as foot areas (length × breadth) were over 210 cm^2 (and all but one were over 235 cm^2), well within the range of the modern adults in our reference samples (except for Samoans; Table 2). Six of the individual prints not in trackways were smaller than this, so may have been made by juveniles; this is discussed further below. Both the '*H. sapiens*' and '*Au. afarensis*' methods described above were used by Dingwall et al. (2013) to estimate body masses. Hatala et al. (2016b) estimated body masses using a random forests model, based on Daasanach experimental data, that included heel-to-hallux and heel-to-2nd toe lengths, forefoot and heel breadths, and average footprint depth.

Happisburgh A series of oval depressions interpreted as hominin footprints, dated to about 0.78–1.0 Ma, were reported in estuarian sediments from Happisburgh, UK by Ashton et al. (2014).

Given the time period, geographical location, and general body size indicated by the prints, the authors favored a possible attribution to *Homo antecessor*. A recent morphological analysis of the prints is consistent with this attribution, finding them to be similar to the presumed *H. erectus* tracks from Ileret, but with some falling closer to modern *H. sapiens* (Wiseman et al., 2020). Ashton et al. (2014: Table 1) provided quantitative information for 12 prints with the most complete outlines. Of these, only the three largest, with estimated statures of >140 cm, were considered to be adults by the authors. These individuals have foot areas of ≥240 cm^2 (while the other nine have foot areas of ≤180^2), so this interpretation is consistent with our data (Table 2). Only these three prints are analyzed here. Body masses were estimated by the authors using Dingwall et al.'s (2013) equations based on the Daasanach.

Le Rozel Hundreds of footprints dated to about 80,000 BP and attributed to archaic *Homo sapiens* (Neandertals) have been discovered at the site of Le Rozel on the Normandy coast of France (Duveau et al., 2019). Here we focus on the 35 most complete footprints from the D3b-4 stratigraphic unit preserving measurable lengths and forefoot breadths (Duveau et al., 2019: Fig. S19 and Duveau, pers. comm.). Although some of these may have been made by the same individual, none are definitively associated (Duveau, pers. comm.), so are treated as separate data points for the present analyses. Footprint length was measured to the 2nd toe and forefoot breadth on a line perpendicular to the heel-2nd toe axis. The average ratio of maximum/heel-to-2nd toe footprint length in our Dasaanach sample (all ages combined) is about 1.02. Consideration of the average angle between the perpendicular and true maximum forefoot breadths in Duveau et al., Fig. S17 (also see Robbins, 1985: Fig. 6.8; Webb et al., 2006: Fig. 4) also suggests a ratio between maximum and perpendicular breadths of about 1.02. Thus, footprint lengths and breadths reported by Duveau et al. were multiplied by 1.02 to approximate the maximum

dimensions used in our study. The 35 footprints from Le Rozel represent a variety of body sizes and likely ages, with a great majority probably made by children and adolescents (Duveau et al., 2019). This provides an opportunity to apply results from our ontogenetic study of modern humans; accordingly, both juveniles and adults from this site are included in our analyses.

Barcin Höyük Barcin Höyük is an early Neolithic settlement in northwestern Turkey dated to about 6400 BCE (Atamtürk et al., 2018). Two footprints impressed within a freshly plastered floor were found; dimensions for the well-preserved right footprint were reported (Atamtürk et al., 2018: Table 1). Although the footprint was made by a bare foot, it is very likely, based on other regional evidence, that occupants of the site habitually utilized footwear, and that the maker of these prints either customarily went barefoot indoors, or removed his/her shoes in this case for symbolic reasons. Thus, an adjustment for a habitually shod condition (using the shod/unshod Indian data from D'Août et al., 2009) was employed here. Body mass was estimated by the original authors using equations from Krishan (2008) and Atamtürk and Duyar (2008).

2.5. Statistics

Least squares regression was used to generate body mass estimation equations in the modern reference samples. Model II regression, in particular Reduced Major Axis (RMA) regression, has been advocated for predicting body mass when the predictor variable in the target sample lies outside the range of the reference sample (Squyres and Ruff, 2015; Ruff et al., 2018; Ruff et al., 2020). However, that is not the case here: adult foot areas in the combined modern reference sample range between 137 and 360 cm^2, while the total range of all adult target samples is 162–360 cm^2. Our combined juvenile reference sample has foot areas of 93 to 268 cm^2, encompassing all but one of the Le Rozel juvenile prints. In addition, as shown below, the

most appropriate estimation equations involve multiple predictor variables or a quadratic fit, neither of which is amenable to RMA analysis.

Precision of the estimation equations was assessed using the standard error of estimate (SEE), percent standard error of estimate [%SEE: (SEE/mean y) × 100], and the mean percent prediction error, %PE: [(actual y – predicted y)/predicted y] × 100, with %PEs taken as absolute values to reflect random error. Analysis of covariance (ANCOVA) was used to assess differences in slopes and elevations of linear regressions, and analysis of variance (ANOVA) and post-hoc pairwise Tukey tests were used for comparisons of indices between groups. Significance was set at $p < 0.05$. All statistical analyses were carried out using SYSTAT (SYSTAT13, 2009).

3. Results

3.1. Prediction of adult body mass

A scatterplot of body mass against foot area in the total combined adult sample is shown in Figure 1. The data distribution is better fit by a quadratic rather than linear regression: the correlation and %SEE of body mass from foot area are both improved using a quadratic fit (r = 0.861, %SEE = 13.7%) relative to a linear fit (r = 0.831, %SEE = 14.9%; this is also true for foot length and foot breadth). Quadratic prediction equations for foot area, foot length, and foot breadth are given in the first half of Table 5. Average %PE using foot area is about 10%.

The pooled sample is broken down into the five reference samples in Figure 2, with linear regressions plotted through each sample (quadratic equations do not improve fit within populations). It is apparent that the different samples show systematic variation in their relationships between body mass and foot area. All regressions are highly statistically significant

($p < 0.0001$), with correlations ranging between 0.67 and 0.83. Slopes are equivalent between samples ($p = 0.40$, ANCOVA), but elevations are highly significantly different ($p < 0.0001$, ANCOVA). Elevational differences follow patterns of variation in BMI (Table 2), with Samoans highest, followed by Machiguenga, Pumé and Hadzabe, and Daasanach. Thus, populations with higher BMIs have systematically larger body masses for their foot areas (or smaller feet for their body masses). Very similar results are obtained for body mass regressed against foot length or foot breadth (results not shown). This suggests that incorporating BMI into body mass prediction equations based on the entire pooled reference sample will improve prediction accuracy.

This has been done in the second half of Table 5, which lists prediction equations for the pooled reference sample based on foot area, foot length, and foot breadth in multiple linear regressions that include BMI. Correlations are quite high (r = 0.949–0.965), as are measures of prediction precision, with SEEs of 4.0–4.8 kg, %SEEs of 7.0–8.4%, and average %PEs of 5.4–6.7%. Of course, in practice the true precision (and accuracy) of the equations will not be as high as this, since BMI must be estimated in the target specimen/sample. As shown in section 4.4., there are various ways of doing this, but they all involve additional error. The effects of this are discussed further in the Discussion section.

We also explored whether variation in foot index (breadth/length) could help predict BMI in footprint makers, for example, whether relatively wider-bodied (higher BMI) individuals or samples have relatively wider feet. Figure 3 is a plot of BMI against foot index in the reference samples. Within the pooled sample there is a general correspondence between the two indices, but the correlation is low (r = 0.385) and there is very large variation in BMI for a given foot index in the central part of the distribution. For example, foot index values for Samoans and Machiguenga are similar, but Samoans have much higher BMIs. Daasanach have higher foot

index values than Hadzabe on average, but lower BMIs. Except for the Daasanach, none of the individual samples show significant within-sample correlations between foot index and BMI. Thus, foot index has only limited value as a predictor of BMI, or body shape, except perhaps at more extreme values for foot index. The conservative interpretation of the distribution shown in Figure 4 is that individuals or samples with foot indices in the lower quartile (below 38) are unlikely to have high BMIs (above 23), while those with foot indices in the higher quartile (above 42) are unlikely to have low BMIs (below 20). Foot indices in the middle two quartiles (38–42) are relatively uninformative in this respect. These results are referenced when considering possible BMI values for our five fossil footprint examples (SOM S1).

3.2. Ontogenetic trends

The ratio of foot area to body mass distinguished by age group is shown for each sample in Figure 4 (note that there are no juvenile Samoan data, so Samoans are not included). Juveniles have relatively larger feet than adults in all samples ($p < 0.001$, t tests). The general pattern of variation between samples is similar in adults and juveniles, although as shown below, these patterns are also affected by the age composition of each juvenile sample.

The Machiguenga and Daasanach samples have the best representation of juveniles, with 12 or more individuals distributed over a wide age range (6.7–15.9 and 4–15 years, respectively) (Table 2). Linear regressions of body mass on foot area by age group are shown in Figure 5 for these samples. As predicted given the results shown in Figure 5, juveniles as a whole have smaller body mass relative to foot area in each sample. However, regression slopes are also significantly different between adults and juveniles, with juveniles having higher slopes ($p < 0.001$, ANCOVA). Proportions change throughout development, approaching and sometimes

overlapping adults in adolescence. The same difference in proportions (line elevations) between Machiguenga and Daasanach adults ($p < 0.0001$, ANCOVA; see also Fig. 2) is also characteristic of juveniles throughout development ($p < 0.0001$, ANCOVA), while regression slopes for juveniles are very similar in the two groups ($p = 0.77$, ANCOVA). This indicates similar developmental trajectories and an early developmental origin of proportional differences between the samples.

The different foot to body size proportions in juveniles and adults may be partially attributable to earlier maturation of the foot than some other regions of the skeleton. Krogman (1962: Table 3) gives the age of epiphyseal fusion of the foot phalanges and metatarsals as 14–16 years; Scheuer and Black (2000) state that 75% of females and males complete epiphyseal fusion of the foot bones by 15 and 17 years, respectively. In contrast, fusion of the knee epiphyses (proximal tibia and distal femur) occurs later, at 17.6–18.6 years in Krogman (1962: Table 6), with 75% completion of fusion at age 19 years in McKern and Stewart's summary (for males) (1957: Table 21). Cross-sectional and longitudinal studies clearly show that peak growth velocity and cessation of growth occur earlier in foot length than in stature (Anderson et al., 1956). Thus, adults have slightly greater stature to foot length proportions, or smaller foot length/stature proportions, than juveniles (Anderson et al., 1956), as also found here for foot area/body mass proportions.

However, the primary factor accounting for age differences in body mass to foot size proportions is likely to be systematic age changes in body shape, i.e., BMI. Figure 6 shows age changes in BMI in the pooled sample (except Samoans). Daasanach adults of uncertain age are not included. A LOWESS line (Cleveland, 1979) is plotted through the data to demonstrate overall trends. Juveniles progressively increase in BMI throughout growth, to about 20 years of

age. In a 2-way ANOVA of BMI with age group and sample as factors, age group is highly significant ($p < 0.0001$), and BMI is lower in juveniles than in adults in every sample ($p \leq 0.01$, t tests).

Because of the relatively thinner bodies (lower BMIs) of juveniles, equations based on adults will systematically overestimate their body masses, with the greatest overestimation in younger children and progressively less bias in older children and adolescents, as shown in Figure 5. Because of this age-dependence of the relationship, body mass prediction equations based on juveniles alone are impractical, since they would rely on knowing either the specific age of the individual or its BMI, both of which are difficult or impossible to estimate from footprints. As an alternative, we suggest initially using equations based on adults (Table 5), and then adjusting the resulting estimates downwards based on the size of the juvenile's foot relative to that of an average adult of the same sample. Figure 7 shows plots of actual body mass/body mass estimated from adult equations against actual foot area/average adult foot area for that sample, pooled over all samples. The latter ratio used sex-specific values, given the smaller feet of adult females relative to males. Results for both the multiple regression equation using the quadratic equation and the equation incorporating BMI (in this case the average BMI for that sample) from Table 5 are shown.

The relationship between foot size relative to adults and overestimation of body mass using adult equations is relatively strong (r = 0.747–0.799). Least squares prediction equations are given in the plots. Applying the method requires knowledge of adult footprint size values for the sample in question, but that is likely to be the case in the vast majority of situations, in part because without presumed adult footprints it is difficult to identify which footprints in a sample are likely to be juvenile. To give an example of how to use this method, consider a juvenile foot

area that measures 145 cm^2, in a sample where the average adult foot area is 200 cm^2. Using the generic adult quadratic equation (1) in Table 5, the initial body mass estimate for the juvenile is 43.7 kg. The ratio of actual/average adult foot size is 145/200, or 0.725, which, when entered into the formula in Figure 7b, gives a body mass adjustment factor of 0.588, and a final body mass estimate of 43.7 × 0.588 = 25.7 kg. Note that while this estimate can be referred to as 'age-adjusted', in fact, no estimate of age per se is required—only the relative size of the footprint compared to those of adults. Of course, where to draw the adult/juvenile boundary for any preserved footprint sample will always be somewhat arbitrary, but this method should produce more accurate results than simply using adult-derived equations on all individuals in a mixed-age group. Further examples are given below in the analysis of the Le Rozel sample (section 4.4.).

3.3. Habitually shod comparisons

Figure 8 shows the ratio of foot area (length × breadth) to body mass in the habitually unshod Indian, shod Indian, and shod European samples studied by D'Août et al. (2009). Unshod Indians have significantly larger feet relative to body mass than shod Indians, and both are significantly larger than shod Europeans (ANOVA $p < 0.0001$; all pairwise differences $p < 0.01$). Variation in BMI between the samples is not a factor, as they do not vary significantly in this regard (ANOVA and all pairwise differences $p > 0.50$). The average difference in foot size for a given body mass between shod and unshod Indians is 8%; the average difference between shod Europeans and unshod Indians is 22%. Given the likely nature of footwear in prehistoric samples, the comparison between shod and unshod Indians is probably more relevant to interpretations of archaeological footprints. Thus, the area of (bare) footprints made by habitually shod individuals in an archaeological context can be converted to equivalent foot areas of

habitually unshod individuals by multiplying by 1.08, prior to application of body mass estimation formulae, as illustrated below for the Barcun Höyük sample.

Our earlier finding that higher BMI individuals have smaller feet relative to body mass suggests that either stress on the plantar surface of the foot increases with increasing BMI, or that there may be compensatory mechanisms to reduce increases in stress. One of these may be to increase the actual contact area of the foot with the substrate relative to the overall dimensions of the foot. Because true foot contact areas were also determined in the original study (D'Août et al., 2009), we can evaluate this possibility by assessing variation in the ratio of actual contact area/our 'area' (length × breadth) measurement relative to BMI. This has been done in Figure 9 for the habitually unshod Indian sample. The correlation between relative foot contact area and BMI is only moderate but highly significant ($r = 0.46$, $p < 0.0001$). Correlations are lower but still significant for the habitually shod Indian and European groups ($r = 0.31$, $p < 0.001$ and $r = 0.38$, $p < 0.01$, respectively). Thus, there is some evidence that higher BMI is associated with relatively greater contact area of the foot, and this is most strongly expressed in habitually unshod individuals.

A summary of the steps involved in estimating body mass from footprint size is given in Table 6. Two flowcharts—one for adults, and one for juveniles—are provided.

3.4. Fossil Applications

Laetoli Table 7 gives body mass estimates for the five Laetoli trackways using the equations in Table 5 based on foot area (length × breadth), except for S2, where foot length was used. Estimates using the generic quadratic equations (1 and 2) range between 44 and 64 kg. Based on skeletal estimates for A.L. 288-1 and other *Australopithecus afarensis* specimens, an average

BMI of 25 is assumed for this taxon (see explanation in SOM S1). Estimates using this value in the BMI equations (4 and 5) range between 51 and 71 kg, and are higher, by an average of 18%, than those using the quadratic equation. Previously published body mass estimates from Masao et al. (2016) are also listed in Table 7. Both the '*H. sapiens*' and '*Au. afarensis*' methods (Dingwall et al., 2013) produce lower estimates than those of the present study. In particular, estimates using the second method, favored by Masao et al., average 40% and 65% lower than our quadratic and BMI-based estimates, respectively (using midpoints of ranges given by Masao et al. (2016). Previous estimates using the '*H. sapiens*' (Daasanach) regression are closer to ours, averaging 12% (quadratic) and 32% (BMI) lower.

Given that the foot size to body size proportions of *A. afarensis* may have varied significantly from those of modern humans (Jungers, 1988a; Masao et al., 2016), we also explored foot to body size proportions in chimpanzees and, following Dingwall et al. (2013) and Masao et al. (2016), A.L. 288-1. Footprint maximum length and breadth across the metatarsal heads were measured on two male adolescent chimpanzees (*Pan troglodytes*), 6.5 and 6.9 years of age and 30.7 and 27.8 kg, walking bipedally over a substrate similar to that used for the Daasanach experiments (Hatala et al., 2016a). As with the modern human footprints, foot area (length × breadth) was considered to be equivalent to footprint area, based on the results shown in Table 3. Because of likely age effects on foot size/body size relationships in chimpanzees as well as humans (see SOM S1), we compared the chimpanzees to juvenile humans of a similar developmental age – 10 to 15.9 years, i.e., late childhood through mid-adolescence (from just before to just after M2 eruption—see Smith, 1991; Smith et al., 1994), derived from our pooled sample (n = 34).

Results of the comparison are shown in Figure 10. The chimpanzees have very large feet relative to body mass compared to humans of a similar developmental age – 3.6 and 5.5 standard deviations from the mean foot/area body mass ratio for our human juveniles (Fig. 10a). Consequently, using a regression based on the juvenile human sample would overestimate body mass in the two chimpanzees by 52% and 78% (Fig. 10b). Thus, if *A. afarensis* had feet that were intermediate in relative size between chimpanzees and modern humans, body masses would be overestimated by some amount within this range if a human reference sample were used.

Figure 11 shows a comparison of foot length relative to stature in our modern human adult and juvenile samples, A.L. 288-1, and the two juvenile chimpanzees (for details on foot length reconstruction for A.L. 288-1, see SOM S1). A stature of 107 cm was used for A.L. 288-1 (Jungers, 1988a). Least squares regressions are plotted through our pooled modern human adult and pooled juvenile samples. An additional modern human adult data point for a small Akka female skeleton whose articulated stature and foot length were reported by Flower (1889) is also included (for details see SOM S1). As shown earlier for foot area, foot length in modern human juveniles is longer relative to stature than in adults, converging with adults in older juveniles. Chimpanzees have foot length/stature proportions that are high for human juveniles as a whole, although close to some younger juveniles (the four human data points lying closest to the chimpanzees are from individuals 6–10 years old). The Akka individual falls almost exactly on a projection of the regression line through our other adult humans. A.L. 288-1 falls above the human juvenile regression and well above the human adult regression, including the Akka individual. It is closer in proportions to our two chimpanzees than to human adults, and about equidistant between chimpanzees and human juveniles. This is probably a conservative comparison, since it is likely that chimpanzee adults have smaller foot length to stature

proportions than chimpanzee juveniles, i.e., even more like those of A.L. 288-1. Thus, A.L. 288-1 has relatively long feet compared to modern human adults, approaching those of chimpanzees.

A similar direct comparison of foot area and body mass is not possible for A.L. 288-1, given lack of a foot breadth reconstruction for the fossil. However, if the average foot index value of 45.8 for the four Laetoli trackways with a preserved breadth is applied to A.L. 288-1's foot length estimate, a breadth value of 7.8 cm is obtained, giving a foot area of 132.6 cm. Figure 12 is a plot of body mass against this foot area in A.L. 288-1 and our modern adult combined sample fit with the quadratic regression. A.L. 288-1's body mass is overestimated by 50% using this regression, and by 72% using the BMI-based formula (Table 5). These are close to the overestimates of body mass in our two chimpanzees using an age-appropriate modern human sample (Fig. 10b). They are also very similar to differences between the present body mass estimates for the Laetoli sample based on modern humans and those derived by Masao et al. (2016) using the '*Au. afarensis*' body mass/foot length method, especially for the two smallest Laetoli trackways (G1 and G3), with average differences of 50% and 73% for quadratic and BMI-based methods, respectively. This is not surprising, given that both results are based on the proportions of A.L. 288-1.

Thus, application of any body mass estimation equation based on modern humans to *A. afarensis* footprints is highly questionable. Masao et al. (2016) attempted to address this problem by using a range of ratios between foot length and body mass for A.L. 288-1 (Dingwall et al., 2013) to predict body mass for the Laetoli footprints. However, as discussed further in the Discussion, there are both statistical and mechanical arguments against using a ratio between foot length and body mass to estimate body mass.

Here, we derive a new ratio method for estimating body mass in *A. afarensis* based on estimated foot area and body mass for A.L. 288-1. Using a body mass of 28.9 kg (Ruff et al., 2018), and a foot area of 132.6 cm, a ratio of body mass/foot area of 0.218 is obtained. This is applied to the five Laetoli trackways in Table 8. Foot area for S2 was derived using its foot length (Table 7) and the average Laetoli foot index of 45.8. As discussed further below, body mass estimates using this technique seem reasonable when compared to those derived for *A. afarensis* from lower limb articular size (Ruff et al., 2018).

Ileret

Footprint dimensions and body mass estimates for the Ileret sample are given in Table 9 for the nine trackways described in Hatala et al. (2017) plus the A2-I2 and I3 prints described by Dingwall et al. (2013), together with body mass estimates presented in these previous studies. Given the general similarities in body proportions between early *H. erectus* (KNM-WT 15000) and modern humans (Walker and Leakey, 1993), only the '*H. sapiens*' results from Dingwall et al. (2013) are shown. Results for all trackways and isolated prints are given in SOM Table S1. For trackways with multiple prints, foot area was calculated separately for each print and then averaged, with the average used to calculate body mass. Thus, average foot areas shown in the tables for these individuals may not correspond exactly to calculations based on average print length and breadth. Based on skeletal reconstructions of KNM-WT 15000 (see SOM S1), a BMI value of 24.0 is assumed for BMI-based estimates of body mass.

Both the quadratic and BMI equations (Table 5) produce body mass estimates that are higher than previous estimates based on the Daasanach sample (Dingwall et al., 2013), averaging 21% higher using the quadratic equation and 31% higher using the BMI-based estimates. Differences are greater between our estimates and those of Hatala et al. (2016b) (for a different

subsample of footprints), averaging 32% and 41% higher using our quadratic and BMI equations, respectively. However, where they overlap, Dingwall et al.'s and Hatala et al.'s estimates are generally very similar, except for higher estimates in Dingwall et al. (2013) for FLT1 and FUT2. These results are influenced by different average footprint dimensions recorded for these two trackways in the two studies, in part because of discovery and association of additional prints (FUT2) as well as reevaluation of existing prints (FLT1), both of which led to slightly smaller average dimensions in the later study. Thus, taking this into account, the two Daasanach-based sets of estimates are quite close, as would be expected. Including all of the isolated footprints as well as trackways (SOM Table S1) reduces the difference between the present and Hatala et al. (2016b) estimates somewhat, with average differences of 22% and 36% for quadratic and BMI equation results, respectively.

As mentioned earlier, six of the Ileret trackways or prints have relatively small foot areas (<200 cm^2), which, however, still overlap extensively with our smaller modern adult reference samples (Machiguenga and Pumé; Table 2). The issue of how to distinguish juvenile footprints is addressed more extensively below. However, it is worth noting here that one of the smallest Ileret footprints, FU-X (169 cm^2; see SOM Table S1), noted as possibly juvenile by Hatala et al. (2016b), produces the largest difference of any individual between body mass estimates using their method and the present methods (77–99% larger in the present study). This further emphasizes the importance of taking developmental stage into account when applying body mass estimation equations.

Happisburgh Footprint and foot dimensions and body mass estimates for the three large adult prints from Happisburgh (Ashton et al., 2014) are given in Table 10, along with the original authors' body mass estimates, which were derived from Dingwall et al.'s (2013) equations based

on the Daasanach sample. Based on skeletal estimates for the Middle Pleistocene Sima de los Huesos sample (Carretero et al., 2012) and a sample of Neandertals, an average BMI of 27 is assumed here for the Happisburgh sample (see SOM S1 and SOM Tables S2 and S3).

Body mass estimates for the three adult Happisburgh prints using the generic quadratic equation (Table 5) range between 53 and 62 kg, which average 13% higher than Ashton et al.'s (2014) estimates (Table 10). Using the BMI-based equation with an assumed BMI of 27 produces estimates between 69 and 75 kg, averaging 43% higher than Ashton et al.'s estimates.

Le Rozel Dimensions of the 35 most complete Le Rozel footprints are given in Table 11, arranged in order from longest to shortest, which was used to determine age categories (from calculated statures) by Duveau et al. (2019). The three longest, which may belong to the same individual, were identified as adult by the original authors. The next 14 longest prints were tentatively assigned as adolescents, although the authors note that "the stature gap between adults and adolescents is small, and footprints placed near the limit between these two classes could be misclassified" (Duveau et al., 2019: 19412). To gain a better idea of the potential range of overlap in foot size between adults and adolescents, the percent difference between the minimum adult value and the mean adult value for foot area was calculated for each of our four modern reference samples that included juveniles. The mean was 75%, and all samples fell between 70% and 78%. Therefore, values for foot area down to 75% of the mean adult value were considered to be potentially made by smaller (typically female) adults. Distributions of foot area values for adults and juveniles in the two best represented living samples— Machiguenga and Daasanach— are shown in Figure S4.

The mean foot area of the three largest prints from Le Rozel is 319.9 cm^2. As shown by the original authors (Duveau et al., 2019) and in SOM S1, these prints were very likely made by

adult males, or possibly one male. To obtain an average foot area over both adult males and females, we again used our reference samples (in this case, all five, including Samoans) to calculate mean male/mean female values, which varied from 1.17 and 1.27 between samples, with a mean of 1.23. This produces a hypothetical mean adult female foot area value of 319.9/1.23 = 260 cm^2, and a pooled adult mean of 290 cm^2 for the Le Rozel sample. This value was used to calculate the juvenile/adult foot area ratio for juveniles or potential juveniles in the sample, to use with the equations in Figure 7 to adjust adult-based body mass estimates. We also consider any foot areas that are 75% or more of 290 cm^2 (i.e., ≥218 cm^2) to be potentially those of small adults (Fig. S4).

Using the generic quadratic equation (Table 5), the estimated average body mass of the three largest footprints is 81.4 kg (range 68–98 kg) (Table 11). Using an average BMI of 27, derived from a sample of 11 adult Neandertals (SOM S1 and SOM Table S3), the average estimated body mass for these prints is 83.7 kg, with a smaller range of estimates (78–90 kg). Five other 'adolescent' prints have estimated foot areas within the potential range of adults, i.e., within 75% of the estimated mean adult value. One of these—2017-103—has a foot area that overlaps with the three definitively adult values, because of its very wide foot (foot index 61.0). Adult body mass estimates for these five individuals range from 53.6 to 68.5 kg (quadratic method) and 69.4 to 78.3 kg (BMI method). If they are considered to be juveniles and adjusted downwards using the juvenile adjustment factor (Table 11), the ranges are 34.0–55.3 kg (quadratic) and 47.3–66.5 kg (BMI), averaging 25–29% lower than the adult estimates, with differences increasing with decreasing foot size (and likelihood of being an adult). Other 'adolescents' range between 19.2 and 31.1 kg (quadratic equation) and 28.6 and 44.3 kg (BMI equation), using the juvenile age adjustment. Estimates for children, with the age adjustment,

range from 5.8 to 28.5 kg (quadratic) and 8.2 to 26.5 kg (BMI). In all cases except the very largest print (2017-86), body mass estimates using the BMI method are larger than those using the generic quadratic method, with estimates averaging about 40% larger for adolescents and children.

To further explore age-related variation in body mass to foot area proportions, body mass or estimated body mass is plotted against foot area in the Machiguenga and Le Rozel samples in Figure 13. The Machiguenga plot (Fig. 13a) clearly demonstrates the large range of body masses associated with individuals with foot areas of about 135–155 cm^2, which corresponds to 75–87% of the mean adult value (Table 2). This group includes both female adults (16 years or older) and adolescents of both sexes (12–15.9 years). Thus, it is not possible to separate female adults from adolescents in this foot size range. The high variability in body mass relative to foot area in this size range is also due to the continuing increase in stature and body mass in late adolescence after foot growth has completed, as discussed earlier. The same pattern is evident in the plot for the Le Rozel sample (Fig. 13b)—the five intermediate-sized footprints (within 75% of the estimated mean adult value) could represent either late adolescents or female adults. Body mass estimates both with and without age-adjustment are shown for these specimens.

The overall shape of the two distributions in Figure 13 is strikingly similar, although the Machiguenga sample does not extend into as low a size (and implied age) range as the Le Rozel sample. The minimum age for the Machiguenga sample is 6.7 years (Table 2). Based on a comparison of foot length with that in a modern US ontogenetic sample (Anderson et al., 1956), the smallest Le Rozel footprint may have been made by a 1-year-old, and several were probably under 4 years of age. Whether our method for age adjustment of body mass values can be extrapolated to individuals that young is not certain, although the ‘growth’ curve in Fig. 13b for

Le Rozel looks reasonable. Adjusted body mass estimates using the BMI-based equation also seem reasonable for modern children with similar foot lengths. Anderson et al. (1956) did not report body masses for their sample, but such data are available for a closely matched sample (Anderson et al., 1965) measured by Reed and Stuart (1959). Modern children in the age range 1–4 years had body masses of 9.9 to 16.4 kg (average of males and females). This compares to adjusted body mass estimates for the five smallest Le Rozel individuals, whose foot lengths fall into the 1–4-year range in Anderson et al.'s (1956) study, of 8.2 to 19.6 kg, using the BMI method. Adjusted body mass estimates for these Le Rozel infants using the quadratic equation seem less reasonable (too small), varying between 6.2 and 13.3 kg. Unadjusted body masses for these individuals using either adult equation are all over 42 kg (Table 11), which are obviously much too high, illustrating the need for age adjustment when applying either method to juveniles.

Barcin Höyük Dimensions of the Neolithic footprint from Barcin Höyük are given in Table 12. Given the likelihood that this individual habitually wore shoes (Atamtürk et al., 2018), foot area was multiplied by 1.08 based on the difference between habitually shod and unshod Indians described in section 4.3 (D'Août et al., 2009). This is considered a more appropriate comparison than that between unshod Indians and shod Europeans, first, because it minimizes possible ethnic (genetic) effects, and second, because the footwear environment of the habitually shod Indians in D'Août et al.'s sample is likely to have been more similar to that of the inhabitants of Barcin Höyük.

Body mass estimates using the generic quadratic and BMI-based equations (Table 5) are given in Table 12, along with previous estimates by Atamtürk et al. (2018) based on a study of habitually shod Turkish subjects (Atamtürk, 2003; also see Atamtürk and Duyar, 2008) and (probable) habitually unshod Indians (Krishan, 2008, see above). Only the previous forefoot

breadth estimates, favored by the authors, are shown. A BMI estimate of 24 for the Barcin Höyük individual can be derived from stature and body mass estimates for a large skeletal sample from Çatalhöyük, another Turkish early Neolithic site that overlapped temporally (7100–5940 BCE) with Barcin Höyük (Larsen et al., 2019; Knüsel et al., 2021) (see SOM S1).

Estimated body mass using the generic equation is 55.6 kg, and using the BMI equation 63.5 kg. Both estimates are less than those using the modern Turkish (71.9 kg) and Indian (65.4 kg) equations, although the BMI-based estimate is close to the Indian-based estimate. Atamtürk et al. (2018) favored the higher Turkish estimate.

There are several factors that probably contribute to the differences in present and previous body mass estimates for this specimen. In both Atamtürk's (2003) and Krishan's (2008) studies, footprints were measured from water or ink on paper prints made while subjects were standing on a hard incompressible surface, which likely affects dimensions relative to either anthropometric foot measurements or measurements of footprints made in a deformable substrate (SOM Fig. S1).[2] Atamtürk's (2003) modern reference sample was habitually shod, which affects foot dimensions, as shown above. Another influence on these results is variation in BMI between the reference samples. The Turkish reference sample (combined sexes) had an average BMI of about 26 (Atamtürk and Duyar, 2008), while the average BMI of the Indian sample was likely much lower. Thus, the Turkish equation gives a higher estimate and the Indian equation a relatively lower estimate, although both are higher than our estimates. Based on results for the closely related Çatalhöyük sample, we would argue that a body shape for the Barcin Höyük individual intermediate between those of the modern Turkish and Indian reference samples is most likely. Our BMI-based estimate for the Barcin Höyük individual is quite close to the average body mass estimated for Çatalhöyük males of 63.9 kg (±4.6 SD) (Knüsel et al., 2021).

The 71.9 kg estimate favored by Atamtürk et al. (2018) is greater than all but three (94%) of the males from Çatalhöyük.

4. Discussion

4.1. Body Shape and Body Mass Estimation

Foot area (maximum length × breadth) is highly correlated with body mass in our pooled adult sample of 193 habitually unshod individuals. As a consequence, a quadratic equation based on foot area can predict body mass with an average %PE of about 10% in this sample. Similar equations based on just foot length or breadth have slightly greater associated errors. This method makes no assumptions about body shape and is theoretically applicable to any adult footprint.

However, there is also strong evidence that body shape significantly affects the relationship between foot size and body mass. Populations that are relatively heavier-bodied for their stature, i.e., have a high BMI, have relatively smaller feet. Thus, if information regarding body shape can be incorporated into prediction equations, prediction accuracy can be significantly improved. Multiple regression equations that include both foot size and an estimated BMI have %PEs of body mass that are only about half as large as those using generic quadratic equations. Of course, these prediction errors under-predict actual error when applied to fossil footprints, since BMI will not be known for the individuals making the prints. As shown in several examples, it is possible to estimate an average BMI for a taxon or population using estimates of stature and body mass derived from appropriate skeletal specimens, and then use this reference value in prediction equations for individual prints or trackways. There is significant uncertainty in such a procedure, however—BMI varies between individuals, even

within populations (coefficients of variation of BMI range between about 8 and 9% in our five living samples); skeletal estimates of stature and body mass in past reference individuals or samples are themselves subject to error; past reference individuals or samples are imperfectly matched, to varying degrees, with target footprint samples. Given these uncertainties, it is reasonable to ask whether use of the BMI-based equations is justifiable, i.e., whether they will actually improve body mass predictions.

One way to assess this is to compare body mass estimates calculated using a range of BMI values with those estimated using the generic quadratic equations. This has been done in Figure 14, using foot areas ranging from 140 cm^2 to 350 cm^2, the approximate total range of variation in our living adult sample (and encompassing virtually all of our adult fossil footprints) and a range of BMI values from 22 to 27, which includes the range of values that we assumed for our fossil footprints based on skeletal estimates from related individuals or samples. If we take the Ileret footprint sample as an example, where an assumed BMI of 24 based on the reconstructed body proportions of KNM-WT 15000 was employed, varying the assumed BMI by ±1 unit (from 23 to 25) results in an average change in estimated body mass of about ±4%; varying the assumed BMI by ±2 units (from 22 to 26) changes estimated body mass by about ±8%. The latter is less than the average %PE of the generic quadratic equation. Thus, moderate changes in assumed BMI do not have very large effects on body mass estimation.

Figure 14 also illustrates the effects of using the generic quadratic versus the BMI-based equations. The average BMI of our pooled living adult sample is 21.8. In most of the foot area range—up to 300 cm^2—the quadratic equation returns body mass estimates that are quite close (within ±8%) to those obtained using the BMI equation with an assumed BMI of about this magnitude (22 in Fig. 14). In other words, the quadratic equation produces estimates that mimic

the average body shape of the pooled modern sample, except in the largest footprint size range (> 300 cm^2), where it mimics the Samoan sample (average BMI = 27.4), which includes almost all the individuals with feet this large and thus drives the quadratic equation in this range. What this means is that the quadratic equations will be highly dependent on the body shape (BMI) of the reference samples, as well as body size-shape scaling relationships characteristic of the reference sample (e.g., larger–bodied and higher–BMI Samoans). In contrast, the BMI-based equations incorporate body shape as a variable, and are thus not as dependent on the particular distribution of body shapes in the pooled reference sample, as long as these encompass the probable range of values in the target footprint samples.

The effects of this factor can be clearly seen in comparisons of quadratic and BMI-based estimates for the Happisburgh and Le Rozel samples. A BMI value of 27 was used here for these samples, based on averages calculated for two higher latitude Middle-Late Pleistocene skeletal samples—Sima de los Huesos and Western Eurasian Neandertals. While there is variability in estimated BMI within these skeletal samples (SOM Tables S2 and S3), all individual BMI estimates are relatively high (over 24), which as discussed further below is consistent with all available information concerning body form in Early-Middle Pleistocene higher latitude hominins. Use of the generic quadratic equation models body shape as much more linear, i.e., with a BMI nearer to 22, for individuals with foot areas less than 300 cm^2, which includes all of the Happisburgh and many of the adult and possibly adult Le Rozel footprints, as well as all of the juvenile Le Rozel footprints. These quadratic equation estimates are thus almost certainly too low.

Thus, whenever feasible, the BMI-based equations are recommended over the generic quadratic equations. The effects of error in BMI estimation can be incorporated, if desired, by

calculating body masses using a range of BMI values. This depends on having some information on probable average body shape in the target sample, derived independently. Foot index (breadth/length) values can give some corroboratory evidence, although the relationship between foot index and BMI is relatively weak. If information on body shape is unavailable or unreliable, the quadratic equations can be employed. It should be recognized, though, that use of the quadratic equations will inherently produce estimates that model body shape as fairly linear, i.e., as equivalent to the average body shape of our living pooled reference sample (except in the larger foot size range).

One other implication of our findings is that in general, prediction equations developed from a population with a particular body shape (BMI) will not produce accurate estimates when applied to populations with different body shapes. The most commonly used body mass prediction equations in human paleontological research were derived from studies of the Daasanach, a very linear population with the lowest average BMI of any of our samples (Dingwall et al., 2013; Hatala et al., 2016b). Given our current results, these equations will produce significant underestimations of body mass when applied to footprints made by individuals with higher BMIs. These would include, in all likelihood, the three footprint samples where the Daasanach-based equations have been applied—Laetoli, Ileret, and Happisburgh (Dingwall et al., 2013; Ashton et al., 2014; Hatala et al., 2016b; Masao et al., 2016). Body mass estimates for the Ileret sample average 21-32% higher using our quadratic foot area equation, and 31–41% higher using our BMI-based equation than previous estimates. For the Happisburgh sample, our new body mass estimates average 13% higher for the quadratic equation, and 43% higher for the BMI-based equation. As shown below, the new estimates are more consistent with previous skeletal estimates of body mass for related samples.

Our results also have broader implications regarding variation in relative foot size. Our observation that differences in foot size/body mass proportions between modern populations are characteristic of juveniles as young as seven years of age (comparisons between the Machiguenga and Daasanach samples) indicates an early development of such proportional differences. This in turn suggests that there may be some fundamental developmental-genetic mechanisms that lead to different foot size/body mass relationships in populations with different overall body shapes.

Finally, the relatively smaller foot of higher-BMI populations has biomechanical implications, suggesting either an increase in stress (force per unit area) or other compensatory mechanisms to reduce stress on the plantar surface with increased BMI. Comparisons within a habitually unshod Indian sample of true plantar surface area to the 'area' (maximum length × breadth) dimension employed here indicated that relatively more of the plantar surface area is in contact with the substrate in higher-BMI subjects, potentially reducing stress. A similar pattern was found in habitually shod Indian and European subjects from the same study, but the relationship was weaker, possibly because of lower foot compliance (Kadambande et al., 2006). A similar phenomenon has been observed in clinical studies of obese versus non-obese children (Dowling et al., 2001). Increased plantar pressure has also been observed in obese versus non-obese children and adults (Dowling et al., 2001; Hills et al., 2001; Birtane and Tuna, 2004). Obesity *per se* is not a factor in the present study comparisons: all of our samples were relatively lean, including the Samoans (R. Wunderlich, pers. obs.). However, it is possible that even within the clinically "normal" range, variation in BMI is associated with changes in both plantar contact surface area distributions as well as plantar pressure magnitudes and distributions. In the future we intend to explore these factors in our unshod samples using available footprint and pressure

pad data. Another factor that should be further explored among habitually unshod populations is the possible effect of burden carrying on foot size relative to body size (Dowling et al., 2001; Wall-Scheffler et al., 2015).

4.2. Estimation of Body Mass in Juveniles

Children have larger feet relative to body mass than adults, with the difference diminishing with age. This is likely brought about by both different growth trajectories of the foot and the rest of the skeleton, as well as increasing BMI with age. As a result, body mass estimation equations developed for adults cannot be used on juveniles without adjustment, and any adjustment factors will be age-dependent. Because age itself cannot be estimated accurately from footprints alone, we suggest using a procedure that involves first calculating the average adult foot area for a footprint sample, then the ratio of foot size in the juvenile print to this value. This ratio is then placed into regressions that produce adjustment factors to apply to body masses estimated using adult formulae. The adjustments appear to provide reasonable body mass estimates for juveniles in the Le Rozel archaic *H. sapiens* (Neandertal) sample (Duveau et al., 2019). When using the BMI-based equations, this assumes that variation in body shape in juveniles parallels variation in adults from the same population or taxon, which appears to be well justified based on comparisons within modern humans (Ruff et al., 2002; Cowgill et al., 2012).

There is extensive overlap between smaller adults and older adolescents in foot size, making identification of juveniles in this size range difficult from footprint size alone. In our living reference samples, the smallest adult foot area averaged 75% of the mean adult foot area, so this can be used as an approximate threshold for identifying possible adult footprints.

However, the mean adult foot area is itself dependent on which individuals are considered adult, so this can be somewhat circular. The procedure is also subject to possible sampling bias; for example, the only definitive adult footprints in the Le Rozel Neandertal sample (Duveau et al., 2019) were very likely those of a male or males. In this case the average difference between adult male and female foot area in our reference samples (23% larger in males) was used to calculate a hypothetical adult female value, and an average adult value. Both adjusted and non-adjusted body masses can be calculated in probable areas of overlap between adults and adolescents, providing a range of values. The 75% threshold for identifying possible adult footprints will also be dependent on the degree of sexual dimorphism characteristic of a taxon/population—greater overall dispersion among adults will lower this threshold and increase overlap between adults and older juveniles. Although sexual dimorphism in body mass is slightly greater in Neandertals than in modern humans (Ruff et al., 2018), the effects of this factor on our analyses of the Le Rozel sample are likely to have been very small.

4.3. Estimation of Body Mass in Habitually Shod Individuals

Comparisons between habitually unshod and shod individuals from the same ethnic group (D'Août et al., 2009) suggest increasing footprint areas by 8% before applying our body mass estimation equations to (bare) footprints made by habitually shod individuals. This adjustment applies to situations involving use of relatively loose footwear of the type likely worn by most pre-industrial populations, i.e., to archaeological samples. Similar comparisons to individuals wearing more confining Western-style footwear are potentially affected by ethnic differences in foot shape, but provisionally suggest a much greater adjustment (+22%) of foot area when applying our equations to such samples. Additional direct studies of footprint size and

body mass in Western industrial populations are recommended before applying any body mass estimation equations, e.g., in a forensic context.

4.4. Specific applications

Laetoli Our body mass estimates for the Laetoli footprints are consistently larger than previous estimates based on equations either derived from the Daasanach sample or reconstructions of A.L. 288-1's foot length and body mass (Masao et al., 2016; the '*Au. afarensis*' method). Because "the body proportions of modern *Homo sapiens* are considerably different from those of the Laetoli putative track-makers" (Masao et al., 2016: p. 17), i.e., *Australopithecus afarensis*, Masao et al. considered the '*Au. afarensis*' estimates to be more realistic. They also note that their '*Au. afarensis*' body estimates are generally concordant with those derived for this taxon by Grabowski et al. (2015). However, those estimates have been questioned on several grounds, with larger body masses argued to be more probable based on preserved skeletal specimens (Ruff et al., 2018). The average body mass for *A. afarensis* derived in the latter study is 49.3 kg (range 29–60 kg), with male and female means of 57.2 and 33.5 kg, respectively. This is still smaller than the BMI-based footprint estimates of the present study (mean 62.0 kg, range 51–71 kg), although closer to the quadratic equation estimates (mean 53.0 kg, range 44–64 kg).

There are several potential explanations for the difference in results between previous skeletal estimates of body mass in *A. afarensis* and the larger estimates produced by our BMI or quadratic regressions applied to footprints. The Laetoli trackways may be sampling a different, generally larger-bodied subset of the taxon than the Afar skeletal specimens. The available fossil material from Laetoli and Hadar does not support such an inference, however (Johanson and White, 1979; White, 1985; White and Suwa, 1987). The average BMI estimate of 25 derived

here for *A. afarensis* may be too large. However, even the generic quadratic equation, based on a pooled sample with a much lower average BMI, produces body mass estimates that are higher than previous skeletal estimates. Given various lines of evidence indicating a relatively wide body and thus high relative body weight to stature in *A. afarensis* (Aiello, 1992; Ruff, 2017), it seems very unlikely that it was characterized by a very linear body build. Taphonomic and post-depositional factors may have affected dimensions of the Laetoli prints, although distortion of the better-preserved prints appears to be minimal, except as noted (White and Suwa, 1987; Masao et al., 2016).

Therefore, the most likely explanation of the divergence in results between skeletal and the present footprint-based body mass estimates in *A. afarensis* is that foot size relative to body mass was different in *A. afarensis* and modern humans, as suggested by Masao et al. (2016; also see Dingwall et al., 2013). Comparisons of reconstructed foot length to stature in A.L. 288-1 support this interpretation, with A.L. 288-1 having proportions more similar to those of chimpanzees than modern human adults. Consequently, body mass estimated from foot area, using the average foot index value of the Laetoli footprint sample to calculate foot breadth in A.L. 288-1, is 50–72% larger than body mass estimated from hind limb joint size in A.L. 288-1.

As an alternative to regressions based on modern humans, Masao et al. (2016) used a range of ratios between foot length and body mass for A.L. 288-1, developed by Dingwall et al (2013), to predict body mass for the Laetoli prints. However, use of ratios in this way assumes isometry between foot length and body mass (Hens et al., 1998). In fact, foot length and body mass are strongly non-isometric (slopes depart from 1.0) in our modern sample, as might be expected from both dimensional differences and mechanical principles: RMA slopes of log-transformed foot length on body mass for individual adult samples range between 0.391 and

0.628 (mean 0.510, standard errors 0.043–0.082) and for the pooled sample 0.474 (standard error 0.023). This will lead to biased estimates of body mass, particularly in individuals furthest from A.L. 288-1 in body size, i.e., large *A. afarensis*. In contrast, similar log-log regressions of foot area on body mass in our modern human samples are isometric, with RMA slopes non-significantly different from 1.0, ranging in individual samples between 0.85 and 1.17 (mean 1.04, standard errors 0.10–0.13) and through the total combined sample 0.97 (standard error 0.04). These results are consistent with mechanical predictions that foot surface area (not length) should be proportional to body mass, producing equivalent stress (force/area) under loading.

Therefore, we developed a new method based on the ratio of body mass to estimated foot area in A.L. 288-1 (0.218) to estimate body mass for the Laetoli footprints. Body mass estimates using this technique seem reasonable when compared to those derived for *A. afarensis* from lower limb articular size of nine specimens (Ruff et al., 2018). The average body mass of the five Laetoli trackways is 47.9 kg, compared to 49.3 kg using skeletal estimates. The coefficient of variation (corrected for small sample size; Sokal and Rohlf, 1981) is 27.2%, compared to 26.3% for skeletal estimates. If the two smaller trackways (G1 and G3) are considered to be made by adult females and the three larger trackways (S1, S2, and G2) by adult males, average male body mass is 56.7 kg, and average female body mass is 34.9 kg, with a M/F ratio of 1.62 (log(M/F) + 1 ratio of 1.48) (see Ruff et al., 2018 for details). These compare favorably with values of 57.2 kg for males, 33.5 kg for females, and a M/F ratio of 1.71 (log(M/F) + 1 ratio of 1.54) based on skeletal dimensions (Ruff et al., 2018). The similarity in footprint and skeletal estimates using these sex (and age) assignments also does not support the tentative suggestion of Masao et al. (2016) that the G2 trackway was made by an adult female and the G1 and G3 trackways by juveniles. As shown earlier, though, it is not possible to distinguish small adults from older

adolescents using footprint size alone. Using modern human footprint samples to identify a threshold distinguishing likely small adults from juveniles (e.g., the 75% of average adult size threshold used for the Le Rozel sample) is obviously not appropriate when size dispersion and sexual dimorphism is much greater than in modern humans, as is the case for *A. afarensis* (McHenry, 1992; Ruff et al., 2018).

Use of the body mass to foot size proportions of A.L. 288-1 as a model for *A. afarensis* assumes that, as in modern humans, foot area scaled isometrically to body mass in small and large (adult) individuals of this taxon. The discovery of additional, larger *A. afarensis* specimens that include associated foot and other skeletal elements will allow testing of this assumption. Whether this method is applicable to other australopith taxa also awaits additional associated fossil material. We do not recommend applying the method to *H. erectus* and later *Homo*, since other body proportions are generally similar to those of modern humans (Walker and Leakey, 1993) and there is no reason to suspect that foot length was relatively increased (also see Bennett et al., 2009).

Ileret Body masses for the Ileret sample estimated from either the quadratic or BMI-based equations are larger than those using the Daasanach equation (Dingwall et al., 2013), which can be attributed to the low BMI of the Daasanach sample. Our BMI-based equation produces estimates that are closest to those derived from skeletal material of East African *H. erectus* or early *Homo* (Ruff et al., 2018). The mean skeletal body mass estimate of two East African *H. erectus* (KNM-WT 15000, as an adult, and OH 28) is 69.4 kg; the mean estimate for three temporally earlier East African 'erectus-like' early *Homo* (KNM-ER 1472, 1481, and 3228), not including KNM 5881/2, which is probably *H. habilis* (sensu stricto) (Ruff et al., 2018), is 59.8 kg, with an overall mean for the five specimens of 63.6 kg. These estimates compare favorably

to a mean body mass estimate of about 65 kg for the Ileret sample (trackways and A2 prints only, or trackways and all prints), using our formula with an assumed BMI of 24, and are all much greater than estimates derived from the Daasanach equation, which average 49–50 kg.

Applying the 'means' method (Plavcan, 1994), male and female body masses using the BMI-based method are 68.8 and 59.6 kg (trackways and A2 prints) or 70.9 and 58.2 kg (trackways and all prints), respectively, yielding estimates of sexual dimorphism of 1.15–1.22 (M/F) or 1.14–1.20 [(log)M/F + 1] (the higher estimates are for the total sample). Estimates of sexual dimorphism in East African *H. erectus* based on skeletal remains are very tenuous given the limited available evidence, but the above values are consistent with a general decline in sexual dimorphism in *H. erectus* compared to australopiths (Antón et al., 2014; Ruff et al., 2018; although also see Spoor et al., 2007). Our results for the total trackway + track sample are consistent with Villmoare et al.'s (2019) conclusions based on analyses of Ileret footprint lengths, i.e., that they are "less dimorphic than gorillas or *A. afarensis* but slightly more dimorphic than modern humans" (p. 9) (modern humans average 1.15 for sexual dimorphism in body mass; Ruff et al., 2018). The average estimated body mass for the Ileret tracks of 65 kg is also consistent with a significant increase in overall body size in early *Homo* (not including *H. habilis*) compared to australopiths (McHenry, 1994; Ruff et al., 2018).

Happisburgh Our new body mass estimates for the Happisburgh sample are similar to those previously obtained for other post-1.7 Ma Early and Middle Pleistocene *Homo* (not including *H. habilis*). The three Happisburgh adult prints produce estimates that average 71.4 kg using an assumed BMI of 27, which compares with means of 69.4 kg for two East African *H. erectus* and 72.1 kg for 19 Middle Pleistocene archaic *Homo* (Ruff et al., 2018). Previous estimates (Ashton et al., 2014) based on the Daasanach equations (Dingwall et al., 2013) are much lower. Ashton et

al. (2014) noted the uncertainty inherent in applying equations derived from a tropically proportioned population to higher latitude specimens, but also suggested that a high body mass relative to stature is "not seen in most European skeletal fossil assemblages" (their Supporting Information, p. 3). In fact, all available evidence from higher latitude Early and Middle Pleistocene hominin specimens indicates that they were quite wide-bodied. This includes the probable cool temperate to 'hyperarctic' body proportions of the Middle Pleistocene Boxgrove tibia (Trinkaus et al., 1999); the "wide and large body type" of the Sima de los Huesos Middle Pleistocene sample (Arsuaga et al., 2015: 11525); the very long clavicle (161.5 cm) of the Early Pleistocene Gran Dolina ATD6-50 *H. antecessor* specimen, most similar to those of larger male Neandertals (Carretero et al., 1999); and the very wide pelvis relative to ulna length of the Middle Pleistocene Jinnuishan 1 specimen (Rosenberg et al., 2006). No European skeletal samples from any time period, including somewhat more linear anatomically modern *H. sapiens* from the terminal Pleistocene and Holocene, exhibit average estimated BMIs approaching those of the Daasanach (Niskanen et al., 2018). Thus, Happisburgh estimates based on that sample are almost certainly much too small. Even use of more moderate BMI estimates of 24 (our estimate for East African *H. erectus*) to 26 still produces average body mass estimates for Happisburgh of 64–69 kg, almost 30–40% larger than previous estimates. The new larger body masses for the Happisburgh sample are consistent with its provisional attribution to *H. antecessor* (Ashton et al., 2014), which has stature estimates based on skeletal remains of 170.5–174.5 cm (Carretero et al., 1999; Lorenzo et al., 1999). However, our new estimates also fall comfortably within the range of other Early and Middle Pleistocene *Homo*, including the Atapuerca sample, as well as Late Pleistocene archaic *Homo* (Neandertals) (Ruff et al., 2018).

Given the small number of Happisburgh probable adult prints, it is difficult to evaluate the level of sexual dimorphism in body mass represented in the sample. All three prints produce estimates (using the BMI method) within about 6 kg, or 9%, which is considerably less than average sexual dimorphism in *Homo* (Ruff et al., 2018), suggesting that the three prints may represent a single sex (or individual), or simply nonrandom sampling of males and females.

Le Rozel The average body mass of 83.7 kg for the three large prints in the Le Rozel sample, using our favored BMI method and assuming a BMI of 27, is about equal to the largest body masses calculated from skeletal remains of Neandertals (Ruff et al., 2018). Estimated statures associated with these three footprints average 174.8 cm (Duveau et al., 2019 and Duveau, pers. comm.), which is close to the maximum estimated for Neandertals from skeletal remains (Duveau et al., 2019: Supplementary Information), so are consistent with the body mass estimates. The juvenile body mass estimates for this sample, using the BMI method and applying the juvenile adjustment, seem reasonable when compared to modern human children, including infants, supporting use of this technique throughout the full developmental age range.

Barcin Höyük A skeletal sample from a temporally, geographically, and culturally similar population from Çatalhöyük, Turkey provides guidance on a reasonable BMI value for this early Neolithic footprint. An adjustment for probable habitual use of footwear is also incorporated. When this is done, body mass estimates are lower than those obtained using a modern Turkish sample. Like the Ileret footprint analyses, this illustrates the dangers in using current local populations as models for past populations (Bennett and Morse, 2014), and the value of appropriate skeletal remains in reconstructing probable body shape.

5. Conclusions

Body mass is highly correlated with foot size in a sample of 193 habitually unshod modern human adults from five populations representing a wide range of body sizes and shapes (Machiguenga, Daasanach, Pumé, Hadzabe, Samoan). A quadratic equation based on foot area (maximum length × breadth) predicts body mass with an average percent prediction error of about 10%. However, when broken down by population, body shape, represented here by body mass index (BMI, body mass/stature^2), has a significant impact on this relationship: populations with higher BMIs have relatively smaller feet. This effect is apparent even among children from the same populations (n = 50), suggesting innate (genetic) influences. Therefore, prediction equations that incorporate BMI are also developed. These have much smaller associated prediction errors, although true errors will be larger because BMI itself must be estimated for target samples. This can be done using mean values from appropriate related skeletal samples where stature and body mass can be independently estimated. We also develop conversions for footprint size to foot size using associated data from a study of footprints made in a natural substrate.

Our analyses of juveniles show that children have relatively larger feet than adults from the same populations but converge with adults in late adolescence. Thus, adult equations cannot be used on footprints made by juveniles without adjustment. Because age is difficult to determine from footprints, we develop a technique based on footprint size relative to average adult footprint size to calculate an adjustment factor to body mass estimates derived from adult formulae. Based on comparisons between habitually shod and unshod individuals from the same ethnic group, we also develop an adjustment to footprints made by habitually shod individuals, multiplying them by 1.08, before applying the present study equations.

When applied to a series of footprint samples spanning from the Pliocene to the Holocene, the equations, particularly the BMI-based equations, generally produce body mass estimates that are consistent with skeletal estimates for the same taxa or regional population. The exception is the footprint sample from Laetoli (*Australopithecus afarensis*, 3.66 Ma), where footprints produce estimates that are higher than skeletally-based estimates for this taxon. Further exploration of foot size/body size relationships in modern humans, chimpanzees, and *A. afarensis* shows that *A. afarensis* (A.L. 288-1) has relatively large feet compared to modern human adults and is closer to modern human children and chimpanzees in this regard. A different method based on the ratio of estimated body mass to foot area of A.L. 288-1 (0.218) is developed and appears to provide more reasonable body mass estimates for the Laetoli footprints.

Ethics Statement:

All study participants provided informed consent in accordance with protocols approved by institutional review boards at the original researchers' home institutions.

Competing interests: The authors declare that they have no competing interests.

Data availability: Access to the raw data for living samples will be considered upon request.

Footnotes

[1] A seventh study, carried out by Hatala et al. (2016b), also developed a method for estimating body mass from footprint dimensions, based on a random forests model applied to a mixed-age Daasanach sample. Since one of the dimensions in the model is average footprint depth (i.e., not foot size per se), it is not included among the studies listed in Table 1.

[2] Atamtürk and Duyar (2008) presented equations based on foot dimensions in the same sample—also while standing on a hard surface—but Atamtürk et al. (2018) utilized the earlier equations based on footprints (Atamtürk, 2003) in their analyses.

Acknowledgments

We would like to thank Jérémy Duveau for making available the complete data set for the Le Rozel sample and for clarifying several issues, Kewal Krishan for providing data and clarifications regarding the Gujjar Indian sample, Izzet Duyar for providing information on the Turkish sample, and Isabelle de Groote for answering some questions regarding the original Happisburgh sample analyses. For the other foot and footprint samples included in the study, we thank the following people and funding sources: Machinguenga: Data collection and analyses were supported by the National Science Foundation (BNS-8504290), the Marian and Adolf Lichstern Fund for Anthropological Research, the Social Sciences Divisional Research Fund of the University of Chicago, and the Harvard Travellers Club. Daasanach: Data collection was accomplished with funding from NSF (BCS-1232522), the Leakey Foundation, and the Wenner Gren Foundation (8592). We also thank the National Museums of Kenya, Koobi Fora Field School, and the Ileret community for logistical support, and Heather Dingwall, Matt Ferry, John Mwangi, Job Naasak, Nyako, Brian Richmond, and Ben Sila for their assistance with data collection. Pumé: Funding for data collection was provided by the University of New Mexico's Latin American Institute and Department of Anthropology, and Sigma Xi. Hadzabe: Data collection was supported by the Marian and Adolf Lichstern Fund for Anthropological Research, and the University of Chicago Social Sciences Divisional Research Grant No. 4-56004 and Center for International Studies. We would also like to thank the Mang'ola village government and the Department of Antiquities, Ministry of Natural Resources, National Institute of Medical Research and the Commission for Science and Technology of Tanzania for issuing research and ethics permits. Samoans: Data were collected with support from the James Madison University College of Science and Mathematics. We would also like to thank the Samoan Rugby Union and their players, and Michael Deasy for facilitating the work. Indians: Data collection was supported by the Fund for Scientific Research–Flanders (project G.0125.05), by the University of Antwerp (BOF grant #1094) and by the Flemish Government through structural support to the Centre for Research and Conservation. We would also like to thank the staff of the Jain Institute of Vascular Sciences in Bangalore, Dr. Ranjendakumar and staff at KGF, and the staff in Mandya. Chimpanzees: Chimpanzee data were collected with support from the NSF (BCS-1232522), the Leakey Foundation, and the Wenner-Gren Foundation (8592), and with help from

Brigitte Demes, Kristin Fuehrer, and Susan Larson. Finally, we would like to thank the editors and three reviewers for their useful comments on the original manuscript.

References

Aiello, L.C., 1992. Allometry and the analysis of size and shape in human evolution. J. Hum. Evol. 22, 127-148.

Altamura, F., Bennett, M.R., D'Aout, K., Gaudzinski-Windheuser, S., Melis, R.T., Reynolds, S.C., Mussi, M., 2018. Archaeology and ichnology at Gombore II-2, Melka Kunture, Ethiopia: everyday life of a mixed-age hominin group 700,000 years ago. Sci. Rep. 8, 2815.

Anderson, M., Blais, M., Green, W.T., 1956. Growth of the normal foot during childhood and adolescence - length of the foot and interrelations of foot, stature, and lower-extremity as seen in serial records of children between 1-18 years of age. Am. J. Phys. Anthropol. 14, 287-308.

Anderson, M., Hwang, S.C., Green, W.T., 1965. Growth of the normal trunk in boys and girls during the second decade of life; related to age, maturity, and ossification of the iliac epiphyses. J. Bone Joint Surg. Am. 47, 1554-1564.

Anil, A., Peker, Ttirgut, T.H. Ulukent, S.C., 1997. An examination of the relationship between foot length, foot breadth, ball girth, height and weight of Turkish university students aged between 17 and 25. Anthropol. Anz. 55, 79-87.

Antón, S.C., Potts, R., Aiello, L.C., 2014. Human evolution. Evolution of early Homo: an integrated biological perspective. Science 345, 1236828.

Arsuaga, J.L., Carretero, J.M., Lorenzo, C., Gomez-Olivencia, A., Pablos, A., Rodríguez, L., Garcia-Gonzalez, R., Bonmatí, A., Quam, R.M., Pantoja-Pérez, A., Martínez, I., Aranburu,

A., Gracia-Tellez, A., Poza-Rey, E., Sala, N., Garcia, N., Alcazar de Velasco, A., Cuenca-Bescos, G., Bermúdez de Castro, J.M., Carbonell, E., 2015. Postcranial morphology of the middle Pleistocene humans from Sima de los Huesos, Spain. Proc. Natl. Acad. Sci. USA 112, 11524-11529.

Ashizawa, K., Kumakura, C., Kusumoto, A., Narasaki, S., 1997. Relative foot size and shape to general body size in Javanese, Filipinas and Japanese with special reference to habitual footwear types. Ann. Hum. Biol. 24, 117-129.

Ashton, N., Lewis, S.G., De Groote, I., Duffy, S.M., Bates, M., Bates, R., Hoare, P., Lewis, M., Parfitt, S.A., Peglar, S., Williams, C., Stringer, C., 2014. Hominin footprints from early Pleistocene deposits at Happisburgh, UK. PLoS One 9, e88329.

Atamtürk, D., 2003. Ayak ve ayak ölçülerinden boy uzunluğu ve vücut ağırlığının tahmini üzerine adli antropolojik bir araştırma. MA Thesis, Hacettepe University.

Atamtürk, D., Duyar, I., 2008. Age-related factors in the relationship between foot measurements and living stature and body weight. J. Forensic Sci. 53, 1296-1300.

Atamtürk, D., Özbal, R., Gerrtisen, F., Duyar, I., 2018. Analysis and interpretation of Neolithic period footprints from Barcin Höyük, Turkey. Mediterr. Archaeol. Archaeom. 18, 163-174.

Bates, K.T., Savage, R., Pataky, T.C., Morse, S.A., Webster, E., Falkingham, P.L., Ren, L., Qian, Z., Collins, D., Bennett, M.R., McClymont, J., Crompton, R.H., 2013. Does footprint depth correlate with foot motion and pressure? J. R. Soc Interface 10, 20130009.

Beguen, C., Vallois, H., 1928. Les Empreintes Prehistoriques. Institute International d'Anthropologie III° Session.

Behrensmeyer, A.K., Laporte, L.F., 1981. Footprints of a Pleistocene Hominid in Northern Kenya. Nature 289, 167-169.

Bennett, M.R., Harris, J.W.K., Richmond, B.G., Braun, D.R., Mbua, E., Kiura, P., Olago, D., Kibunjia, M., Omuombo, C., Behrensmeyer, A.K., Huddart, D., Gonzalez, S., 2009. Early hominin foot morphology based on 1.5-million-year-old footprints from Ileret, Kenya. Science 323, 1197-1201.

Bennett, M.R., Morse, S.A., 2014. Human Footprints: Fossilized Locomotion? Springer, Heidelberg.

Bennett, M.R., Reynolds, S.C., Morse, S.A., Budka, M., 2016. Laetoli's lost tracks: 3D generated mean shape and missing footprints. Sci. Rep. 6, 21916.

Birtane, M., Tuna, H., 2004. The evaluation of plantar pressure distribution in obese and non-obese adults. Clin. Biomech. 19, 1055-1059.

Brown, J.H., West, G.B., 2000. Scaling in Biology. Oxford University Press, Oxford.

Calder, W.A., III, 1984. Size, Function, and Life History. Cambridge University Press, Cambridge.

Cameron, N., Hiernaux, J., Jarman, S., Marshall, W.A., Tanner, J.M., Whitehouse, R.H., 1981. Anthropometry. In: Weiner, J.S., Louirie, J.A. (Eds.), Practical Human Biology. Academic Press, London, pp. 27-52.

Carretero, J.M., Lorenzo, C., Arsuaga, J.L., 1999. Axial and appendicular skeleton of *Homo antecessor*. J. Hum. Evol. 37, 459-499.

Carretero, J.M., Rodriguez, L., Garcia-Gonzalez, R., Arsuaga, J.L., Gomez-Olivencia, A., Lorenzo, C., Bonmati, A., Gracia, A., Martinez, I., Quam, R., 2012. Stature estimation from complete long bones in the Middle Pleistocene humans from the Sima de los Huesos, Sierra de Atapuerca (Spain). J. Hum. Evol. 62, 242-255.

Charteris, J., Wall, J.C., Nottrodt, J.W., 1981. Functional reconstruction of gait from the Pliocene hominid footprints at Laetoli, Northern Tanzania. Nature 290, 496-498.

Cleveland, W.S., 1979. Robust locally weighted regression and smoothing scatterplots. J. Amer.Stat Assoc. 74, 829-836.

Cowgill, L.W., Eleazer, C.D., Auerbach, B.M., Temple, D.H., Okazaki, K., 2012. Developmental variation in ecogeographic body proportions. Am. J. Phys. Anthropol. 148, 557-570.

Crompton, R.H., Pataky, T.C., Savage, R., D'Aout, K., Bennett, M.R., Day, M.H., Bates, K., Morse, S., Sellers, W.I., 2012. Human-like external function of the foot, and fully upright gait, confirmed in the 3.66 million-year-old Laetoli hominin footprints by topographic statistics, experimental footprint-formation and computer simulation. J. R. Soc. Interface 9, 707-719.

D'Août, K., Meert, L., Van Gheluwe, B., De Clercq, D., Aerts, P., 2010. Experimentally generated footprints in sand: Analysis and consequences for the interpretation of fossil and forensic footprints. Am. J. Phys. Anthropol. 141, 515-525.

D'Août, K., Pataky, T.C., De Clercq, D., Aerts, P., 2009. The effects of habitual footwear use: foot shape and function in native barefoot walkers. Footwear Sci. 1, 81-94.

Day, M.H., Wickens, E.H., 1980. Laetoli Pliocene hominid footprints and bipedalism. Nature 286, 385-387.

Dingwall, H.L., Hatala, K.G., Wunderlich, R.E., Richmond, B.G., 2013. Hominin stature, body mass, and walking speed estimates based on 1.5 million-year-old fossil footprints at Ileret, Kenya. J. Hum. Evol. 64, 556-568.

Domjanic, J., Seidler, H., Mitteroecker, P., 2015. A combined morphometric analysis of foot form and its association with sex, stature, and body mass. Am. J. Phys. Anthropol. 157, 582-591.

Dowling, A.M., Steele, J.R., Baur, L.A., 2001. Does obesity influence foot structure and plantar pressure patterns in prepubescent children? Int. J. Obesity 25, 845-852.

Duveau, J., Berillon, G., Verna, C., Laisne, G., Cliquet, D., 2019. The composition of a Neandertal social group revealed by the hominin footprints at Le Rozel (Normandy, France). Proc. Natl. Acad. Sci. USA 116, 19409-19414.

Fawzy, I.A., Kamal, N.N., 2010. Stature and body weight estimation from various footprint measurements among Egyptian population. J. Forensic Sci. 55, 884-888.

Franciscus, R.G., Holliday, T.W., 1992. Hindlimb skeletal allometry in Plio-Pleistocene hominids with special reference to A.L. 288-1 ("Lucy"). Bull. Mém. Soc. Anthropol Paris n.s. 4, 5-20.

Grabowski, M., Hatala, K.G., Jungers, W.L., Richmond, B.G., 2015. Body mass estimates of hominin fossils and the evolution of human body size. J. Hum. Evol. 85, 75-93.

Hatala, K.G., Demes, B., Richmond, B.G., 2016a. Laetoli footprints reveal bipedal gait biomechanics different from those of modern humans and chimpanzees. Proc. Roy. Soc. London, Ser. B 283, 20160235.

Hatala, K.G., Harcourt-Smith, W.E.H., Gordon, A.D., Zimmer, B.W., Richmond, B.G., Pobiner, B.L., Green, D.J., Metallo, A., Rossi, V., Liutkus-Pierce, C.M., 2020. Snapshots of human anatomy, locomotion, and behavior from Late Pleistocene footprints at Engare Sero, Tanzania. Sci. Rep. 10, 7740.

Hatala, K.G., Roach, N.T., Ostrofsky, K.R., Wunderlich, R.E., Dingwall, H.L., Villmoare, B.A., Green, D.J., Braun, D.R., Harris, J.W.K., Behrensmeyer, A.K., Richmond, B.G., 2017. Hominin track assemblages from Okote Member deposits near Ileret, Kenya, and their implications for understanding fossil hominin paleobiology at 1.5 Ma. J. Hum. Evol. 112, 93-104.

Hatala, K.G., Roach, N.T., Ostrofsky, K.R., Wunderlich, R.E., Dingwall, H.L., Villmoare, B.A., Green, D.J., Harris, J.W., Braun, D.R., Richmond, B.G., 2016b. Footprints reveal direct evidence of group behavior and locomotion in *Homo erectus*. Sci. Rep. 6, 28766.

Hatala, K.G., Wunderlich, R.E., Dingwall, H.L., Richmond, B.G., 2016c. Interpreting locomotor biomechanics from the morphology of human footprints. J. Hum. Evol. 90, 38-48.

Hens, S.M., Konigsberg, L.W., Jungers, W.L., 1998. Estimation of African ape body length from femur length. J. Hum. Evol. 34, 401-411.

Hills, A.P., Hennig, E.M., McDonald, M., Bar-Or, O., 2001. Plantar pressure differences between obese and non-obese adults: A biomechanical analysis. Int. J. Obes. Relat. Metab. Disord. 25, 1674-1679.

Hilton, C.E., Greaves, R.D., 2008. Seasonality and sex differences in travel distance and resource transport in Venezuelan foragers. Curr. Anthropol. 49, 144-153.

Hoffmann, P., 1905. Conclusons drawn from a comparative study of the feet of barefooted and shoe-wearing peoples. J. Bone Jt. Surg. 3, 105-136.

Hollander, K., Heidt, C., BC, V.D.Z., Braumann, K.M., Zech, A., 2017. Long-term effects of habitual barefoot running and walking: A systematic review. Med. Sci. Sports Exerc. 49, 752-762.

Houston, V.L., Luo, G., Mason, C.P., Mussman, M., Garbarini, M., Beattie, A.C., 2006. Changes in male foot shape and size with weightbearing. J. Am. Podiatr. Med. Assoc. 96, 330-343.

Johanson, D.C., White, T.D., 1979. A systematic assessment of early African hominids. Science 203, 321-330.

Jungers, W.L., 1982. Lucy's limbs: Skeletal allometry and locomotion in *Australopithecus afarensis*. Nature 297, 676-678.

Jungers, W.L., 1988a. Lucy's length: Stature reconstruction in *Australopithecus afarensis* (A.L. 288-1) with implications for other small-bodied hominids. Am. J. Phys. Anthropol. 76, 227-231.

Jungers, W.L., 1988b. New estimates of body size in australopithecines. In: Grine, F.E. (Ed.), Evolutionary History of the "Robust" Australopithecines. Aldine de Gruyter, New York, pp. 115-125.

Kadambande, S., Khuranaa, A., Debnatha, U., Bansalb, M., Hariharana, K., 2006. Comparative anthropometric analysis of shod and unshod feet. The Foot 16, 188-191.

Knüsel, C.J., Milella, M., Betz, B., Dori, I., Garofalo, E., Glencross, B., Haddow, S.D., Ledger, M., Anastasiou, E., Mitchell, P., Pearson, J., Pilloud, M.A., Ruff, C.B., Sadvari, J.W., Tibbetts, B., Larsen, C.S., 2021. Bioarchaeology at Neolithic Çatalhöyük: Indicators of Health, Well-being and Lifeway in their Social Context. In: Hodder, I. (Ed.), Peopling the landscape of Çatalhöyük: reports from the 2009-2017 seasons. Çatalhöyük Research Project Series Volume 13; British Institute at Ankara Monograph 53. British Institute at Ankara, London, pp. 315-355.

Krishan, K., 2007. Individualizing characteristics of footprints in Gujjars of North India--forensic aspects. Forensic Sci Int. 169, 137-144.

Krishan, K., 2008. Establishing correlation of footprints with body weight - Forensic aspects. Forensic Sci. Int. 179, 63-69.

Krogman, W.M., 1962. The Human Skeleton in Forensic Medicine. CC Thomas, Springfield, Illinois.

Larsen, C.S., Knusel, C.J., Haddow, S.D., Pilloud, M.A., Milella, M., Sadvari, J.W., Pearson, J., Ruff, C.B., Garofalo, E.M., Bocaege, E., Betz, B.J., Dori, I., Glencross, B., 2019. Bioarchaeology of Neolithic Çatalhöyük reveals fundamental transitions in health, mobility, and lifestyle in early farmers. Proc. Natl. Acad. Sci. USA 116, 12615-12623.

Leakey, M.D., Hay, R.L., 1979. Pliocene Footprints in the Laetolil Beds at Laetoli, Northern Tanzania. Nature 278, 317-323.

Leonard, W.R., Katzmarzyk, P.T., 2010. Body size and shape: Climatic and nutritional influences on human body morphology. In: Meuehlenbein, M.P. (Ed.), Human Evolutionary Biology. Cambridge Univ. Press, Cambridge, pp. 157-169.

Lockley, M., Roberts, G., Kim, J.Y., 2008. In the footprints of our ancestors: An overview of the hominid track record. Ichnos 15, 106-125.

Lorenzo, C., Arsuaga, J.L., Carretero, J.M., 1999. Hand and foot remains from the Gran Dolina Early Pleistocene site (Sierra de Atapuerca, Spain). J. Hum. Evol. 37, 501-522.

Martin, R., 1928. Lehrbuch der Anthropologie. Fischer, Jena.

Masao, F.T., Ichumbaki, E.B., Cherin, M., Barili, A., Boschian, G., Iurino, D.A., Menconero, S., Moggi-Cecchi, J., Manzi, G., 2016. New footprints from Laetoli (Tanzania) provide evidence for marked body size variation in early hominins. Elife 5, e19568.

McHenry, H.M., 1992. Body size and proportions in early hominids. Am. J. Phys. Anthropol. 87, 407-431.

McHenry, H.M., 1994. Behavioral ecological implications of early hominid body size. J. Hum. Evol. 27, 77-87.

McKern, T.W., Stewart, T.D., 1957. Skeletal Age Changes in Young American Males, Analyzed from the Standpoint of Identification Headquarters Quartermaster Research and Development Command, Tech, Rep. EP-45, Natick, MA.

Morse, S.A., Bennett, M.R., Liutkus-Pierce, C., Thackeray, F., McClymont, J., Savage, R., Crompton, R.H., 2013. Holocene footprints in Namibia: The influence of substrate on footprint variability. Am. J. Phys. Anthropol. 151, 265-279.

Musiba, C.M., Tuttle, R.H., Hallgrimsson, B., Webb, D.M., 1997. Swift and sure-footed on the Savanna: A study of Hadzabe gaits and feet in Northern Tanzania. Am. J. Hum. Biol. 9, 303-321.

Niskanen, M., Ruff, C.B., Holt, B., Sládek, V., Berner, M., 2018. Temporal trends and geographic variation in body size and shape of Europeans from the Late Pleistocene to recent times. In: Ruff, C.B. (Ed.), Skeletal Variation and Adaptation in Europeans: Upper Paleolithic to the Twentieth Century. Wiley-Blackwell, Hoboken, pp. 49-89.

Pales, L., 1976. Les Emprientes de Pieds Humains dans les Cavernes. Archives de l'Institut de Paleontologie Humanine, Memoire 36. Masson, Paris.

Plavcan, J.M., 1994. Comparison of four simple methods for estimating sexual dimorphism in fossils. Am. J. Phys. Anthropol. 94, 465-476.

Pontzer, H., 2012. Ecological energetics in early *Homo*. Curr Anthropol. 53, Suppl. 6, S346-348.

Raichlen, D.A., Gordon, A.D., Harcourt-Smith, W.E.H., Foster, A.D., Haas, W.R., 2010. Laetoli footprints preserve earliest direct evidence of human-like bipedal biomechanics. PLoS One. 5, e9769.

Reed, R.B., Stuart, H.C., 1959. Patterns of growth in height and weight from birth to eighteen years of age. Pediatrics 24, 904-921.

Roach, N.T., Du, A., Hatala, K.G., Ostrofsky, K.R., Reeves, J.S., Braun, D.R., Harris, J.W.K., Behrensmeyer, A.K., Richmond, B.G., 2018. Pleistocene animal communities of a 1.5 million-year-old lake margin grassland and their relationship to *Homo erectus* paleoecology. J. Hum. Evol. 122, 70-83.

Roach, N.T., Hatala, K.G., Ostrofsky, K.R., Villmoare, B., Reeves, J.S., Du, A., Braun, D.R., Harris, J.W., Behrensmeyer, A.K., Richmond, B.G., 2016. Pleistocene footprints show intensive use of lake margin habitats by *Homo erectus* groups. Sci. Rep. 6, 26374.

Robbins, L.M., 1985. Footprints: Collection, Analysis and Interpretation. Charles C. Thomas, Springfield, IL.

Robbins, L.M., 1986. Estimating height and weight from size of footprints. J. Forensic Sci. 31, 143-152.

Robbins, L.M., 1987. Hominid footprints from Site G. In: Leakey, M.D., Harris, J.M. (Eds.), Laetoli: A Pliocene Site in Northern Tanzania. Clarendon Press, Oxford, pp. 497-502.

Rosenberg, K.R., Lü, Z., Ruff, C.B., 2006. Body size, body proportions and encephalization in a Middle Pleistocene archaic human from northern China. Proc. Natl. Acad. Sci. USA 103, 3552-3556.

Ruff, C.B., 1994. Morphological adaptation to climate in modern and fossil hominids. Yearb. Phys. Anthropol. 37, 65-107.

Ruff, C.B., 2010. Body size and body shape in early hominins - implications of the Gona pelvis. J. Hum. Evol. 58, 166-178.

Ruff, C.B., 2017. Mechanical constraints on the hominin pelvis and the "obstetrical dilemma". Anat. Rec. 30, 946-955.

Ruff, C.B., Burgess, M.L., Squyres, N., Junno, J.-A., Trinkaus, E., 2018. Lower limb articular scaling and body mass estimation in Pliocene and Pleistocene hominins. J. Hum. Evol. 115, 85-111.

Ruff, C.B., Niskanen, M., 2018. Introduction to special issue: Body mass estimation - Methodological issues and fossil applications. J. Hum. Evol. 115, 1-7.

Ruff, C.B., Niskanen, M., Junno, J.A., Jamison, P., 2005. Body mass prediction from stature and bi-iliac breadth in two high latitude populations, with application to earlier higher latitude humans. J. Hum. Evol. 48, 381-392.

Ruff, C.B., Squyres, N., Junno, J.-A., 2020. Body mass estimation in hominins from humeral articular dimensions. Am. J. Phys. Anthropol. 173, 480-499.

Ruff, C.B., Trinkaus, E., Holliday, T.W., 2002. Body proportions and size. In: Zilhão, J., Trinkaus, E. (Eds.), Portrait of the Artist as a Child: The Gravettian Human Skeleton from the Abrigo do Lagar Velho and its Archaeological Context. Instituto Português de Arqueologia, Lisbon, pp. 365-391.

Scheuer, L., Black, S., 2000. Developmental Juvenile Osteology. Academic Press, San Diego.

Schmid, P., 1983. Eine rekonstruktion des skelettes von A.L. 288-1 (Hadar) und deren konsequenzen. Folia Primatol. 40, 283-306.

Schmid, P., 2004. Functional interpretation of the Laetoli footprints. In: Meldrum, D.J., Hilton, C.E. (Eds.), The Emergence of Modern human Walking, Running, and Resource Transport. Kluwer Academic/Plenum Publishers, New York, pp. 49-62.

Schmidt-Nielson, K., 1984. Scaling: Why is Animal Size So Important? Cambridge Univ. Press, Cambridge.

Sjøvold, T., 1990. Estimation of stature from long bones utilizing the line of organic correlation. Hum. Evol. 5, 431-447.

Smith, B.H., 1991. Standards of human tooth formation and dental age assessment. In: Kelley, M.A., Larsen, C.S. (Eds.), Advances in Dental Anthropology. Wiley-Liss, New York, pp. 143-168.

Smith, B.H., Crunnett, T.L., Brandt, K.L., 1994. Ages of eruption of primate teeth: A compendium for aging individuals and comparing life histories. Yearb. Phys Anthropol. 37, 177-231.

Sokal, R.R., Rohlf, F.J., 1981. Biometry, 2nd ed. W.H. Freeman, New York.

Spoor, F., Leakey, M.G., Gathogo, P.N., Brown, F.H., Anton, S.C., McDougall, I., Kiarie, C., Manthi, F.K., Leakey, L.N., 2007. Implications of new early *Homo* fossils from Ileret, east of Lake Turkana, Kenya. Nature 448, 688-691.

Squyres, N., Ruff, C.B., 2015. Body mass estimation from knee breadth, with application to early hominins. Am. J. Phys. Anthropol. 158, 198-208.

SYSTAT13, 2009. SYSTAT Software, Inc., Chicago.

Trinkaus, E., Stringer, C.B., Ruff, C.B., Hennessy, R.J., Roberts, M.B., Parfitt, S.A., 1999. Diaphyseal cross-sectional geometry of the Boxgrove 1 Middle Pleistocene human tibia. J. Hum. Evol. 37, 1-25.

Tsung, B.Y., Zhang, M., Fan, Y.B., Boone, D.A., 2003. Quantitative comparison of plantar foot shapes under different weight-bearing conditions. J. Rehabil. Res. Dev. 40, 517-526.

Tuttle, R., Webb, D., Weidl, E., Baksh, M., 1990. Further progress on the Laetoli trails. J. Archaeol. Sci. 17, 347-362.

Tuttle, R.H., 1987. Kinesiological inferences and evolutionary implications from Laetoli bipedal trails G-1, G-2/3 and A. In: Leakey, M.D., Harris, J.M. (Eds.), Laetoli: A Pliocene Site in Northern Tanzania. Clarendon Press, Oxford, pp. 503-523.

Villmoare, B., Hatala, K.G., Jungers, W., 2019. Sexual dimorphism in *Homo erectus* inferred from 1.5 Ma footprints near Ileret, Kenya. Sci. Rep. 9, 7687.

Walker, A., Leakey, R., 1993. The Nariokotome *Homo erectus* Skeleton. Harvard University Press, Cambridge.

Wall-Scheffler, C.M., Wagnild, J., Wagler, E., 2015. Human footprint variation while performing load bearing tasks. PLoS One 10, e0118619.

Weaver, T.D., 2003. The shape of the Neandertal femur is primarily the consequence of a hyperpolar body form. Proc. Natl. Acad. Sci. USA 100, 6926-6929.

Webb, D., Bernardo, D.V., Hermenegildo, T., 2006. Evaluating and improving footprint measurement: Orientation and lengths. Anthropologie 44, 277-287.

White, T.D., 1980. Evolutionary implications of Pliocene hominid footprints. Science 208, 175-176.

White, T.D., 1985. The hominids of Hadar and Laetoli: An element-by-element comparison of the dental samples. In: Delson, E. (Ed.), Ancestors: The Hard Evidence. Alan R. Liss, New York, pp. 138-152.

White, T.D., Suwa, G., 1987. Hominid footprints at Laetoli: Facts and interpretations. Am. J. Phys. Anthropol. 72, 485-514.

WHO, 1995. Physical Status: The Use and Interpretation of Anthropometry. World Health Organization, Geneva.

Wiseman, A.L.A., Stringer, C.B., Ashton, N., Bennett, M.R., Hatala, K.G., Duffy, S., O'Brien, T., De Groote, I., 2020. The morphological affinity of the Early Pleistocene footprints from Happisburgh, England, with other footprints of Pliocene, Pleistocene, and Holocene age. J. Hum. Evol. 144, 102776.

Wunderlich, R.E., Cavanagh, P.R., 2001. Gender differences in adult foot shape: Implications for shoe design. Med. Sci. Sports Exerc. 33, 605-611.

Xiong, S.P., Goonetilleke, R.S., Zhao, J.H., Li, W.Y., Witana, C.P., 2009. Foot deformations under different load-bearing conditions and their relationships to stature and body weight. Anthropol Sci. 117, 77-88.

Figure Legends

Figure 1. Body mass versus foot area in pooled adult sample, with quadratic regression (see Table 5 for equation).

Figure 2. Body mass versus foot area (maximum length × forefoot breadth) in five habitually unshod adult samples. Least squares regressions fit through each sample. Regression slopes are equivalent, but elevations are highly significantly different, with higher-BMI samples having relatively larger body mass for foot area.

Figure 3. Body mass index (BMI, [body mass/stature^2] × 100) versus foot index ([foot breadth/foot length] × 100) in five adult samples. The two variables are only weakly correlated, but very low and very high foot index values are generally associated with low and high BMI values.

Figure 4. Box plots of foot area/body mass in adults (filled) and juveniles (under 16 years, open) in four samples. Juveniles have significantly larger feet for their body mass in all samples.

Figure 5. Body mass versus foot area in Machiguenga (blue circles) and Daasanach (orange squares) by age group: filled symbols adults; open symbols: juveniles. Least squares regressions fit through each sample/age group. Juveniles have smaller body masses for their foot size, but approach adults in adolescence. Difference in body mass/foot size proportions observed between the two adult samples are also characteristic of juveniles.

Figure 6. Body mass index (BMI) versus age in pooled juvenile and adult sample, fit with LOWESS regression. BMI increases through late adolescence.

Figure 7. Actual/adult predicted body mass versus actual/adult foot area in pooled juvenile sample, with least squares regressions: b) body mass predicted using quadratic equation in Table 5; a) body mass predicted using BMI equation in Table 5. SEE = standard error of estimate. The formulae in the figures are used to calculate body mass adjustment factors to apply to preliminary estimates for juveniles derived from adult equations.

Figure 8. Foot area (length × breadth)/body mass in habitually unshod and shod Indians and habitually shod Europeans. All pairwise differences between samples are significant.

Figure 9. True foot contact area/'area' (length × breadth) versus body mass index (BMI) in habitually unshod Indians, with least squares regression. Relatively more of the foot is in contact with the support surface with increasing BMI.

Figure 10. a) Foot area/body mass ratio in pooled modern human 10–15.9-year-olds and adolescent chimpanzees. b) Body mass versus foot area in same samples, with least squares regression through humans (circles); stars: chimpanzees. Chimpanzees have relatively larger feet and thus human regressions will overestimate their body masses.

Figure 11. Foot length versus stature in pooled modern adults (blue circles) and juveniles (green crosses) from the present study, Akka adult female (filled blue circle), adolescent chimpanzees

(filled black stars), and A.L. 288-1 (filled brown hexagon). A.L. 288-1 has a foot length to stature proportion that is intermediate between those of human children and chimpanzees, and closer to chimpanzees than to adult humans.

Figure 12. Body mass versus foot area in modern human pooled sample, with quadratic regression (circles), and A.L. 288-1 (filled brown hexagon). Body mass in A.L. 288-1 estimated using BMI = 25 in equation in Table 5; foot area estimated from foot length using average foot index of Laetoli prints (see text). The quadratic equation will overestimate body mass in A.L. 288-1 by 50%.

Figure 13. Body mass versus foot area in juveniles (open symbols) and adults (filled circles). a) Machiguenga. Blue diamonds: males; red circles: females. Note the large spread of body mass values at foot areas of about 135–155 cm^2. b) Le Rozel Neandertals. Body mass estimated from foot area using BMI = 27 (Table 5). Blue diamonds: probable adult male(s); orange hexagons: smaller adults or juveniles; green triangles: juveniles. Juvenile estimates adjusted using equation in Figure 7b. Both adult and juvenile (adjusted) estimates shown for small adults/juveniles.

Figure 14. Body mass estimated from foot area using the BMI and quadratic equations in Table 5 for foot areas of 140–350 cm^2 and BMIs of 22–27. Dashed line = equivalence. BMI-based estimates are generally larger than quadratic equation estimates, except in the largest foot area range.

Figure

Click here to access/download;Figure;Fig. 1.tif

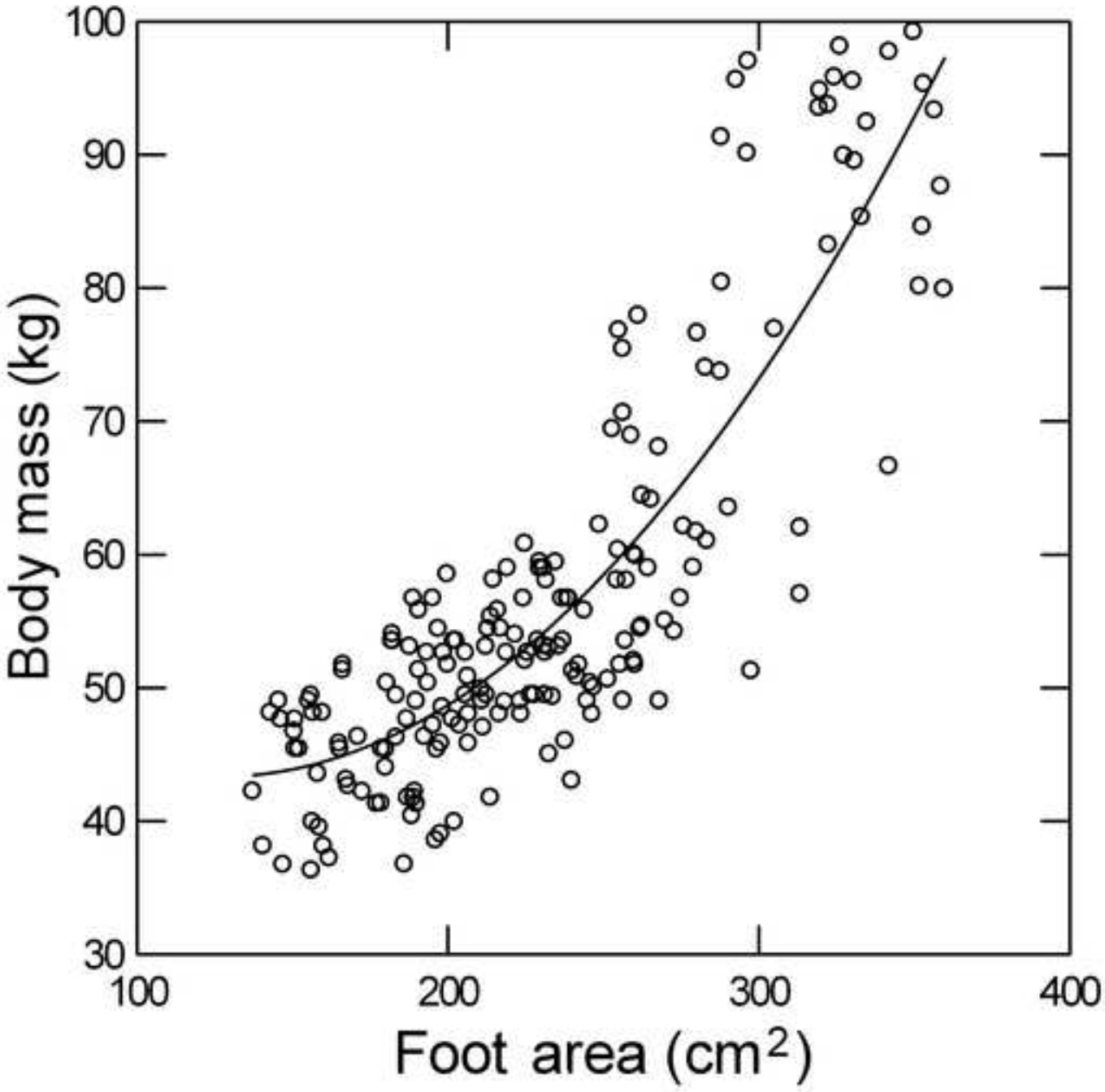

Figure

Click here to access/download;Figure;Fig. 2.tif

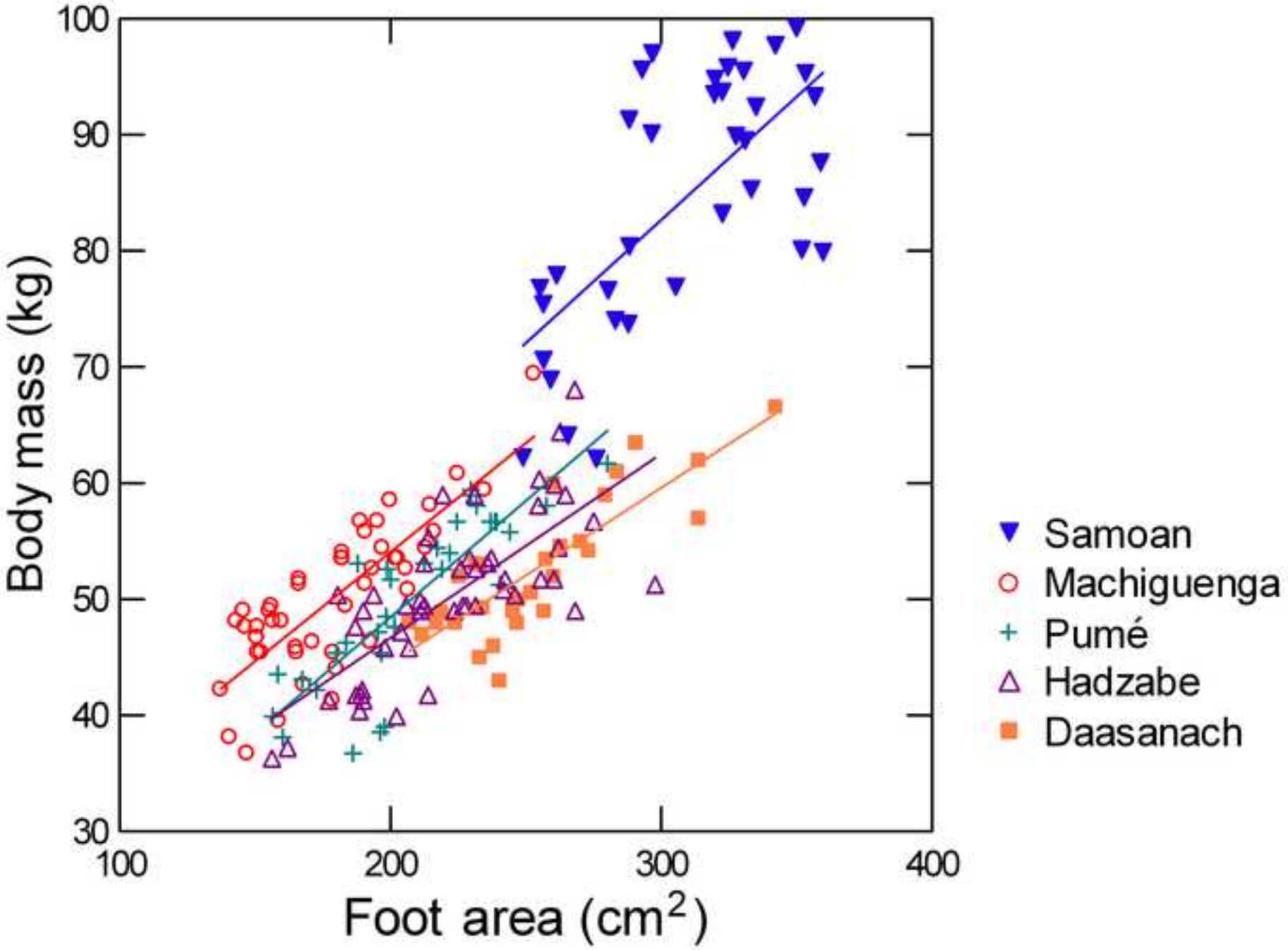

Figure

Click here to access/download;Figure;Fig. 3.tif

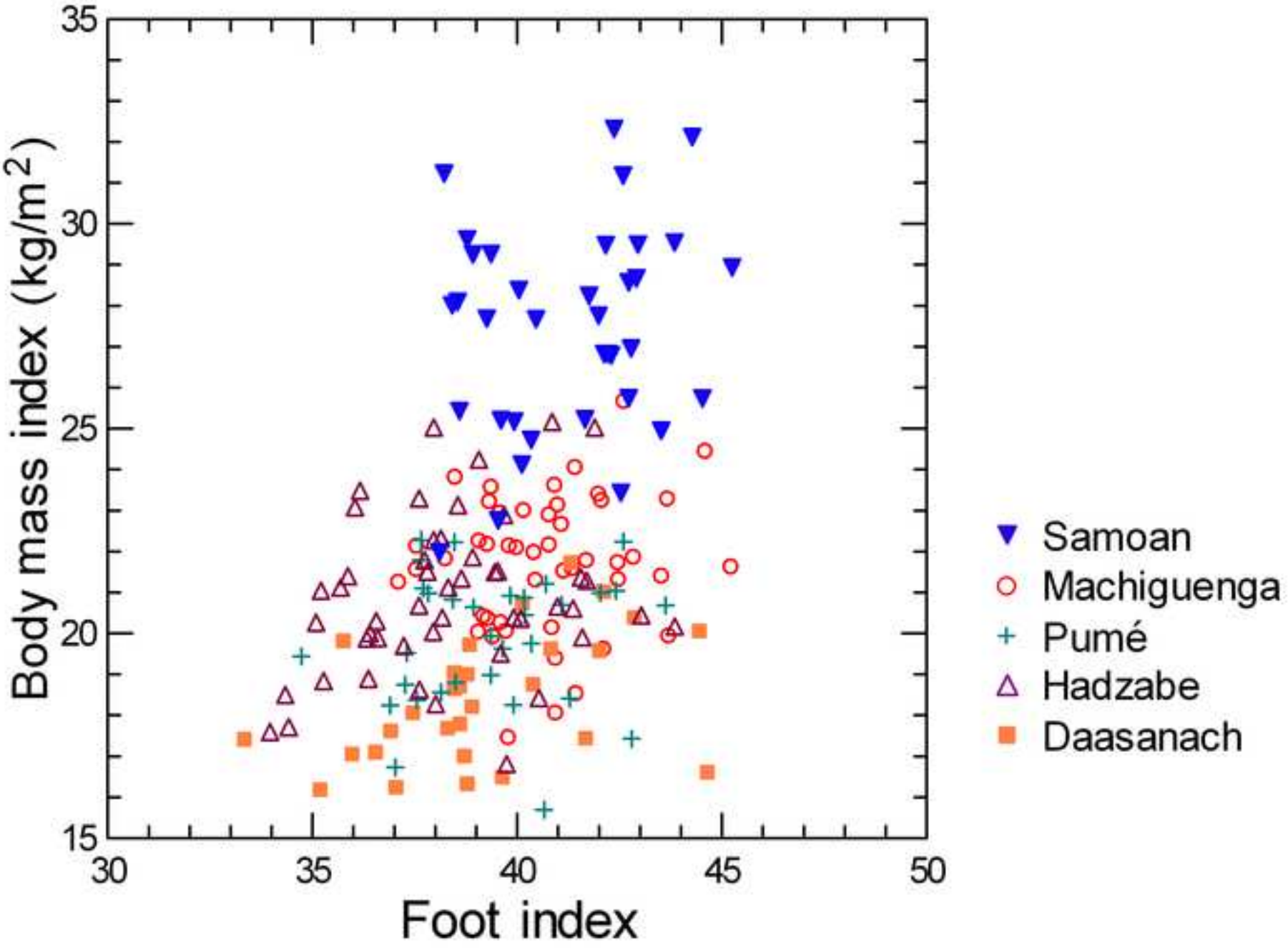

Figure

Click here to access/download;Figure;Fig. 4.tif

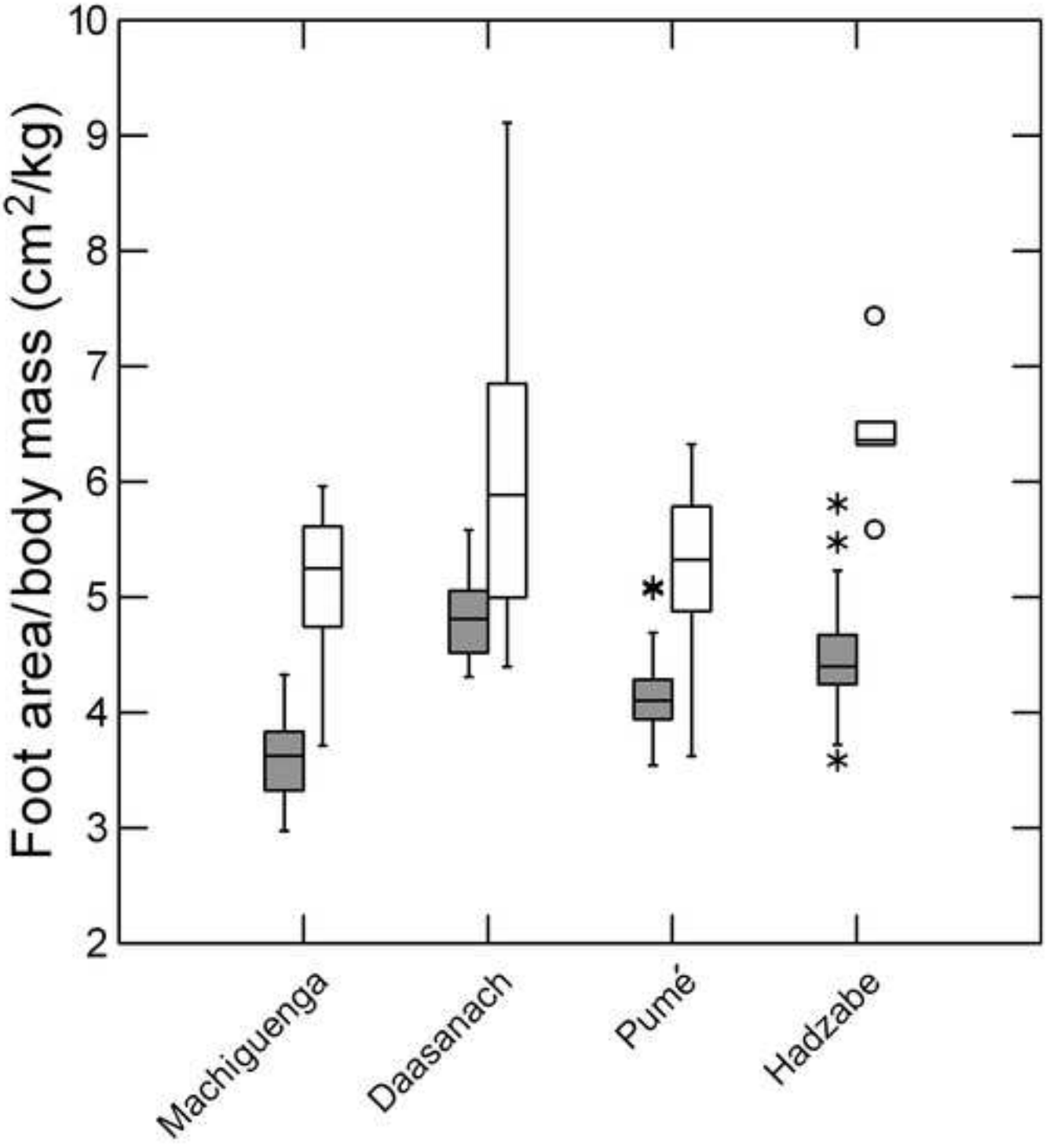

Figure

Click here to access/download;Figure;Fig. 5.tif

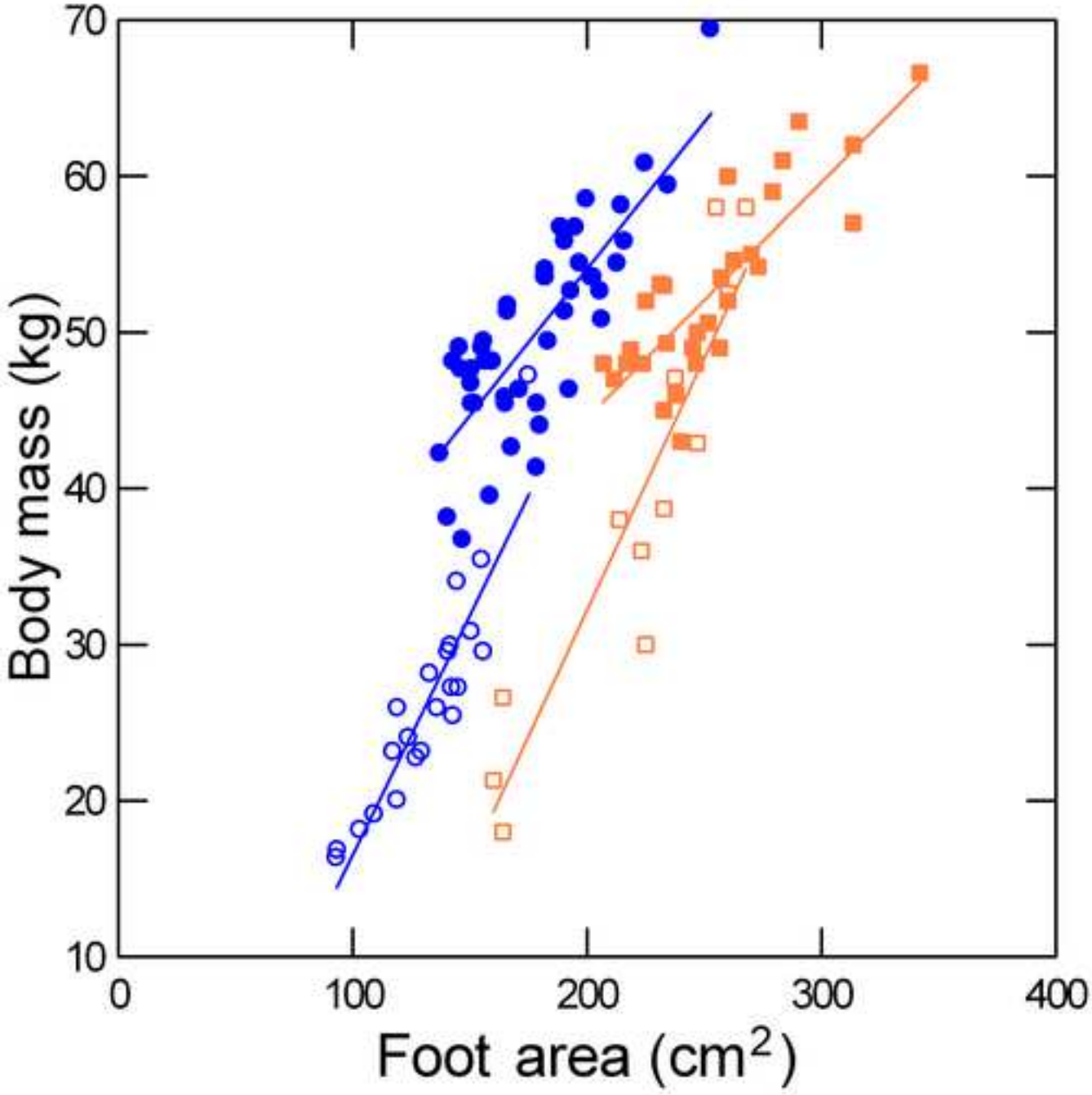

Figure

Click here to access/download;Figure;Fig. 6.tif

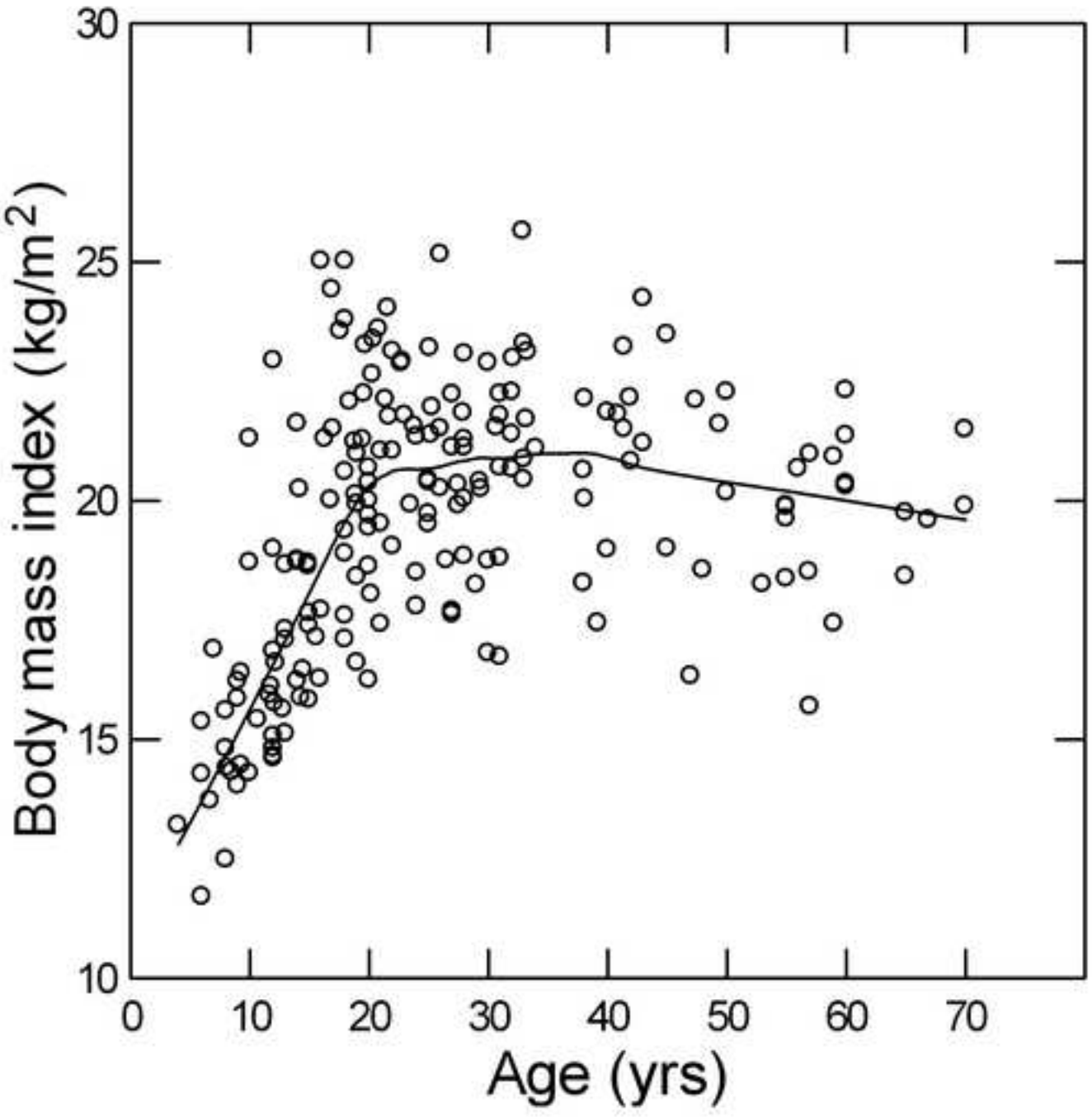

Figure

Click here to access/download;Figure;Fig. 7.tif

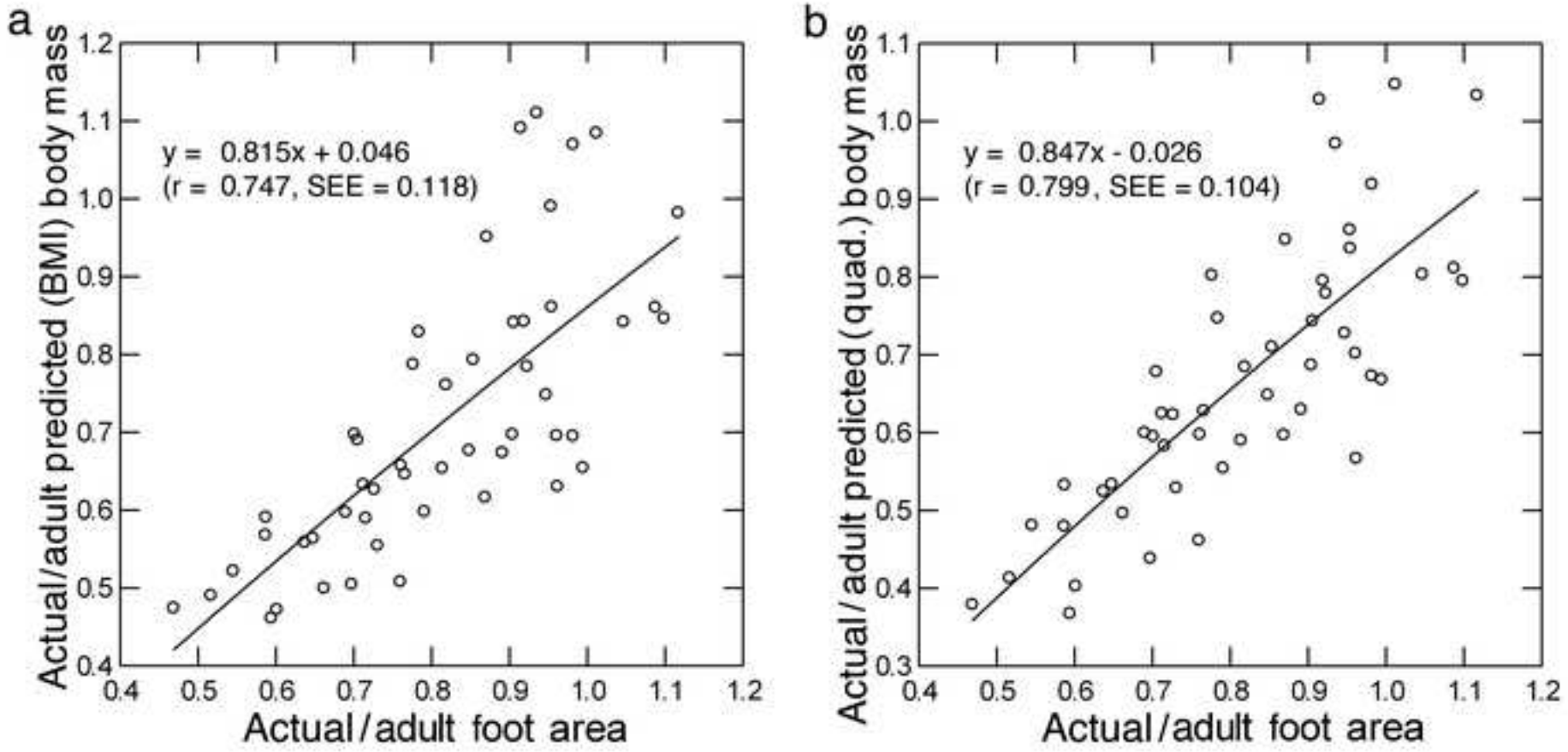

Figure

Click here to access/download;Figure;Fig. 8.tif

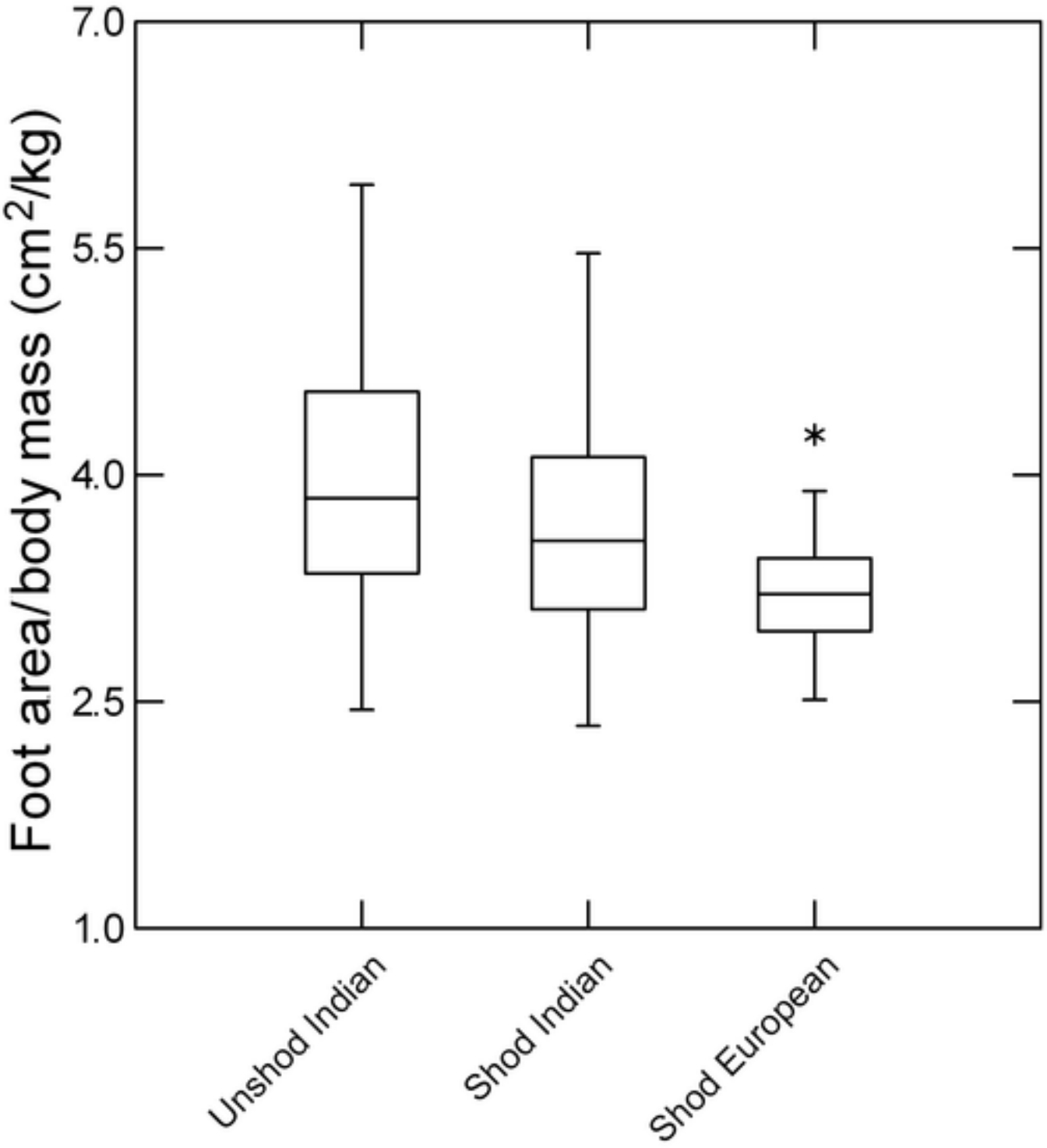

Figure

Click here to access/download;Figure;Fig. 9.tif

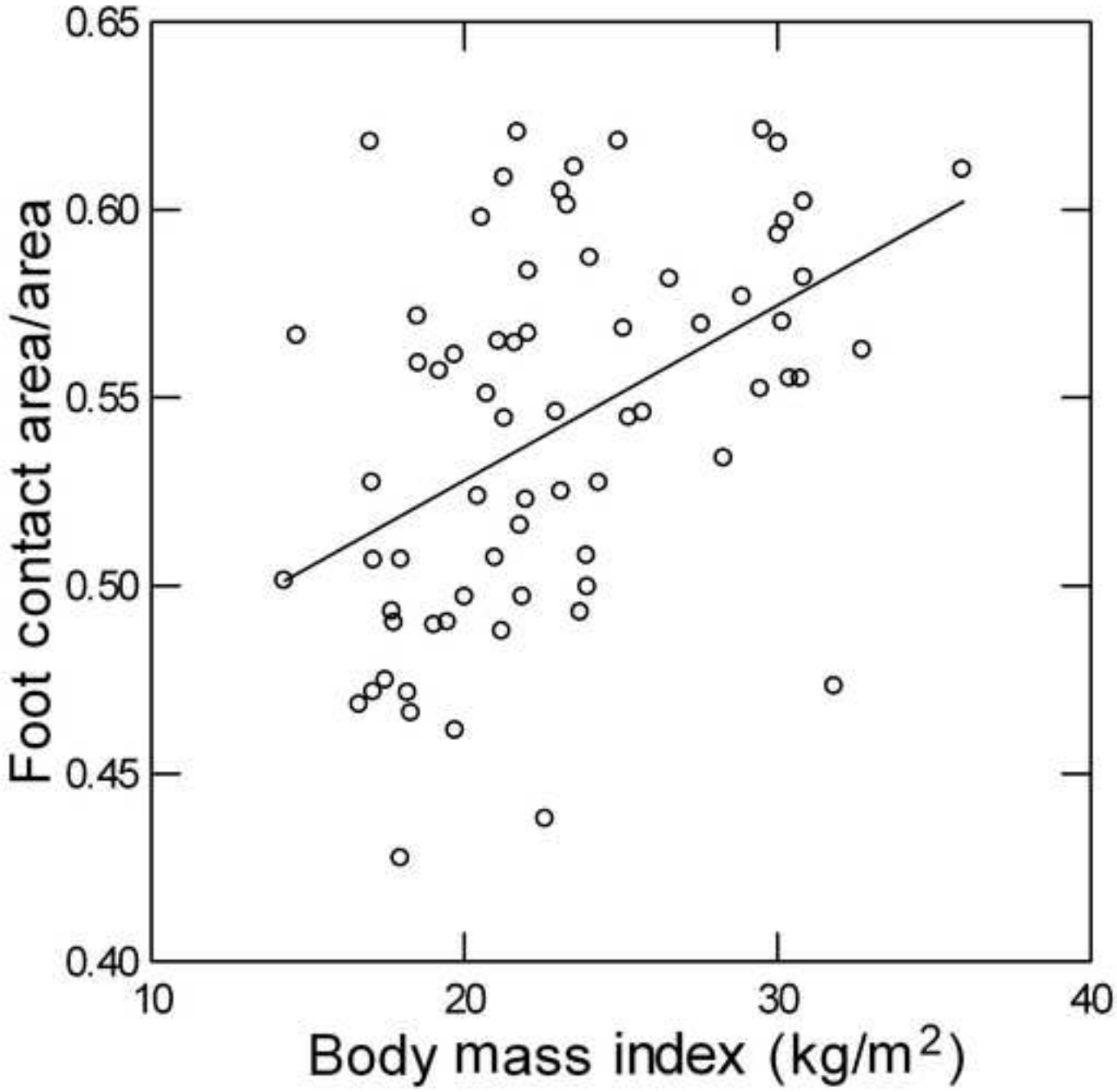

Figure

Click here to access/download;Figure;Fig. 10.tif

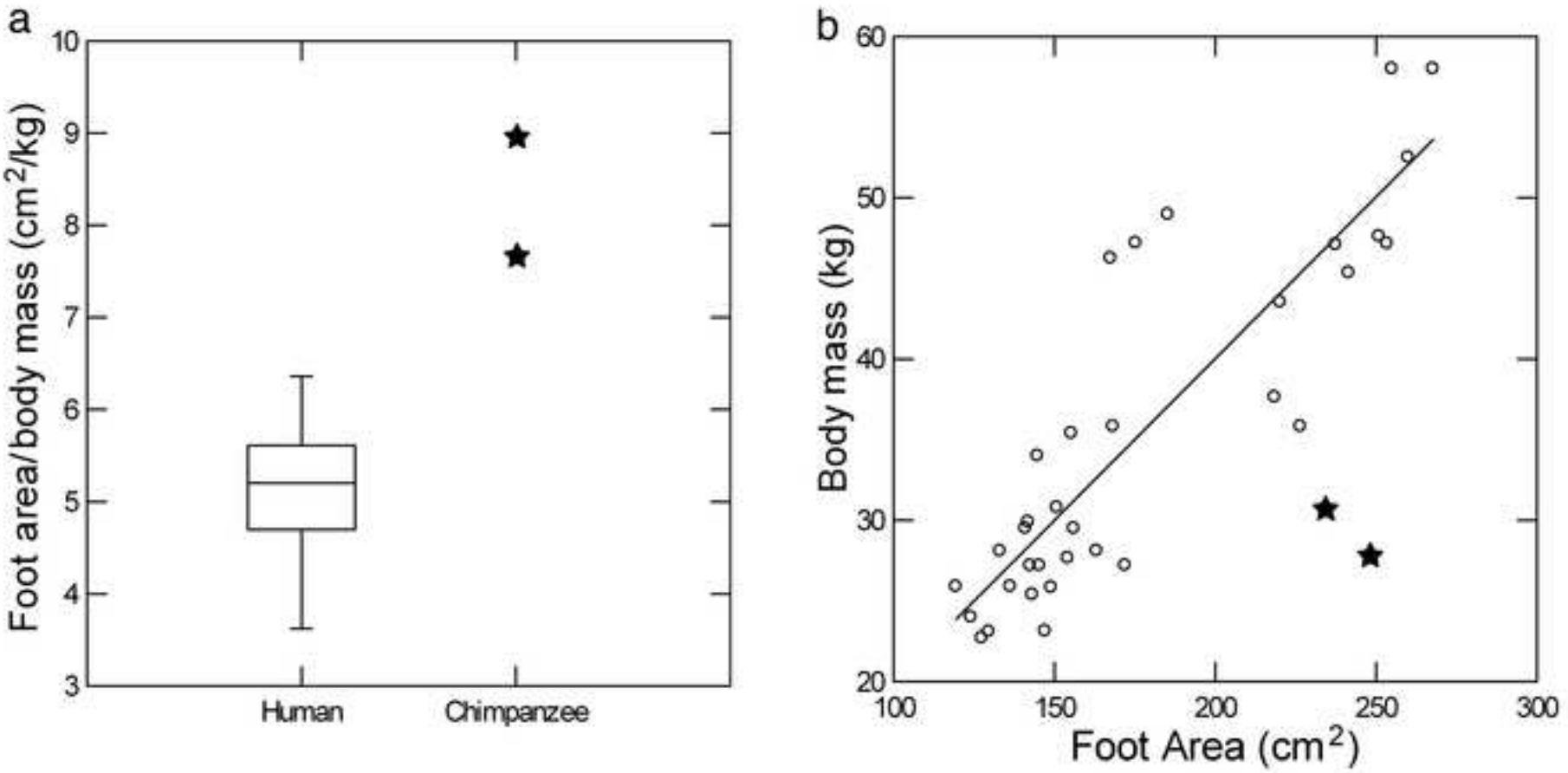

Figure

Click here to access/download;Figure;Fig. 11.tif

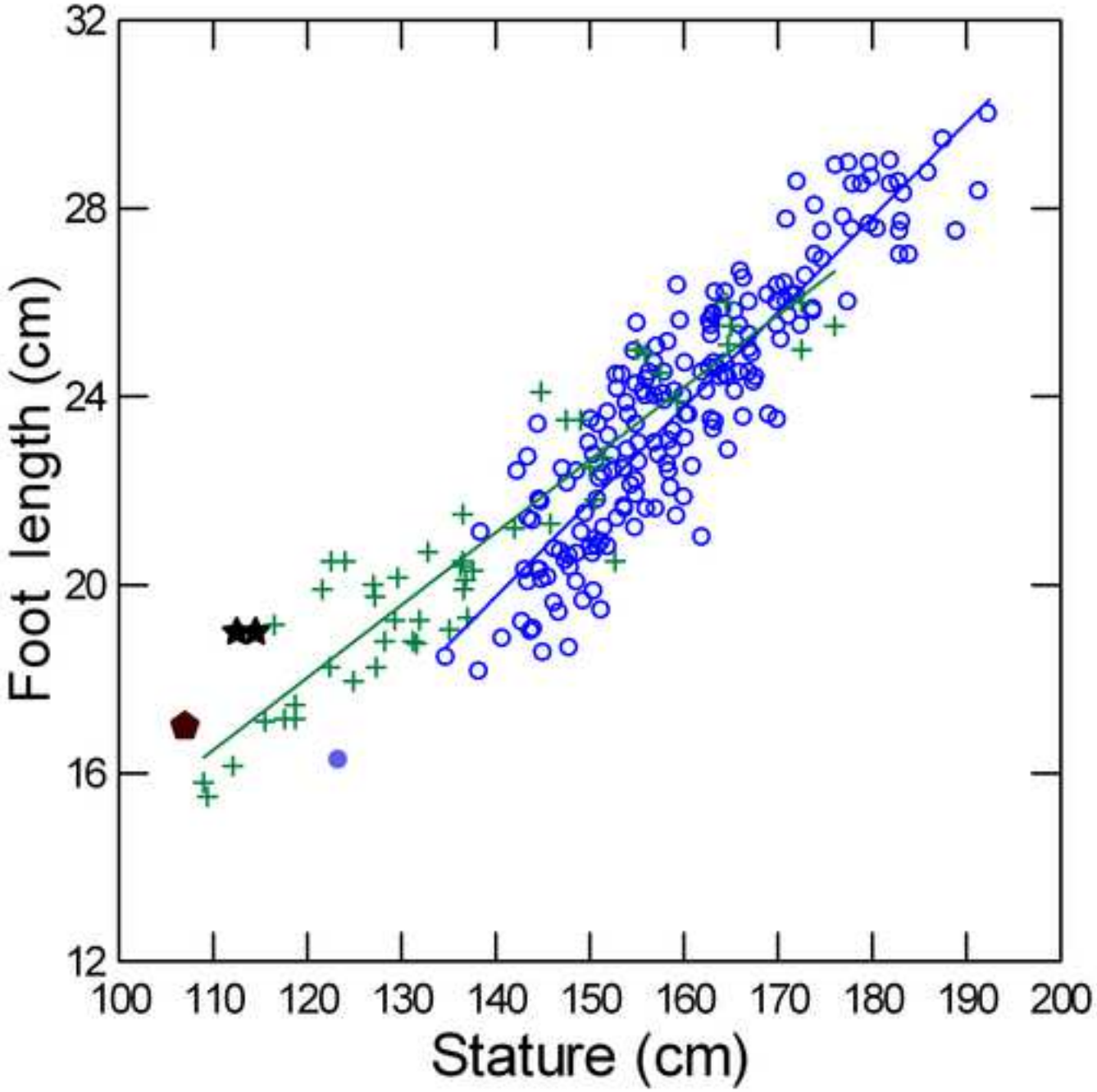

Figure

Click here to access/download;Figure;Fig. 12.tif

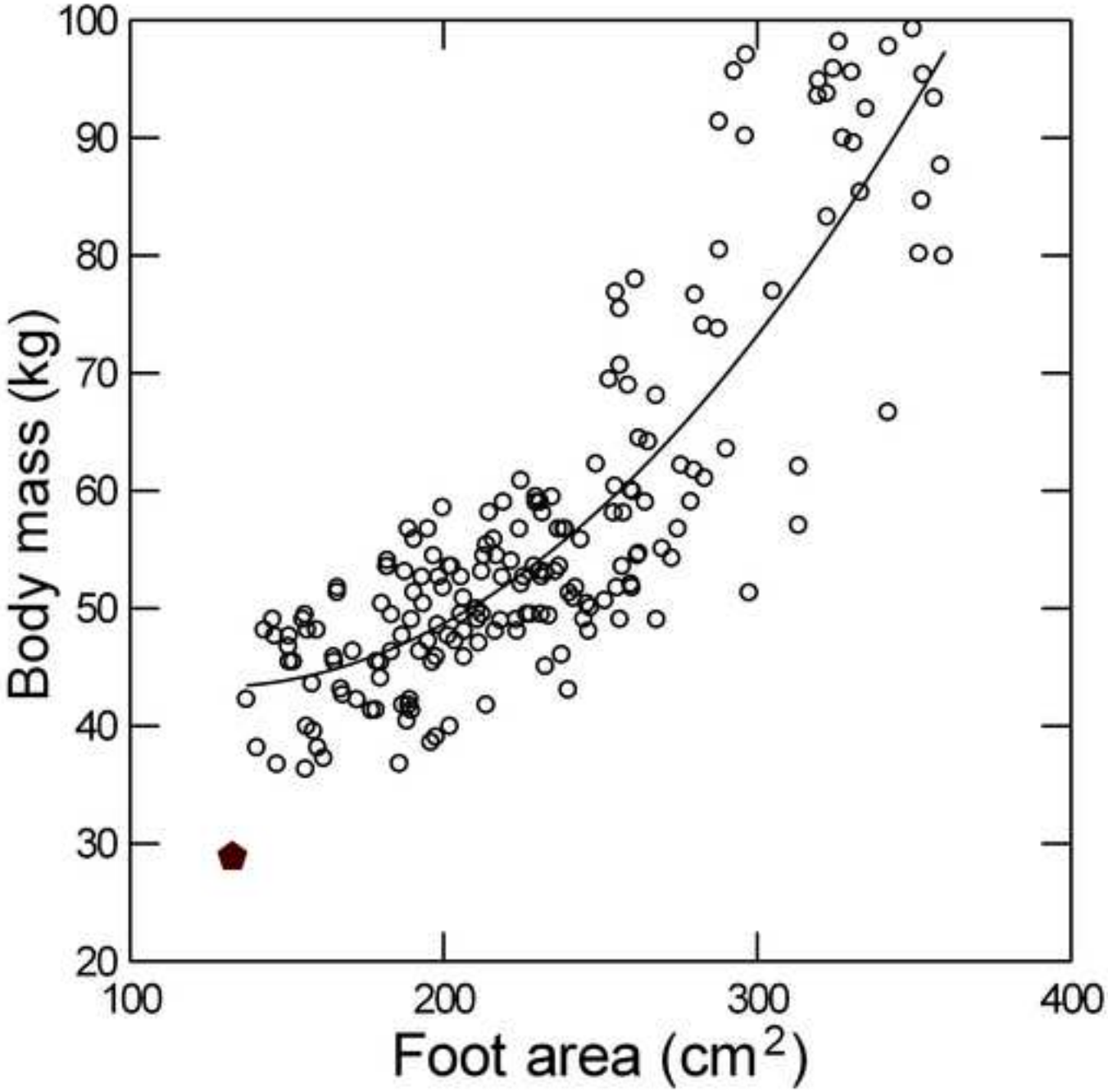

Figure

Click here to access/download;Figure;Fig. 13.tif

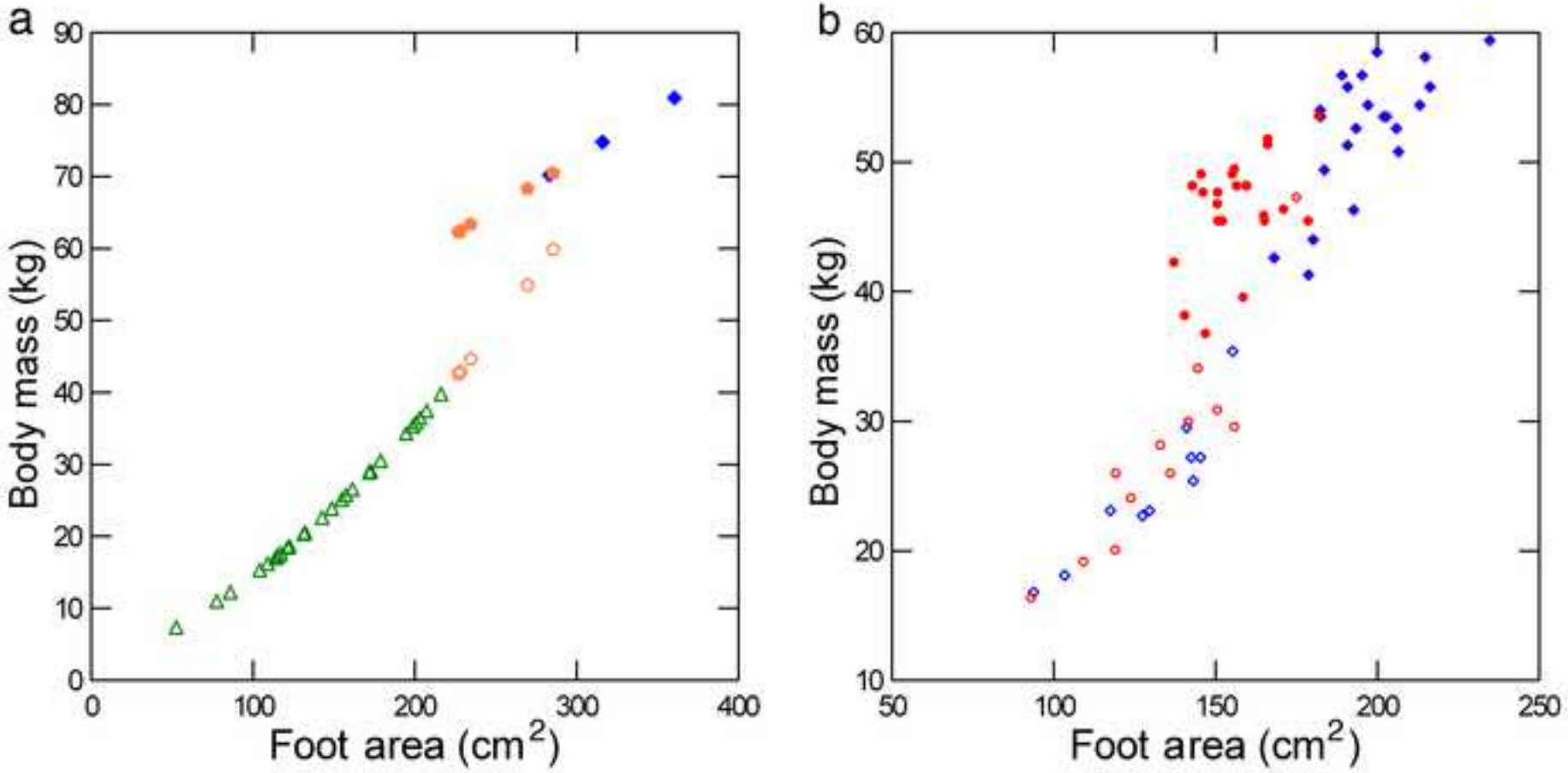

Figure

Click here to access/download;Figure;Fig. 14.tif

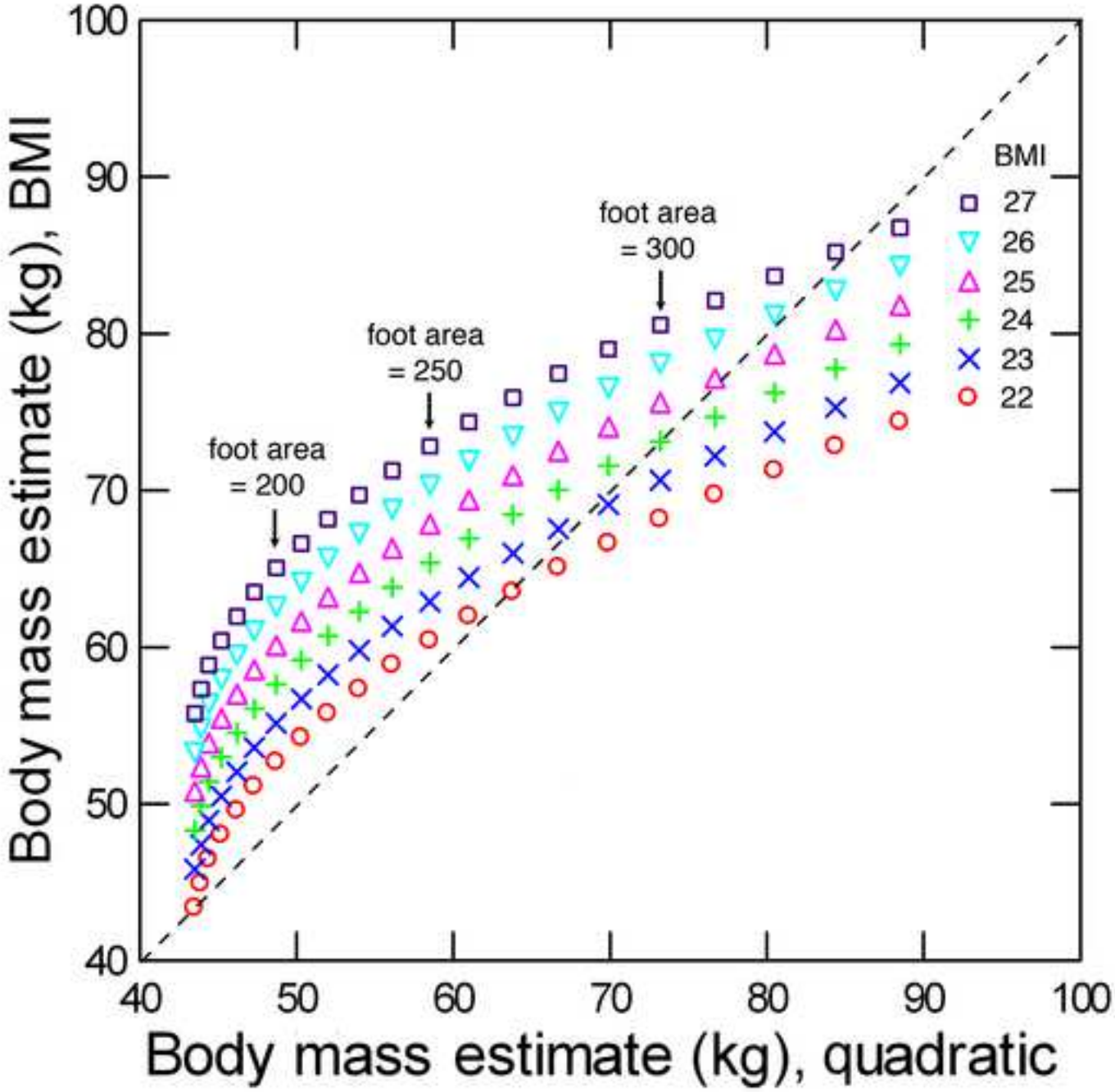

Table 1

Past studies of human body mass estimation from foot size.

Study	Sample	Method
Robbins, 1986	Shod US, mixed ages	Footprint, paper, standing
Anil et al., 1997	Shod Turkish, young adults	Foot, standing
Atamtürk and Duyar, 2008	Shod Turkish, adults	Foot, standing
Krishan, 2008	Unshod (?) Gujjar Indians, adult males	Footprint, paper, standing
Fawzy and Kamal, 2010	Shod Egyptian, young adult males	Footprint, paper, standing
Dingwall et al., 2013	Unshod Daasanach, adults	Footprint, naturalistic, walking and running
Bennett and Morse, 2014	Shod British, mixed ages	Footprint, paper, standing
Domjanic et al., 2015	Shod Croatian, young adults	Foot scans, standing

Table 2

Modern unshod reference samples.

		Adults[a]												Juveniles	
			Body mass		Stature		BMI		Foot length		Foot breadth		Foot area		
Population	Ref[b]	*n* (M/F)[c]	Mean	SD	Mean	SD	Mean	SD	Mean	SD	Mean	SD	Mean	SD	*n*	Age range
Machiguenga	1	47(24/23)	50.1	6.3	151.7	7.4	21.7	1.7	21.0	1.6	8.5	0.7	178.9	26.9	22	6.7–15.9
Daasanach	2	29(15/14)	52.6	5.9	169.1	9.0	18.4	1.6	25.5	1.8	9.9	0.7	253.9	32.3	12	4–15
Pumé	3	32(17/15)	50.1	7.2	158.4	7.9	19.9	1.6	22.9	1.6	9.0	0.8	208.1	30.2	11	12–15
Hadzabe	4	49(22/27)	50.3	6.8	154.9	7.4	20.9	1.9	24.0	1.5	9.2	0.8	222.8	31.9	5	6–12
Samoan	5	36(26/10)	84.5	11.0	175.4	8.8	27.4	2.5	27.3	1.4	11.3	0.8	308.8	34.9	---	---

Body mass in kg; stature, foot length, and foot breadth in cm; foot area in cm^2. BMI: [body mass/(stature in m)^2]. Age range in years.

[a] Individuals 16 years of age or older.

[b] Ref = References: 1: Tuttle et al., 1990; 2: Hatala et al., 2016; 3: Hilton, unpub. data; 4: Musiba et al., 1997; 5: Wunderlich, unpub. data.

[c] M = male; F = female.

Table 3

Footprint to foot conversion factors.

	Foot/footprint							
	Area		Length		Breadth		Index[b]	
Trial condition	Mean	SE[a]	Mean	SE	Mean	SE	Mean	SE
Normal walking	1.003	0.016	0.984*	0.006	1.020	0.012	1.038*	0.014
Jog and run	0.967*	0.014	0.991*	0.006	0.974*	0.012	0.983	0.012

[a] Standard error of the mean

[b] (Foot breadth/foot length) x 100.

* $p < 0.05$, paired t test between foot and footprint dimension. Only these ratios were used as conversion factors (see text).

Table 4

Footprint test samples.

Site	References[a]	Taxon[b]	Date	#Trackways/prints
Laetolil	1	*A. afarensis*	~3.66 Ma	4/
Ileret	2	(*H. erectus*)	~1.52 Ma	9/
Happisburgh	3	(*H. antecessor*?)	~0.78–1.0 Ma	/3
Le Rozel	4	archaic *H. sapiens*	~80,000 BP	/35[c]
Barcun Hoyük	5	*H. sapiens*	~6400 BC	/1

[a] References: 1 = Masao et al., 2016; 2 = Hatala et al., 2017; 3 = Ashton et al., 2014; 4 = Duveau et al., 2019; 5 = Atamtürk et al., 2018.

[b] Parentheses indicate probable (*H. erectus*) or possible (*H. antecessor*) attributions.

[c] Includes both adults and juveniles. All other samples adults only.

Table 5

Body mass prediction equations.

Equation[a]	r	SEE	%SEE	%PE
Quadratic				
(1) Body mass = –0.250 × Foot area + 0.00099 × Foot area^2 + 59.1	0.861	7.80	13.7%	10.1%
(2) Body mass = –21.9 × Foot length + 0.546 × Foot length^2 + 265.4	0.808	9.03	15.9%	11.4%
(3) Body mass = –25.8 ×Foot breadth + 1.84 × Foot breadth^2 + 133.3	0.853	8.01	14.1%	10.0%
Linear, with BMI				
(4) Body mass = 0.155 × Foot area + 2.48 × BMI – 32.9	0.965	3.97	7.0%	5.4%
(5) Body mass = 2.88 × Foot length + 2.85 × BMI – 73.9	0.961	4.20	7.6%	5.8%
(6) Body mass = 6.60 ×Foot breadth + 2.44 × BMI – 59.0	0.949	4.79	8.4%	6.7%

[a] Body mass in kg; foot area in cm^2; foot length and breadth in cm. Foot area = foot length x foot breadth. BMI = body mass index.

SEE = standard error of estimate; %SEE = percent standard error of estimate; %PE = absolute value of percent prediction error.

Table 6

Flowchart of steps in estimating body mass from footprint size. Dotted lines = optional steps.

1) Adults

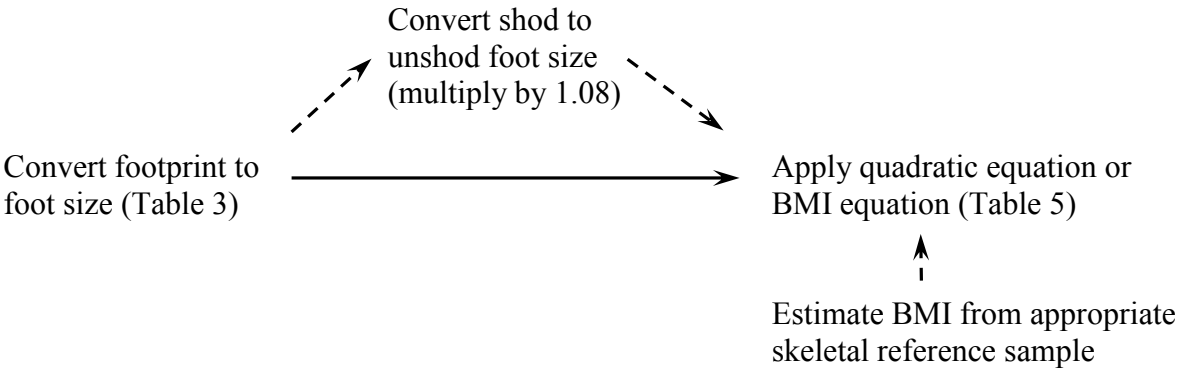

2) Additional steps for juveniles

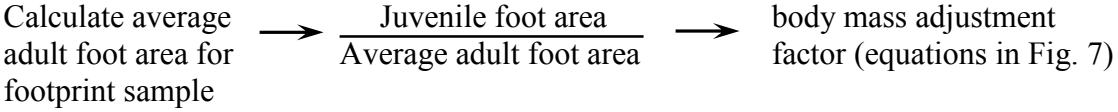

Apply body mass adjustment factor to juvenile body mass, calculated using adult equations

Table 7

Body mass estimates for the Laetoli sample.

	Dimension[a]				Body mass estimate (kg)			
					Present[b]		Previous[c]	
Trackway	Print length	Print breadth	Foot area	Foot length	Quadratic	BMI = 25	Masao-1	Masao-2
S1	26.1	10.4	271.4		64.2	71.2	53.6	41.3–48.1
S2	23.1			22.7	49.6	62.7	46.7	36.5–42.4
G1	18.0	7.9	142.2		43.6	51.1	39.3	28.5–33.1
G2	22.5	11.7	263.3		61.9	69.9	52.6	35.6–41.4
G3	20.9	8.5	177.7		45.9	56.6	43.2	33.1–38.5
Mean					53.0	62.3	47.1	37.8[d]

[a] Print length and breadth, foot length in cm, foot area in cm^2. Foot area = print length × print breadth. Foot length calculated from print length using equation in Table 3.

[b] Calculated using equations (1), (2), (4), and (5) in Table 5. BMI = body mass index.

[c] Estimates from Masao et al., 2016: Masao-1 = '*H. sapiens*' method; Masao-2 = '*Au. afarensis'* method (see text).

[d] Mean of the midpoints of ranges.

Table 8

Body mass estimates for the Laetoli sample using body mass/foot area ratio.

Trackway	Foot area	Body mass[a]
S1	271.4	59.2
S2	244.9 [b]	53.4
G1	142.2	31.0
G2	263.3	57.4
G3	177.7	38.7

[a] Foot area × 0.218, based on A.L. 288-1 (see text).
[b] Foot area calculated from foot length (see text).

Table 9

Body mass estimates for the Ileret sample.

				Body mass estimate (kg)			
	Dimension[a]			Present[b]		Previous	
Trackway	Print length	Print breadth	Foot area	Quadratic	BMI = 24	Dingwall[c]	Hatala[d]
FE1-HT1	26.8	9.0	242.1	56.6	64.1		
FLT1	25.5	8.0	211.7	49.3	58.2	48.0	35.3
FU-AD	26.0	11.0	280.8	68.9	71.1		51.1
FU-E	25.3	10.7	267.1	64.1	68.6		50.2
FU-O	28.0	9.5	262.0	62.6	67.9		50.8
FUT1A	25.6	10.1	256.1	60.6	66.6	50.6	50.3
FUT1B	26.7	9.6	254.1	60.0	66.3	52.1	53.2
FUT2	26.8	11.0	284.2	69.4	71.4	60.3	53.4
FUT3	25.3	9.3	235.1	54.8	62.9	44.5	46.4
A2-I2	21.1	7.7	173.7	44.6	51.8	41.5	
A2-I3	26.5	10.0	261.9	62.4	67.7	52.7	
Mean				59.4	65.1		
Mean[c]				57.3	63.6	50.0	
Mean[d]				61.2	66.6		48.8

[a] Print length and breadth in cm, foot area in cm^2. Foot area = print length × print breadth.
[b] Calculated using equations (1) and (4) in Table 5. BMI: body mass index.
[c] Estimates from Dingwall et al., 2013. All means are for specimens included in that study.
[d] Estimates from Hatala et al., 2016b. All means are for specimens included in that study.

Table 10

Body mass estimates for the Happisburgh sample.

				Body mass estimate (kg)		
	Dimension[a]			Present[b]		Previous
Print	Print length	Print breadth	Foot area	Quadratic	BMI = 27	Ashton[c]
8	24	11	261	62.1	75.0	53
11	25	9	228	53.0	68.9	48
33	26	9	235	54.8	70.3	49

[a] Print length and breadth in cm, foot area in cm^2. Foot area = print length × print breadth.
[b] Calculated using equations (1) and (4) in Table 5. BMI = body mass index.
[c] Estimates from Ashton et al., 2014, using foot area equation from Dingwall et al., 2013.

Table 11

Body mass estimates for the Le Rozel sample.

		Dimension[b]				Body mass estimate (kg)					
						Quadratic			BMI = 27		
Print	Age class[a]	Print length	Print breadth	Foot area	Foot area/290[c]	Adult[d]	Age adj.[e]	Juvenile[f]	Adult[d]	Age adj.[e]	Juvenile[f]
2017–86	adult	29.0	12.4	360.5		97.6			89.9		
2017–87	adult	28.1	10.1	283.2		67.7			78.0		
2017–47	adult	25.2	12.5	316.1		79.0			83.1		
2017–71	adolescent[g]	23.8	11.3	269.7	0.930	63.7	0.762	48.5	75.9	0.804	61.0
2017–64	adolescent	23.8	9.1	216.2	0.746	51.3	0.605	31.1	67.6	0.654	44.2
2017–52	adolescent[g]	23.7	9.6	226.9	0.782	53.3	0.637	34.0	69.2	0.684	47.3
2017–56	adolescent	23.4	8.9	207.3	0.715	49.8	0.579	28.9	66.2	0.629	41.6
2017–73	adolescent[g]	22.5	10.4	234.5	0.809	54.9	0.659	36.2	70.4	0.705	49.6
2017–103	adolescent[g]	22.5	12.7	285.6	0.985	68.5	0.808	55.3	78.3	0.849	66.5
2017–105	adolescent	22.1	9.0	198.7	0.685	48.5	0.554	26.9	64.9	0.604	39.2
2016–35	adolescent	21.9	8.9	194.6	0.671	47.9	0.542	26.0	64.2	0.593	38.1
2017–49	adolescent	21.8	9.3	203.2	0.701	49.2	0.568	27.9	65.6	0.617	40.5
2017–32	adolescent[g]	21.7	10.5	228.3	0.787	53.6	0.641	34.3	69.4	0.687	47.7
2017–22	adolescent	20.9	8.3	172.8	0.596	45.5	0.479	21.8	60.8	0.532	32.3
2017–57	adolescent	19.8	8.0	157.4	0.543	44.3	0.434	19.2	58.5	0.488	28.6
2017–110	adolescent	19.7	10.2	200.8	0.692	48.8	0.560	27.4	65.2	0.610	39.8
2017–18	adolescent	19.6	8.8	171.8	0.592	45.4	0.476	21.6	60.7	0.529	32.1
2017–95	child	19.2	7.8	148.7	0.513	43.8	0.408	17.9	57.1	0.464	26.5
2015–47	child	18.7	7.0	131.4	0.453	43.3	0.358	15.5	54.4	0.415	22.6

2017–41	child	18.4	7.8	142.7	0.492	43.6	0.391	17.0	56.2	0.447	25.1
2015–53	child	18.4	9.7	178.8	0.617	46.1	0.496	22.9	61.8	0.549	33.9
2017–75	child	17.6	8.8	154.8	0.534	44.1	0.426	18.8	58.1	0.481	27.9
2017–104	child	17.3	9.3	161.4	0.556	44.5	0.445	19.8	59.1	0.499	29.5
2016–39	child	17.2	6.3	109.0	0.376	43.6	0.292	12.8	51.0	0.352	18.0
2016–56	child	16.7	6.2	104.1	0.359	43.8	0.278	12.2	50.2	0.339	17.0
2017–102	child	16.7	7.3	122.5	0.422	43.3	0.332	14.4	53.0	0.390	20.7
2015–49	child	16.5	7.0	115.5	0.398	43.4	0.311	13.5	52.0	0.370	19.2
2016–25	child	16.5	7.3	121.4	0.418	43.3	0.328	14.2	52.9	0.387	20.5
2016–33	child	16.4	8.1	132.3	0.456	43.4	0.360	15.6	54.6	0.418	22.8
2017–101	child	16.1	7.1	113.9	0.393	43.5	0.307	13.3	51.7	0.366	18.9
2017–112	child	15.9	7.2	114.1	0.393	43.5	0.307	13.3	51.7	0.367	19.0
2017–07	child	15.7	7.4	117.0	0.403	43.4	0.316	13.7	52.2	0.375	19.6
2016–60	child	15.0	5.7	85.9	0.296	44.9	0.225	10.1	47.4	0.288	13.6
2016–03	child	14.1	5.5	77.5	0.267	45.7	0.200	9.2	46.1	0.264	12.2
2015–04	child	11.6	4.5	52.5	0.181	48.7	0.127	6.2	42.2	0.194	8.2

Abbreviations: adj = adjusted; BMI = body mass index.

[a] Age class as assigned by Duveau et al., 2019.

[b] Original (Duveau et al., 2019) foot lengths and breadths multiplied by 1.02 (see text). Print length and breadth in cm, foot area in cm^2. Foot area = print length × print breadth.

[c] Foot area divided by estimated average foot area of adults of 290 cm^2 (see text).

[d] Calculated using equations (1) and (4) in Table 5.

[e] Age adjustment factor, calculated using equations in Figure 8.

[f] Adult age × age adjustment factor.

[g] Possible adult (see text).

Table 12

Body mass estimates for the Barcin Höyük footprint.

Dimension[a]				Body mass estimate (kg)			
				Present[b]		Atamtürk et al., 2018	
Print length	Print breadth	Print area	Foot area[a]	Quadratic	BMI = 24	Turkish[c]	Indian[d]
24.5	9.7	237.7	256.7	55.6	63.5	71.9	65.4

[a] Print length and breadth in cm, print area (print length × breadth) in cm^2. Foot area = print area × 1.08.
[b] Calculated using equations (1) and (4) in Table 5.
[c] Calculated using forefoot breadth equation for a Turkish sample (Atamturk and Duyar, 2008).
[d] Calculated using forefoot breadth equation for Indians in Krishan, 2008.

Supplementary Online Material (SOM):

Body mass estimation from footprint size in hominins

Christopher B. Ruff[a,*], Roshna E. Wunderlich[b], Kevin G. Hatala[c], Russell H. Tuttle[d], Charles E. Hilton[e], Kristiaan D'Août[f], David M. Webb[g], Benedikt Hallgrímsson[h], Charles Musiba[i], Michael Baksh[j]

[a] *Center for Functional Anatomy and Evolution, Johns Hopkins University School of Medicine, 1800 E. Monument St., Baltimore, MD 21111, USA*

[b] *Department of Biology, James Madison University, MSC 7801, Harrisonburg, VA 22807, USA*

[c] *Department of Biology, Chatham University, Buhl Hall, Woodland Rd., Pittsburgh, PA 15232, USA*

[d] *Department of Anthropology, University of Chicago, 1126 East 59th Street, Chicago, IL 60637, USA*

[e] *Department of Anthropology, University of North Carolina, 301 Alumni Bldg., University of North Carolina, Chapel Hill, NC 27599-3115 USA*

[f] *Department of Musculoskeletal and Ageing Science, Institute of Life Course and Medical Sciences, University of Liverpool, 6 West Derby Street, Liverpool L7 8TX, UK*

[g] *Department of Anthropology and Sociology, Kutztown University, Kutztown, PA 19530, USA*

[h] *Department of Cell Biology & Anatomy, Alberta Children's Hospital Research Institute, McCaig Institute for Bone and Joint Health, Cumming School of Medicine, University of Calgary, 3330 Hospital Dr. NW, Calgary, Alberta T2N 4N1, Canada*

[i] *Department of Anthropology, University of Colorado Denver, NC Building, Suite 4002, 1200 Larimer Street, Denver, CO 80217, USA*

[j] *10878 Aviary Ct., San Diego, CA 92131, USA*

***Corresponding author:**

Email address: cbruff@jhmi.edu (C.B. Ruff)

SOM S1

Supplementary methods

Laetoli

The best available specimen from which to estimate an average BMI for *Australopithecus afarensis* is A.L. 288-1 ('Lucy'). An average stature estimate of 107 cm was derived by Jungers (1988) based on Model II regressions on femur length in human 'pygmies' and *Pan paniscus*. Ruff et al. (2018) obtained a body mass estimate of 28.9 kg from femoral head breadth, which is near the middle of other previous estimates (see Brassey et al., 2018: Fig. 3). Together these yield a BMI estimate of 25.2 kg/m^2. BMI can be estimated more tenuously for two other larger *A. afarensis* specimens: KSD-VP-1/1 and A.L. 827-1. Body mass for KSD-VP-1/1 has been estimated as 59.5 kg based on its estimated femoral head breadth (Ruff et al., 2018). Its maximum tibia length has been reconstructed as 355 mm (Lovejoy et al., 2016). Body mass for the largely complete A.L. 827-1 femur has been estimated as 56.0 kg based on its head breadth (Ruff et al., 2018); its maximum length has been estimated as 368 mm (Ward et al., 2012). Which stature estimation formulae to use with these two specimens is unclear—among non-human primates they are longer than all but large male gorillas so a comparison between human and non-human hominid estimates similar to that for A.L. 288-1 (Jungers, 1988) is not feasible. If the human formulae for male Holocene Europeans (for the tibia, northern Europeans) derived by Ruff et al. (2012) are used, statures of 161.7 cm and 142.9 cm are obtained for KSD-VP-1/1 and A.L. 827-1, respectively, yielding BMI estimates of 22.8 and 27.4 kg/m^2, respectively, which bracket the value for A.L. 288-1. Equations using a higher latitude modern human reference sample characterized by moderate to low limb length to stature or body mass proportions, i.e., northern Europeans, seem more appropriate than more 'generic' equations (e.g., Sjøvold, 1990) given the reconstructed lower limb length to trunk height or body mass

proportions of australopiths (Jungers, 1982; Schmid, 1983; Franciscus and Holliday, 1992; although also see Pontzer, 2012).

Based on this evidence we assume an average BMI of 25 kg/m^2 for *A. afarensis* here. The average foot index of the Laetoli footprints, converted to anthropometric index using the ratio in Table 3, is 45.8, which is quite high for modern humans (Fig. 4) and consistent with a relatively high BMI.

Chimpanzees

Foot length and area, calculated from footprint dimensions using the ratios in Table 3, for the two chimpanzee subjects, A and B, were: A) 19.0 cm and 234.3 cm^2, and B) 19.0 cm and 248.2 cm^2, respectively. It is likely that foot size is larger relative to body mass in juvenile compared to adult chimpanzees, as in humans and many other primates (Young and Heard-Booth, 2016). Since body mass continues to increase after skeletal maturation in chimpanzees (Leigh and Shea, 1996; Brimacombe et al., 2015), a probable increase in BMI in adult relative to juvenile chimpanzees likely also contributes to a relatively larger foot in juvenile chimpanzees, as in humans. Body mass and stature of the two chimpanzees were A) 30.7 kg and 114.5 cm, and B) 27.8 kg and 112.5 cm, respectively.

Foot length in A.L. 288-1 and dimensions of Akka individual

A.L. 288-1's fleshy foot length was derived by adding White and Suwa's (1987) estimate of 12.53 cm for calcaneal to 2nd metatarsal head length, based on a least squares regression through African apes (their Table 3), to their 40.2 cm estimate for summed ray 2 phalangeal lengths (their Table 4), and increasing this by 2.73%, following their recommendation, yielding an estimate of 17.0 cm. This is intermediate between previous estimates of 16.5 cm (White and Suwa, 1987) and 17.26 cm (Jungers, 1988). For the modern Akka individual, following Flower's (1889) recommendation, we added 1.3 cm (half an inch) to skeletal height, yielding a stature of

123 cm, and increased Flower's measured skeletal foot length by 2.73% (White and Suwa, 1987), producing a fleshy foot length of 16.2 cm.

Ileret

Because of its relative completeness, geographic and temporal proximity to Ileret, and probable membership in the same species (*H. erectus*), the KNM-WT 15000 juvenile skeleton provides the most appropriate model for estimating BMI in the Ileret sample. At the time of his death, KNM-WT 15000's stature has been estimated to be slightly less than 157 cm and his body mass to be 50–53 kg (Ruff, 2007), yielding BMI's of 20.3–21.5 kg/m^2. However, as shown earlier (Fig. 7), BMI increases significantly among adolescents. Depending on his exact age at death and number of years of remaining growth, KNM-WT 15000's adult BMI would likely have been about 3±1 units larger (Fig. 6). We have estimated adult body mass for this specimen as 76.7 kg (Ruff et al., 2018) and stature as about 180 cm (Ruff and Burgess, 2015), yielding a BMI of 23.7 kg/m^2. Thus, an adult BMI of about 24 kg/m^2 is consistent with both juvenile and adult body size estimates for KNM-WT 15000, and is used here for the Ileret sample. [Using the midpoint of Cunningham et al.'s (2018) range of estimates for KNM-WT 15000's adult stature (169 cm) and body mass (71 kg) based on chimpanzee and modern human growth models yields a BMI of 24.9 kg/m^2.] The average foot index of the Ileret sample (using averages for the nine trackways plus the 22 additional single prints) is 38.5, which falls in the middle range of values for our modern sample, so is consistent with a wide range of BMIs, including this value (Fig. 3).

Note that Hatala et al. (2017) did not calculate a body mass estimate for FE1-HT1 because it is missing a heel-to-2nd toe length, necessary for application of their method. Here we assumed that heel-to-hallux length, which was available for this specimen, is equivalent to its maximum length, since the average difference between the two length measurements is only 1.4 mm in the entire Ileret sample (including averages for the other eight trackways and the 22

individual prints). Although technically not trackways, the two A2 prints are included in Table 8 because they increase the sample size for comparison with Dingwall et al.'s (2013) results.

Happisburgh

Using body mass estimates from Ruff et al. (2018) and stature estimates from Carretero et al. (2012) based on a generic modern human equation (Sjøvold, 1990), or from Ruff et al. (2012) based on Holocene Europeans, BMIs averaging 26.2 kg/m^2 (Sjøvold stature) or 27.0 kg/m^2 (Ruff et al. stature) are obtained for three femora from the Sima de los Huesos sample (F-X, XII, XIII) (SOM Table S2). A BMI of 26.7 kg/m^2 is obtained for the Jinnuishan specimen (using the Sjøvold equation for stature) (SOM Table S2). These estimates are very close to those for 11 Neandertals, which average 27.0 kg/m^2 (see below and SOM Table S3). Therefore, it is most parsimonious to assume that, like Neandertals, the Happisburgh individuals were characterized by high BMIs. A value of 27 kg/m^2 is used here. The average foot index for the three large adult Happisburgh prints (applying the conversion in Table 3) is 40.3, which is in the intermediate range for modern humans, encompassing a wide range of BMIs (Fig. 4). However, most Happisburgh prints have higher foot index values than this, with a mode of 40.0–44.9 for footprint index (Ashton et al., 2014: Fig. 6), which translates to 41.5–46.6 for foot index, in the upper range for modern humans and most consistent with a relatively high BMI (Fig. 3).

Le Rozel

Based on previous body mass and stature estimates, BMI estimates for 11 adult Neandertals average 27.0 kg/m^2 (range 24.2–33.0 kg/m^2; SOM Table S3), so this average value was used in BMI-based body mass estimation for adults from the Le Rozel sample. The average foot index of the three definitively adult footprints from Le Rozel is 45.0, and the average over all 35 prints is 45.8 (converted using the ratio in Table 3), which falls at the top of our modern human range and is consistent with a high BMI.

Duveau et al. (2019) estimated statures based on the three largest footprint lengths of 184.8, 178.4, and 160.7 cm, which all fall within or above previous stature estimates based on skeletal remains of male Neandertals (158.5—177 cm, *n* = 15; Duveau et al., 2019: SOM Table S10). Previous stature estimates for female Neandertals are shorter, barely overlapping estimates from the three large Le Rozel prints (147.5—161, *n* = 5; Duveau et al., 2019: SOM Table S10). Thus, these three large prints were very likely made by a male or males.

Barcin Höyük

Atamtürk et al. (2018) considered the Barcin Höyük footprint to have been mostly likely made by a male, and we agree, based on its size and comparisons to our reference samples (Table 1). Matched body mass and stature estimates were available for 52 adult males from Çatalhöyük (Knüsel et al., 2021), yielding an average BMI of 24 kg/m^2, so we used this value when employing the BMI-based body mass estimation equation. The foot index of the Barcin Höyük print is 41.1, in the intermediate range for our modern reference samples and consistent with a wide range of BMIs, including this value (Fig. 3).

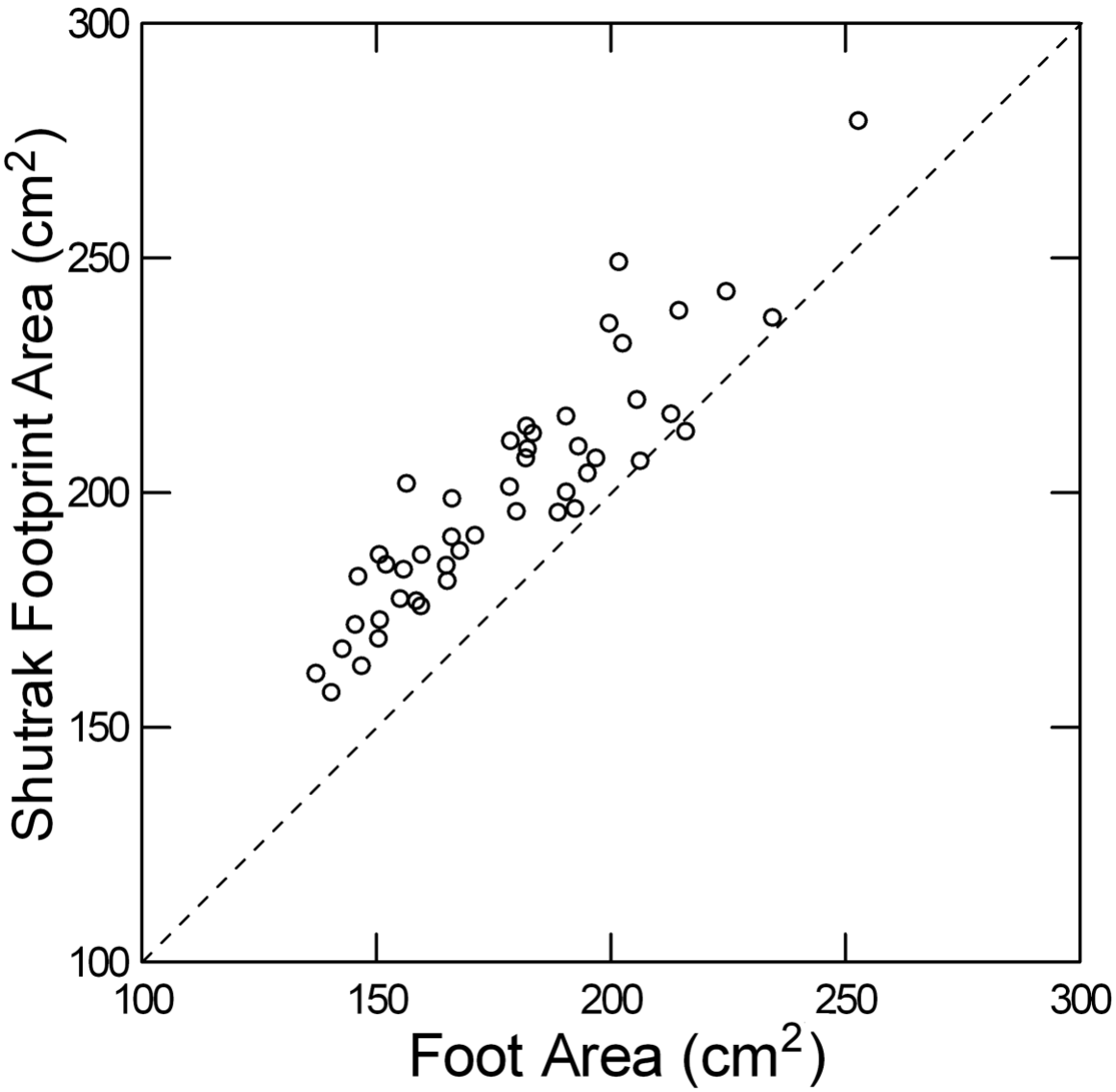

SOM Figure S1. Foot area (maximum length x forefoot breadth), measured anthropometrically on the relaxed foot, versus footprint area measured using Shutrak pressure sensitive paper as subjects walked, in Machiguenga adults (Tuttle et al., 1990). Dashed line indicates equivalence. Shutrak footprint areas average 11% larger than foot areas.

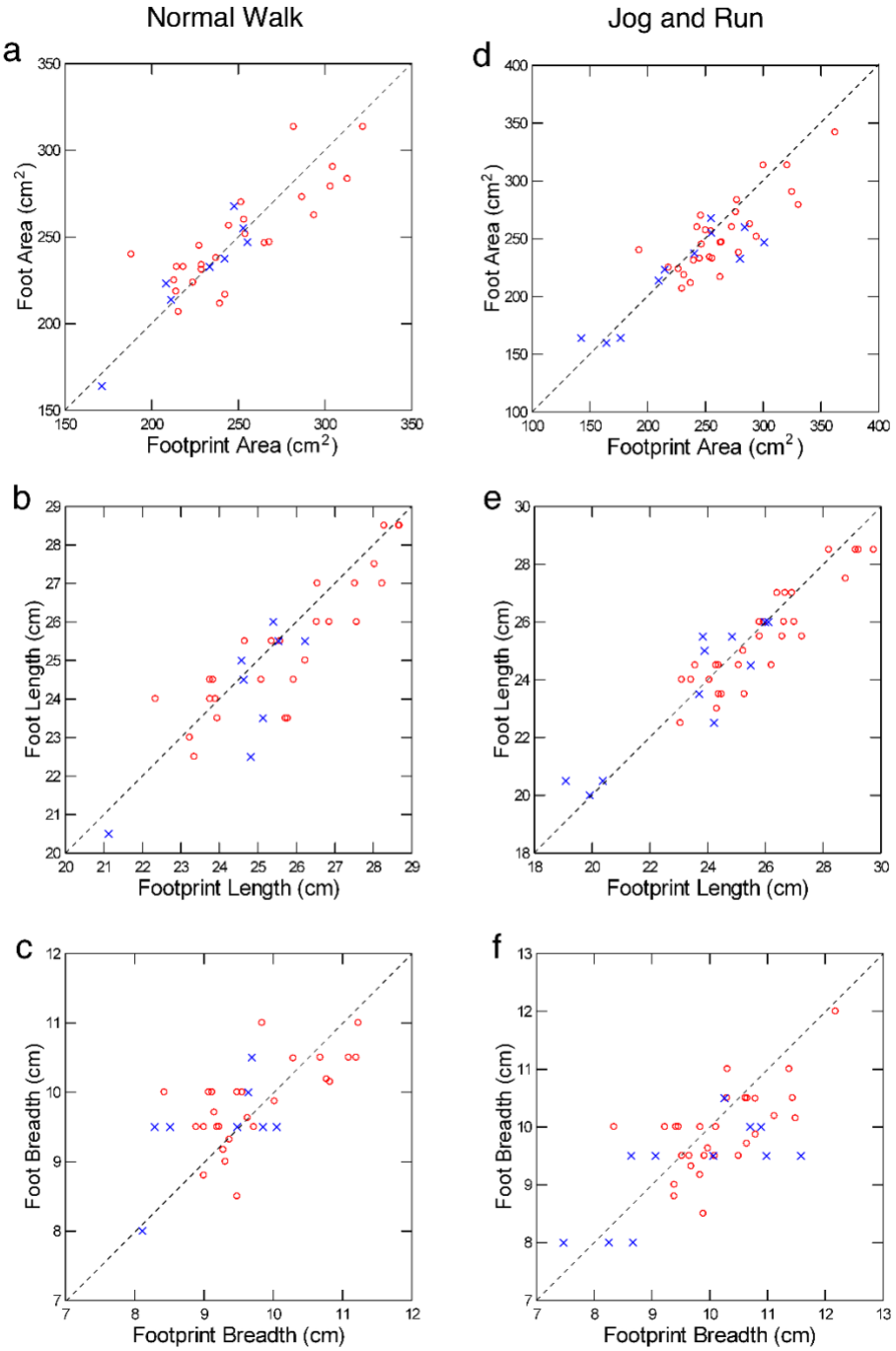

SOM Figure S2. Foot versus footprint dimensions in adult Daasanach sample. Dashed line = equivalence. Circles: adults; x's: juveniles. a-c: 'normal walk' condition; d-f: 'jog and run' condition.

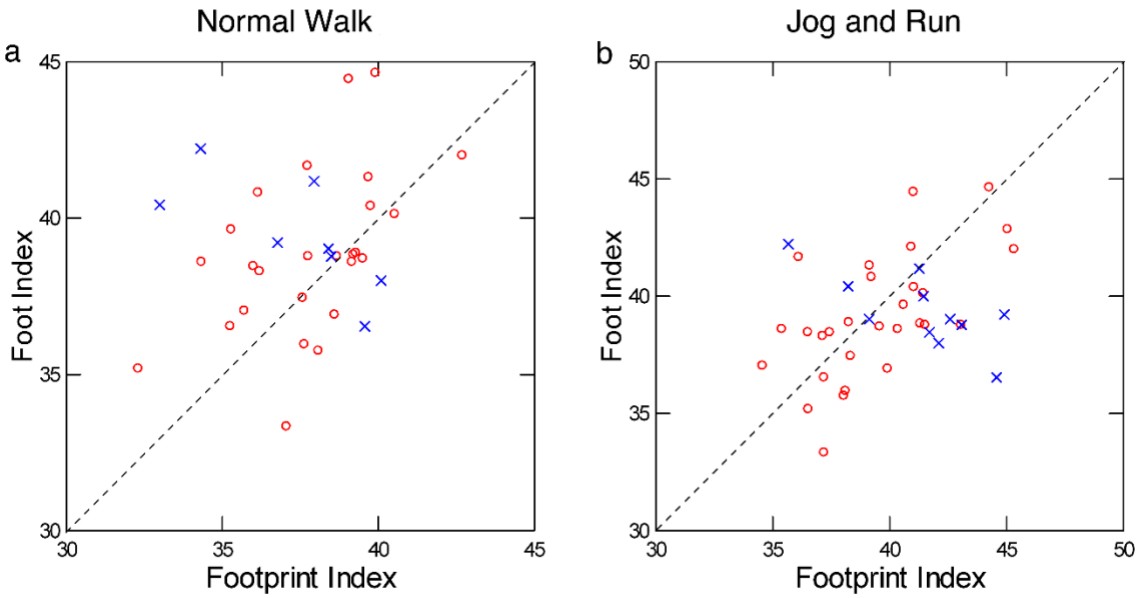

SOM Figure S3. Foot index (breadth/length) versus footprint index in adult Daasanach sample. Dashed line = equivalence. Circles: adults; x's: juveniles. a-c: 'normal walk' condition; d-f: 'jog and run' condition

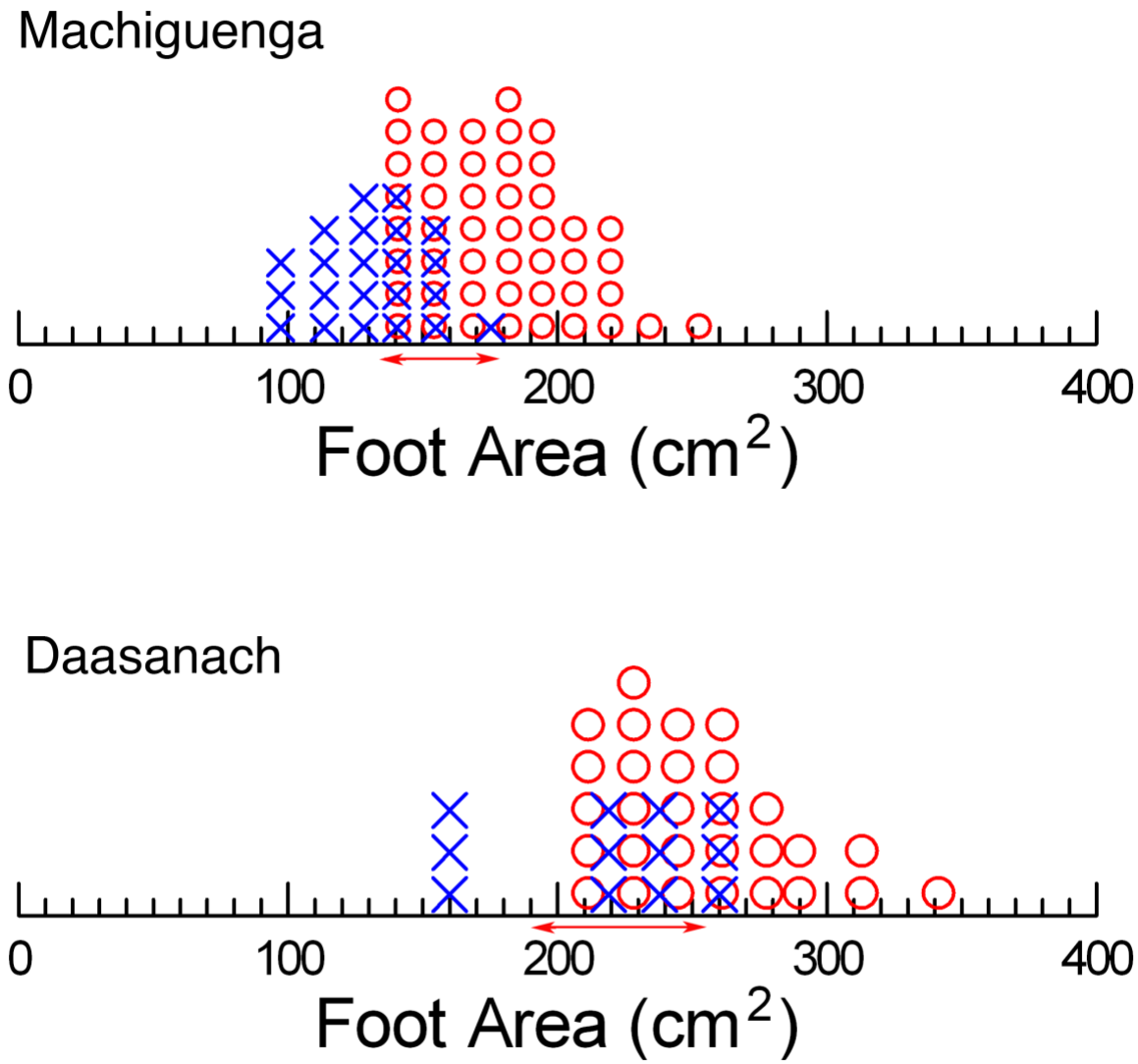

SOM Figure S4. Foot area in Machiguenga and Daasanach adults (red circles) and juveniles (under 16 years, blue crosses). Red arrows indicate range encompassing 75% of adult mean through adult mean.

SOM Table S1

Results for the complete Ileret footprint sample, including all trackways and isolated prints. Body mass estimates using equations in Table 5 for foot area. Previous estimates from Dingwall et al., 2013 and Hatala et al., 2016.

					Body mass estimate (kg)				
					Present			Previous	
Trackway	Print	Print length	Print breadth	Foot area	Quadratic	BMI = 24		Hatala	Dingwall
FE1-HT1		26.8	9.0	242.0	64.1	56.6			
FLT1		25.5	8.0	204.0	58.2	49.3		48.0	35.3
FU-AD		26.0	11.0	287.0	71.1	68.9			51.1
FU-E		25.3	10.7	271.0	68.6	64.1			50.2
FU-O		28.0	9.5	266.0	67.9	62.6			50.8
FUT1A		25.6	10.1	258.2	66.6	60.6		50.6	50.3
FUT1B		26.7	9.6	255.9	66.3	60.0		52.1	53.2
FUT2		26.8	11.0	288.7	69.4	71.4		53.4	60.3
FUT3		25.3	9.3	233.9	54.8	62.9		46.4	44.5
	A2-I2	21.1	7.7	162.5	44.6	51.8			41.5
	A2-I3	26.5	10.0	265.0	62.4	67.7			52.7
	FE1-H1	23.0	7.5	172.5	45.4	53.4			
	FE1-H2	21.0	7.5	157.5	44.3	51.0			
	FE1-H3	21.0	7.5	157.5	44.3	51.0			
	FE3-H11	24.5	9.5	232.8	54.5	62.7		49.4	
	FE3-H13	29.5	12.0	354.0	94.7	81.5		63.4	
	FE3-H17	29.0	10.5	304.5	74.8	73.8		60.0	
	FE3-H18	25.5	9.0	229.5	53.9	62.2			
	FE3-H4	23.5	10.5	246.8	57.7	64.9			
	FE3-H6	26.0	9.5	247.0	57.7	64.9		53.8	
	FE8-H1	29.0	9.5	275.5	65.4	69.3		56.2	
	FU-AA	30.5	11.0	335.5	86.7	78.6		58.8	
	FU-AB	26.5	7.0	185.5	46.8	55.4		40.4	
	FU-AC	25.0	9.0	225.0	53.0	61.5		47.1	
	FU-C	26.5	10.9	288.9	69.5	71.4		55.7	
	FU-J	26.0	8.9	231.4	54.3	62.5		51.1	
	FU-N	24.0	8.6	206.4	49.7	58.6		40.6	
	FU-P	27.0	9.0	243.0	56.8	64.3		52.7	
	FU-T	25.5	10.8	275.4	65.3	69.3		52.4	
	FU-W	24.0	11.1	266.4	62.8	67.9		50.3	
	FU-X	20.5	8.3	169.1	45.1	52.8		26.5	

Print length and breadth in cm, foot area in cm^2. BMI: body mass index, kg/m^2.

SOM Table S2

Estimated body mass, stature, and body mass index for three Sima de los Huesos femora from Atapuerca, Spain (Arsuaga et al., 2015), and the Jinnuishan specimen from China (Rosenberg et al., 2006). Body mass estimated from femoral head breadth using equation in Ruff et al. (2018). Stature for Atapuerca specimens estimated from maximum femoral length using Holocene European equation for males in Ruff et al. (2012) and generic modern human formula (pooled sexes) in Sjøvold (1990) as cited by Carretero et al. (2012). Stature for Jinnuishan 1 estimated using Sjøvold (1990) equation based on maximum ulnar length.

Specimen	Body mass (kg) (Ruff et al., 2018 eq.)	Stature (cm) (Ruff et al., 2012 eq.)	Stature (cm) (Sjøvold, 1990 eq.)	BMI (Ruff et al., 2012 stature)	BMI (Sjøvold, 1990 stature)
Atap. F-X	80.7	167.4	170.0	28.8	27.9
Atap. F-XII	72.1	165.3	167.8	26.4	25.6
Atap. F-XIII	70.6	165.3	167.8	25.9	25.1
Mean				27.0	26.2
Jinnuishan 1	74.2		166.7		26.7

BMI = Body mass index, kg/m^2.

SOM Table 3

Estimated body mass, stature, and body mass index (BMI) in 11 Neandertals. Body mass estimated from femoral head breadth using equation in Ruff et al. (2018); statures estimated from long bone lengths in Ruff et al. (1997), based on US white equations in Trotter and Gleser (1952).

Specimen	Body mass (Ruff et al., 2018 eq.)	Stature (Ruff et al., 1997)	BMI
Amud 1	77.9	175	25.4
La Chapelle-aux-Saints 1	79.8	162	30.4
Font-de-Forêt 1	71.0	172	24.0
La Ferrassie 1	83.4	171	28.5
La Ferrassie 2	65.1	152	28.2
Kebara 2	69.3	166	25.1
Regourdou 1	65.1	164	24.2
Shanidar 5	68.7	168	24.3
Spy 1	70.8	161	27.3
Spy 2	83.4	159	33.0
Tabun 1	62.0	154	26.1
Mean			27.0

Body mass in kg, stature in cm. BMI = Body mass index, kg/m^2.

SOM References

Arsuaga, J.L., Carretero, J.M., Lorenzo, C., Gomez-Olivencia, A., Pablos, A., Rodríguez, L., Garcia-Gonzalez, R., Bonmatí, A., Quam, R.M., Pantoja-Pérez, A., Martínez, I., Aranburu, A., Gracia-Tellez, A., Poza-Rey, E., Sala, N., Garcia, N., Alcazar de Velasco, A., Cuenca-Bescos, G., Bermúdez de Castro, J.M., Carbonell, E., 2015. Postcranial morphology of the middle Pleistocene humans from Sima de los Huesos, Spain. Proc. Natl. Acad. Sci. 112, 11524-11529.

Ashton, N., Lewis, S.G., De Groote, I., Duffy, S.M., Bates, M., Bates, R., Hoare, P., Lewis, M., Parfitt, S.A., Peglar, S., Williams, C., Stringer, C., 2014. Hominin footprints from early Pleistocene deposits at Happisburgh, UK. PLoS One. 9, e88329.

Atamtürk, D., Özbal, R., Gerrtisen, F., Duyar, I., 2018. Analysis and interpretation of Neolithic period footprints from Barcin Höyük, Turkey. Mediterr. Archaeol. Archaeom. 18, 163–174.

Brassey, C.A., O'Mahoney, T.G., Chamberlain, A.T., Sellers, W.I., 2018. A volumetric technique for fossil body mass estimation applied to *Australopithecus afarensis*. J. Hum. Evol. 115, 47–64.

Brimacombe, C.S., Kuykendall, K.L., Nystrom, P., 2015. Epiphyseal fusion in *Pan troglodytes* relative to dental age. Am. J. Phys. Anthropol. 157, 19–29.

Carretero, J.M., Rodriguez, L., Garcia-Gonzalez, R., Arsuaga, J.L., Gomez-Olivencia, A., Lorenzo, C., Bonmati, A., Gracia, A., Martinez, I., Quam, R., 2012. Stature estimation from complete long bones in the Middle Pleistocene humans from the Sima de los Huesos, Sierra de Atapuerca (Spain). J. Hum. Evol. 62, 242–255.

Cunningham, D.L., Graves, R.R., Wescott, D.J., McCarthy, R.C., 2018. The effect of ontogeny on estimates of KNM-WT 15000's adult body size. J. Hum. Evol. 121, 119–127.

Dingwall, H.L., Hatala, K.G., Wunderlich, R.E., Richmond, B.G., 2013. Hominin stature, body mass, and walking speed estimates based on 1.5 million-year-old fossil footprints at Ileret, Kenya. J. Hum. Evol. 64, 556–568.

Duveau, J., Berillon, G., Verna, C., Laisne, G., Cliquet, D., 2019. The composition of a Neandertal social group revealed by the hominin footprints at Le Rozel (Normandy, France). Proc. Natl. Acad. Sci. 116, 19409–19414.

Flower, W., 1889. Description of two skeletons of Akkas, a Pygmy race from central Africa. J. Roy. Anth. Inst. 18, 3–19.

Franciscus, R.G., Holliday, T.W., 1992. Hindlimb skeletal allometry in Plio-Pleistocene hominids with special reference to A.L. 288-1 ("Lucy"). Bull. et Mém. de la Société d'Anthropologie de Paris. n.s. 4, 5-20.

Hatala, K.G., Roach, N.T., Ostrofsky, K.R., Wunderlich, R.E., Dingwall, H.L., Villmoare, B.A., Green, D.J., Harris, J.W., Braun, D.R., Richmond, B.G., 2016. Footprints reveal direct evidence of group behavior and locomotion in *Homo erectus*. Sci. Rep. 6, 28766.

Jungers, W.L., 1988. Lucy's length: Stature reconstruction in *Australopithecus afarensis* (A.L. 288-1) with implications for other small-bodied hominids. Am. J. Phys. Anthropol. 76, 227–231.

Knüsel, C.J., Milella, M., Betz, B., Dori, I., Garofalo, E., Glencross, B., Haddow, S.D., Ledger, M., Anastasiou, E., Mitchell, P., Pearson, J., Pilloud, M.A., Ruff, C.B., Sadvari, J.W., Tibbetts, B., Larsen, C.S., 2021. Bioarchaeology at Neolithic Çatalhöyük: Indicators of Health, Well-being and Lifeway in their Social Context, in: Hodder, I. (Ed.), Peopling the landscape of Çatalhöyük: reports from the 2009-2017 seasons. Çatalhöyük Research Project Series Volume 13; British Institute at Ankara Monograph 53. British Institute at Ankara, London, pp. 315–355.

Leigh, S.R., Shea, B.T., 1996. Ontogeny of body size variation in African apes. Am. J. Phys. Anthropol. 99, 43–65.

Lovejoy, C.O., Latimer, B.M., Spurlock, L., Haile-Selassie, Y., 2016. The pelvic girdle and limb bones of KSD-VP-1/1. In: Haile-Selassie, Y., Su, D.F. (Eds.), The Postcranial Anatomy of *Australopithecus afarensis*. Springer, Dordrecht, pp. 155–178.

Pontzer, H., 2012. Ecological energetics in early *Homo*. Curr Anthropol. 53, Supp. 6, S346-348.

Rosenberg, K.R., Lü, Z., Ruff, C.B., 2006. Body size, body proportions and encephalization in a Middle Pleistocene archaic human from northern China. Proc. Natl. Acad. Sci. USA 103, 3552–3556.

Ruff, C.B., 2007. Body size prediction from juvenile skeletal remains. Am. J. Phys. Anthropol. 133, 698–716.

Ruff, C.B., Burgess, M.L., 2015. How much more would KNM-WT 15000 have grown? J. Hum. Evol. 80, 74–82.

Ruff, C.B., Burgess, M.L., Squyres, N., Junno, J.-A., Trinkaus, E., 2018. Lower limb articular scaling and body mass estimation in Pliocene and Pleistocene hominins. J. Hum. Evol. 115, 85–111.

Ruff, C.B., Holt, B.M., Niskanen, M., Sladek, V., Berner, M., Garofalo, E., Garvin, H.M., Hora, M., Maijanen, H., Niinimaki, S., Salo, K., Schuplerova, E., Tompkins, D., 2012. Stature and body mass estimation from skeletal remains in the European Holocene. Am. J. Phys. Anthropol. 148, 601–617.

Schmid, P., 1983. Eine rekonstruktion des skelettes von A.L. 288-1 (Hadar) und deren konsequenzen. Folia Primatol. 40, 283-306.

Sjøvold, T., 1990. Estimation of stature from long bones utilizing the line of organic correlation. Hum. Evol. 5, 431–447.

Trotter, M., Gleser, G.C., 1952. Estimation of stature from long bones of American whites and Negroes. Am. J. Phys. Anthropol. 10, 463–514.

Ward, C.V., Kimbel, W.H., Harmon, E.H., Johanson, D.C., 2012. New postcranial fossils of *Australopithecus afarensis* from Hadar, Ethiopia (1990-2007). J. Hum. Evol. 63, 1–51.

White, T.D., Suwa, G., 1987. Hominid footprints at Laetoli: Facts and interpretations. Am. J. Phys. Anthropol. 72, 485–514.

Young, J.W., Heard-Booth, A.N., 2016. Grasping primate development: Ontogeny of intrinsic hand and foot proportions in capuchin monkeys (*Cebus albifrons* and *Sapajus apella*). Am. J. Phys. Anthropol. 161, 104–115.